Improvement of semi-active control suspensions based on gain-scheduling control

Husam Hammood

School of Computing, Science & Engineering

University of Salford

Salford, UK

Submitted in Partial Fulfilment of the Requirement of the Degree of Doctor of Philosophy

2018

LIST of CONTENTS

LIST OF FIGURES

LIST OF TABLES

DEDICATION

This PhD Thesis is dedicated to all members of my family:

My parents, who live abroad and kept their hearts with me.

My wife, for her support and patience with me throughout my PhD.

My children, as I spent most of my time on research and not as much time with them as would have liked.

ACKNOWLEDGEMENTS

I would like to acknowledge with deep appreciation the academic guidance, understanding and continuous encouragement provided by my supervisor, Professor T X Mei throughout this study. His patience and inspirational guidance was extremely valuable on the successful completion of this work.

Also, I would like to thank my parents, my brothers and sisters, my wife, and my family for supporting me throughout this PhD study and my life in general. Thank all my friends for their encouragement and support during my study for the PhD degree.

I would like to acknowledge the financial and academic support of University of Dhi Qar and University of Salford, particularly the award of scholarship that provided me the necessary financial support for this research, library facilities, and the computer facilities.

Last but not least, I would like to acknowledge the Ministry of Higher Education and Scientific Research (MOHESR) in Iraq, for the financial support for my family and me during my PhD journey. Special thanks to Iraqi Cultural Attaché in London for the guidance and continuous support.

ABSTRACT

This study presents the development of a non-linear control strategy for a semi-active suspension controller using a gain-scheduling structure controller. The aim of the study is to overcome the constraints of conventional control strategies and improve semi-active suspension to achieve performance close to that of full active control. Various control strategies have been investigated to improve the performance of semi-active vibration control systems. A wide range of semi-active control strategies have also been experimentally tested by researchers in the attempt to enhance the performance of semi-active suspension systems. However, the findings published in the literature indicate that there appears to be a ceiling to performance improvements with the control strategies that have been proposed to date, which is about the half of what could be achieved with full active control. The main constraint for semi-active devices such as Magnetorheological (MR) dampers is that they are only capable of providing active control forces by dissipating energy, in their active mode, and they switch to work as simple passive dampers, the passive mode, when energy injection is demanded by the associated control laws. The split in durations of time between the active and passive modes for the conventional semi-active control strategies is around 50:50. This study will focus on the development of a novel semi-active control strategy that aims to extend the duration of the active mode and hence reduce the duration of the passive mode for semi-active suspensions by using a gain-scheduling control structure that dynamically changes the control force demanded by the operating conditions. The proposed control method is applied to both vertical and lateral suspensions of a railway vehicle in this study and the improvements in ride quality are evaluated with several different track data. For the purpose of performance comparison, a semi-active controller based on skyhook damping control integrated with MR dampers and also a vehicle with passive suspensions are used as the benchmark, and are used as a reference case

for assessment of the proposed design. Numerical simulations are carried out to assess the performance of the proposed gain-scheduling controller. The simulation results obtained illustrate the performance improvement of the proposed control strategy over conventional semi-active control approaches, where the ride quality of the new controller is shown to be significantly improved and comparable with that of full active control. Potentially, this kind of adaptive capability with variable control approaches can be used to deliver the level of the performance that is currently only possible with fully active suspension without incurring the associated high costs and power consumption.

CHAPTER ONE

1 INTRODUCTION

1.1 Introduction

Suspension systems play an essential part in improving the ride quality and stability of the vehicle system. It reduces the motion and acceleration of the sprung mass in the system. Conventional passive suspensions have some advantages such as design simplicity and cost-effectiveness. However, the performance due to the wide frequency range of excitations induced by track irregularities may be limited because of the associated fixed design, in which the damping and spring cannot be controlled when the system and/or operating conditions change.

Therefore, in the last decade, controllable suspension systems, which include full-active and semi-active systems, have been proposed by using computer-based control devices and controllable actuators [1, 2]. Although full-active suspension systems can provide high control performance over a wide frequency range of vibrations, the cost and high power requirement of the actuators imposes significant obstacles to their commercial adoption. A promising alternative to full-active suspension system is a semi-active suspension.

The semi-active suspension offers advantages over passive suspension for desirable performance whilst also providing a more cost-effective solution than full-active suspensions[3]. During the past decade, the semi-active suspension has been investigated by a number of researchers as used in railway vehicles, automotive and vibration control applications [4, 5]. More recently, MR dampers, which can change the damping ratio by suitable magnetic fields, have been studied by some researchers for use in the vibration control

of vehicle suspension because of their fast response, low power consumption and ability to control the damping ratio [6].

However, the tracking of the desired damping force is a significant issue in semi-active suspension systems. The variable dampers are only capable of dissipating energy, but cannot develop a positive force when the damper velocity reverses and hence the semi-active controller will simply apply a damping force using passive mode; therefore, a semi-active damper cannot create the necessary forces, or apply the same level of control, in the same way as a full-active control in such conditions.

This study will focus on the development of a novel semi-active control strategy that aims to extend the duration of the active mode and hence reduce the duration of the passive mode for semi-active suspensions by using a gain-scheduling control structure that dynamically changes the control force demanded according to the operating conditions.

1.2 Identification of the Problem

Many control strategies have been studied for the semi-active suspension systems in the attempt to achieve high levels of performance. Most semi-active control strategies are based on achieving a control force equivalent to the behaviour of the skyhook control strategy[7]. Some linear feedback control methods and intelligent strategies have also been investigated in the semi-active suspension system [8, 9]. More recently, many control strategies including fuzzy logic control [10], skyhook, ground-hook and hybrid control[11], neural network predictive control algorithm[12], semi-active fuzzy control [13], and adaptive vibration control [14] have been explored.

However, the findings published in the literature indicate that there appears to be a ceiling on performance improvements with the control strategies proposed to date, which is about the half of what could be achieved with full-active control. The main constraint for semi-active

devices such as MR dampers is that they are only capable of providing active control forces by dissipating energy, i.e., in their active mode, and are switched to work as simple passive dampers, i.e., the passive mode, when energy injection is demanded by the appropriate control laws. The split in durations of time between the active and passive modes for the conventional semi-active control strategies is around 50:50. In the full-active suspension system, the force-velocity diagram (Figure1.1) shows that the actuator force versus actuator relative velocity it works in all four quarters, which means the energy can be injected into the suspension system or dissipated from the suspension system.

However, the semi-active damper can only be dissipated energy from the system, which follows from the possibility to work only in the first and third quarter of the force-velocity diagram, as shown in Figure 1.1. Therefore, the semi-active damper is not able to develop a damping force in the opposite direction as the relative damper velocity, and it is switched to the minimum damper setting, i.e., in their passive mode, as the damper is transmitting the force rather than dissipating energy.

This study will focus on the development of a novel semi-active control strategy that aims to extend the duration of the active mode and hence reduce the duration of the passive mode for semi-active suspensions by using a gain-scheduling control structure that dynamically changes the control force demanded according to the operating conditions.

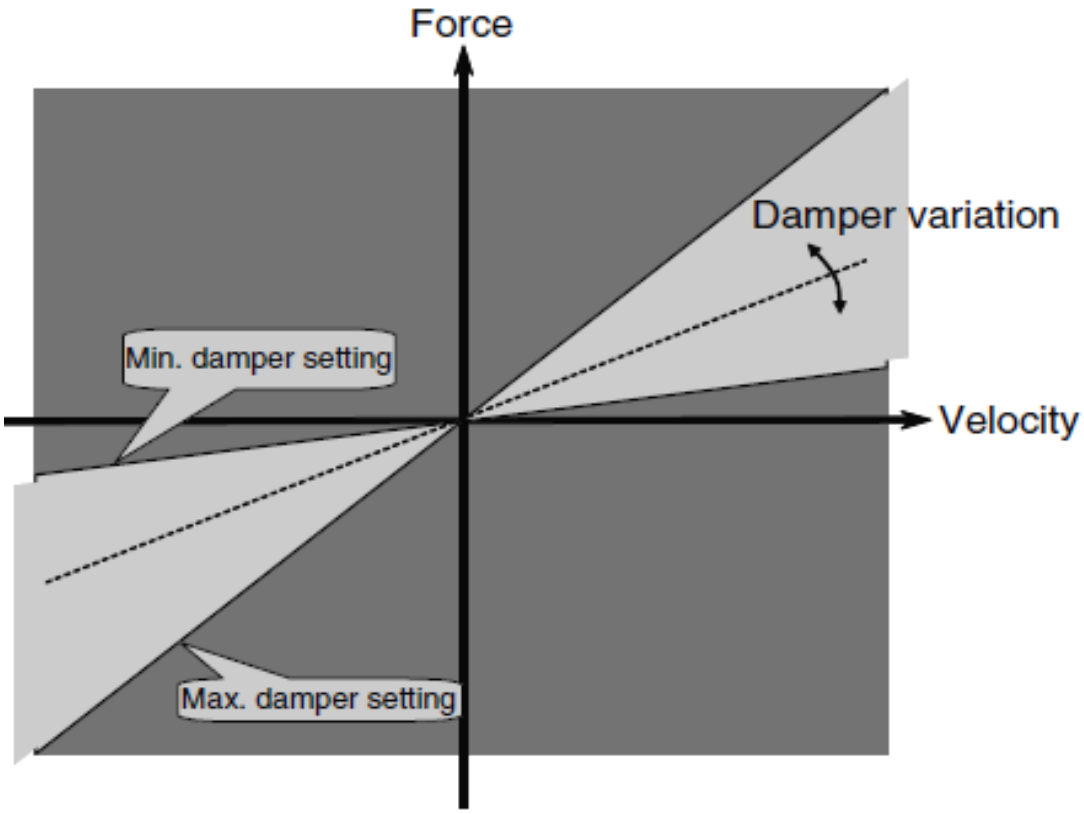

Figure 1.1: Force – velocity diagram for semi-active damper[15]

1.3 Research Motivation, Aim and Objectives

The aim of the research is to overcome the constraints of conventional linear control strategies and improve semi-active suspension to achieve a performance close to that of full-active control. The improved performance may be used to deliver the same level of the performance that is currently only possible with full-active suspension systems without incurring the associated high costs and power consumption.

The improved performance can be used to deliver a better ride quality or will be used to enable higher railway vehicle speeds while maintaining the same level of passenger comfort. The other possibility is to provide the same ride quality on less well-maintained or lower quality track.

In order to achieve this aim, the following research objectives have been identified:

- Undertake a comprehensive literature review of current full-active and semi-active control strategies for suspension systems.
- Undertake a comprehensive literature review of semi-active suspension control of the MR damper.
- Work on the modelling and simulation of a railway vehicle as a case study and control design for active/semi-active suspension control.
- Develop an adaptive control strategy for a semi-active suspension in order to minimise the use of minimum level of damper settings as much as possible.
- Verify the development of the proposed control strategy via the MR damper model and assess the associated system performance.
- Discuss dynamic performance and draw conclusions from the research carried out, and further make recommendations as to how the proposed control design for semi-active suspension of a railway vehicle can improve ride quality.
- Publish results of research in journals, and present the same at conferences.

1.4 Contributions of This Thesis

This thesis presents the development of a non-linear control strategy for semi-active suspension that can be used to deliver a level of the performance that is only currently possible with full-active suspension without incurring the associated high costs and power consumption. This thesis is believed to make the following contributions to the present research field:

- A new semi-active control strategy using a gain-scheduling structure controller, which can be used to improve semi-active suspension performance, has been developed and optimised through simulation.

- The proposed control method is applied to both vertical and lateral secondary suspensions of the railway vehicle in this study and the improvements in the ride quality are evaluated with several different track data.

1.5 The Layout of the Thesis

The thesis is organised as follows:

In chapter 1, the introduction and an overview of the study are given, as well as a brief description of the motivation, aims, and objectives of this research.

In chapter 2, the background of thesis and an overview of different categories of control suspensions are presented. The advantages and limitations are briefly discussed.

In chapter 3, the comprehensive literature review of full-active and semi-active suspension systems for railway vehicles is presented. The use of an MR damper-based semi-active suspension for railway vehicles is also discussed. The literature review highlights the importance of this research.

In chapter 4, the modelling of the conventional railway vehicle in vertical and lateral directions are introduced. Vehicles with passive suspension, full-active and conventional semi-active controls are introduced as benchmarks and are used for comparative assessment of the proposed semi-active controlled suspension design.

In chapter 5, both the modelling and control of semi-active MR dampers are presented.

In chapter 6, the proposed semi-active suspension based on gain-scheduling control is introduced. The design process, tuning, and applications for the secondary suspension system of the railway vehicle are also presented.

In Chapter 7, the numerical simulation results of vertical secondary suspension performed in the Matlab Simulink environment to evaluate and analyse the performance of different control strategies for the secondary suspension system of the railway vehicle are discussed.

In Chapter 8, the results of lateral suspension used to assess the performance of different control strategies for the secondary suspension system of the railway vehicle are further analysed.

In chapter 9, a summary of the main conclusions from this thesis and recommendations for future work are given.

CHAPTER TWO

2 BACKGROUND

2.1 Introduction

Increased velocity is one way for railway vehicles to compete with other means of transportation. However, higher velocity usually causes increased forces and accelerations on the vehicle, which negatively affect ride comfort. Therefore, some form of active technology in the secondary suspension system might represent a solution to improved ride quality in cases where conventional passive suspension systems cannot be further optimised. The improved performance can be used to deliver better ride quality or will be used to enable higher railway vehicle speeds while maintaining the same level of passenger comfort. The other possibility is to provide the same ride quality on lower quality track. In this regard, the active secondary suspension can be used in the lateral and/or vertical directions when different actuator configurations are installed.

The concepts of full-active suspension in railway vehicles have been studied theoretically and experimentally for decades, generally showing significant ride quality improvements compared to passive suspension systems. In full-active suspension systems, actuators, which are operating by the external power supply, are used to generate the necessary damping force to suppress the vibrations. However, active suspensions have disadvantages regarding their weight, size, high power consumption, and fail-safety issues[16].

Therefore, full-active suspension systems have not yet been implemented for in-service operation. Generally speaking, full-active suspension system solutions are excessively expensive in relation to the potential benefits they can deliver. Compared to conventional

passive suspension, full-active suspension systems must be safe and reliable in order to be considered a feasible option for industrial railway implementation[16, 17].

During the past decade, among the many different types of controlled suspension systems, the semi-active suspension has been investigated by a number of researchers for use in railway vehicles, automotive, and vibration control applications [5]. The semi-active suspension offer advantages over passive suspension in terms of its more desirable performance and, on the other hand, provides a more cost-effective solution when compared with full-active suspensions.

Semi-active suspension systems usually use controllable dampers to change the damping force, and do not add energy to the suspension system such as semi-active hydraulic damper changes the size of an orifice in the hydraulic flow valve to adjust the damping force, an electrorheological (ER) damper applies different of the electric field to control the viscosity of the ER damper.

More recently, Magnetorheological (MR) dampers, which can change the damping ratio by suitable magnetic fields, have been studied for railway vehicles in semi-active suspension by many researchers, because of their low power consumption, fast response, and the capability to control the damping ratio.

The fundamental idea of the semi-active controlled suspension system is to regenerate the action of skyhook damping as closely as possible, but an MR damper cannot develop a positive force when the relative velocity reverses because it would require a negative damper setting. In this instance, the semi-active controller will simply apply a minimum damper setting, and hence a semi-active damper cannot create the necessary forces. However, if a control strategy can be found that manages the desired control force so as to minimise the use of the minimum damper setting, this would represent an improved damping efficiency of the damper and

thereby increase energy dissipation, and for which there is significant potential for future implementation.

2.2 Railway Vehicle Suspension Systems

Prior to developing the controller, a model of a railway vehicle, which is shown in Figure 2.1, is constructed as the benchmark model for assessment and comparative studies of control strategies. The railway vehicle studied in the research is composed of one vehicle body, two bogies, and four wheelsets. The two bogies, which are identified simply as the front and rear bogies, are connected to the vehicle body by the secondary suspension. Each of the two bogies is also connected to two wheelsets by the primary suspension. The primary and the secondary suspensions are provided in the vertical and lateral directions. The main aim of active technology in railway vehicle suspension can fall into one of two categories: improving running stability and wheelset guidance through controlling the primary suspension, and improving ride quality through controlling the secondary suspension.

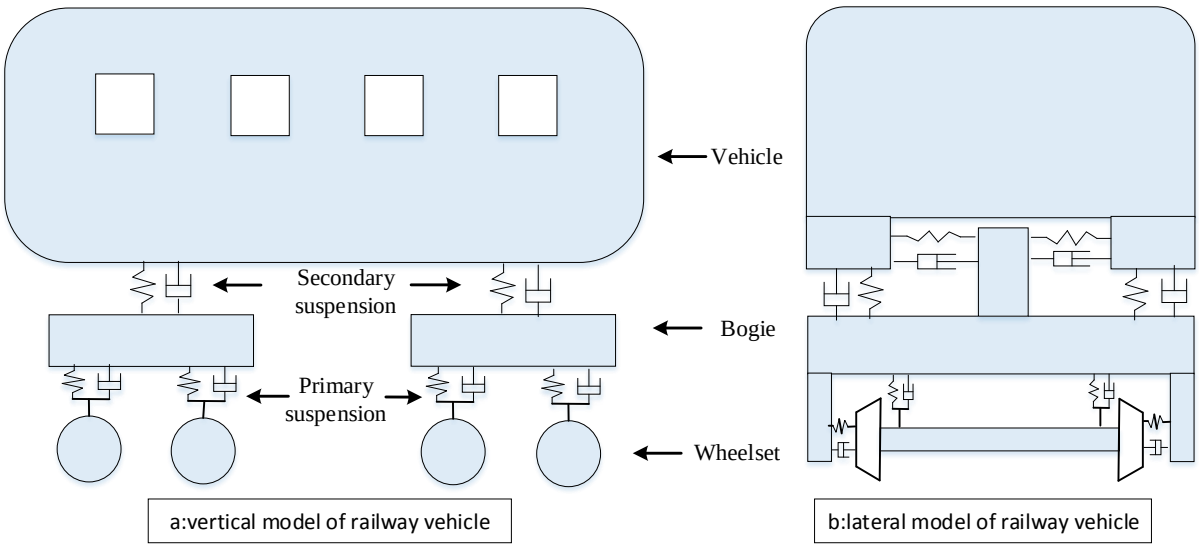

Figure 2.1: Diagram of a railway vehicle model (a) vertical model; (b) lateral model

2.2.1 Primary Suspension

The most significant challenge in the primary suspension of railway vehicles is to achieve a good compromise between stability and guidance, which with a passive suspension is difficult. The critical speed of the railway vehicle on the straight track is a function of an exceedingly stiff wheelset guidance, especially in the longitudinal direction, and is often integrated with a stiff yaw damping between vehicle and bogie. However, the curving performance is thereby negatively affected, since a high primary suspension stiffness reduces the radial steering ability, which causes larger track shift forces and a higher amount of wheel and rail wear. With the actively controlled primary suspension, the stiffness can be adapted to the running conditions[16]. Active technology in the primary suspension can improve the curving performance whilst maintaining an adequate level of running on the straight track. The concept of active primary suspension has been under investigation for decades and has been theoretically and practically developed and improved. There are a variety of approaches to enhance stability and guidance through an active technology, which has been categorised and summarised by Goodall et al. [18]. However, high cost and reliability issue have prevented the implementation of this technology for active primary suspension.

2.2.2 Secondary Suspension

The aim of the secondary suspension is to isolate the vehicle body from track irregularities. There are two elements of the suspension that have an influence on its performance, namely a spring element and a damper. For a passive suspension, the designer has to assume the most frequent condition of running (such as characteristics of railway track, vehicle speed, and acceptable level of acceleration) and find the best suspension stiffness and damping for these conditions. However, the performances due to the wide frequency range of excitations induced by rail track irregularities may be limited, the parameters of the passive damper are fixed, which means that once the system is designed, the damping cannot be varied. The purpose of active

control of the secondary suspension is to provide better isolation of the vehicle from excitations transmitted from track irregularities than the passive damping can offer by itself, and hence improves passenger comfort. The secondary suspension is usually controlled in the lateral direction, including the yaw mode, or in the vertical direction, including the pitch mode. It is important to realise that the improved performance offered by an active suspension can be employed from an operational point of view through a variety of methods.

Figure 2.2 illustrated the general relationship of ride quality with railway vehicle speed, which shows the accelerations on the vehicle body increases with speed. As shown in Figure 2.2, active technology in secondary suspension can be used in order to achieve one or more of the following options. The first option is simply to improve passenger ride comfort, but if the passenger ride comfort is already good, further improvement at unchanged railway vehicle speed and track conditions is little justification for the extra cost of the active technology in secondary suspension. The second option shows the possibility of increasing vehicle speed and using the improved performance to maintain good ride quality, with the reduced journey time and enhanced utilisation of the railway vehicle bringing benefits that offer a clear rationale for the use of an active technology in secondary suspension. The third option is to operate the railway vehicle on a lower quality track, with the active technology in secondary suspension again being used to maintain acceptable ride quality, in this option, the significant savings in track maintenance that arise from the reduced need to ensure high track quality, can be used to justify the active technology in secondary suspension.

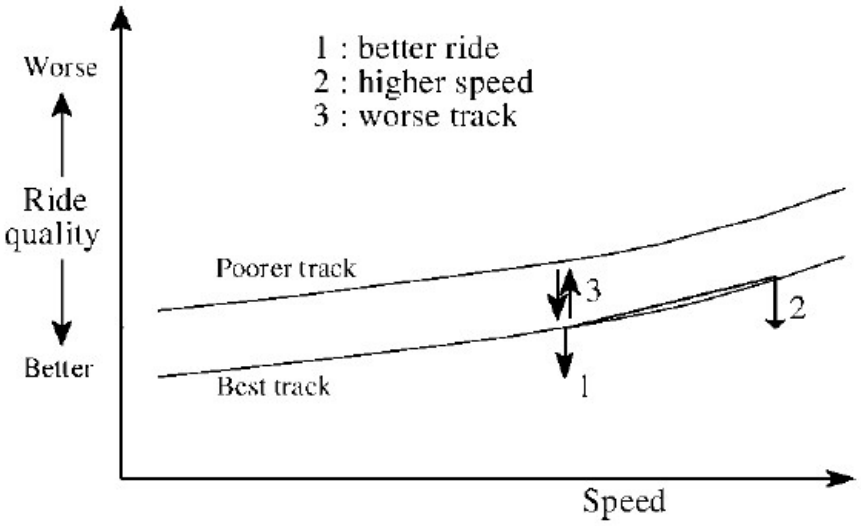

Figure 2.2: Use of improved active secondary suspension performance[19]

2.3 Control Schemes in Suspension

The suspension system can be categorised depends on the control bandwidth and external power supply to the system in terms of three categories, which are passive, full-active, and semi-active suspension systems. A passive suspension is a conventional suspension system that consists of a spring and damper, and which means the damping rate is fixed. A semi-active suspension system has the same configuration as the passive suspension, but with a controllable damping rate for the damper. A full-active suspension consists of a spring and an actuator that supply additional force. Figure 2.3 shows a schematic of a quarter of the railway vehicle system with a conventional passive, semi-active and full-active damper.

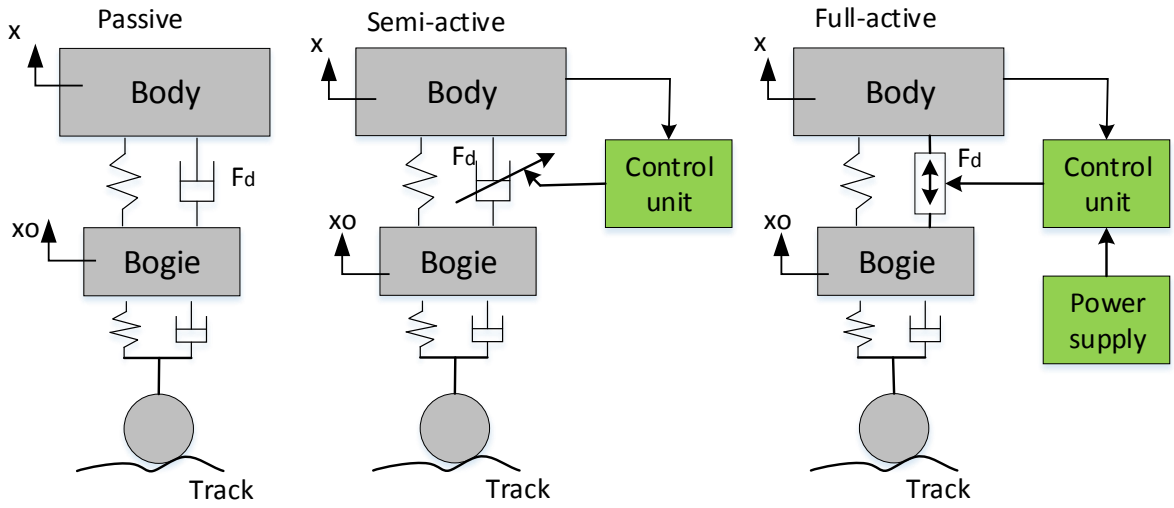

Figure 2.3: Conventional passive, semi-active, and full-active suspension systems[20]

2.3.1 Passive Suspension Systems

Passive suspension systems for railway vehicles using springs and pneumatic or oil dampers have some advantages such as cost-effectiveness and design simplicity. However, the performance due to the wide frequency range of excitations induced by rail track irregularities may be limited, and the parameters of the passive damper are fixed, which means that once the system is designed, the damping cannot be adapted. In addition, a fixed passive damper may become ineffective due to other phenomena such as instability of the vehicle, which is velocity dependent. In fact, when the railway vehicle velocity reaches a critical value, the amplitude of the railway vehicle vibration grows exponentially with time and theoretically reaches infinity in a linear system[21]. Figure 2.4 shows the relationship between damping force (F_d) and relative velocity ($\dot{x}$-$\dot{x}_o$) for a conventional passive damper, where the magnitude and direction of the force exerted depend only on the relative velocity across the damper.

In many applications, the relationship between the damping force and the relative velocity for the conventional passive damper is nonlinear, and the gradient tends to decrease as the relative velocity increases. However, in the passive model considered in this study, the slope of the force-velocity curve is constant.

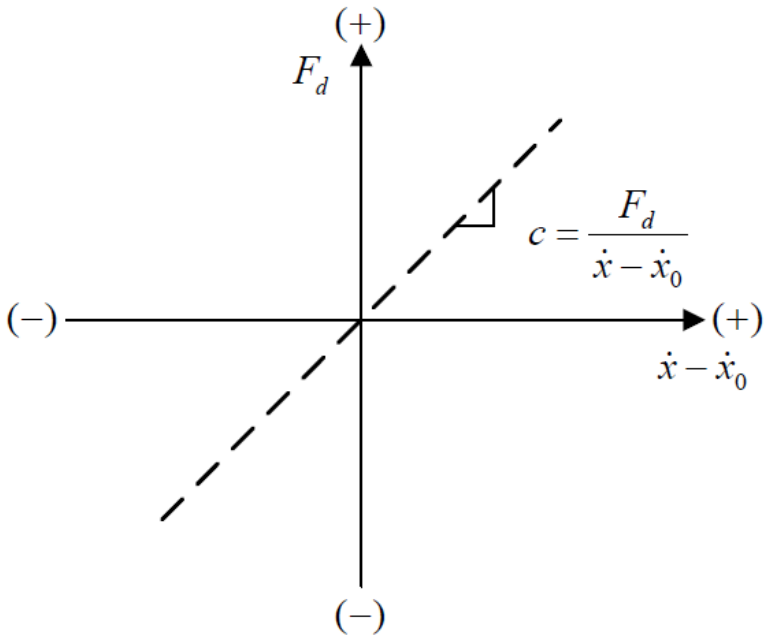

Figure 2.4: Force-velocity diagram for a passive damper[22]

2.3.2 Full-Active Suspension Systems

In general, the principle of an active suspension system is based on the idea of controlling a specific variable system, such as vehicle acceleration, according to the feedback signals, as illustrated in Figure 2.5. In order to incorporate a control loop in the suspension system of railway vehicles, actuators, sensors and controller must be included in the railway vehicle system. Actuators can replace conventional passive dampers, for instance, between the vehicle-body and bogies. They should actively generate the necessary damping force, according to the desired force from the system controller. The desired force is determined based on the vehicle output signals measured by appropriate sensors. The feedback signals, in turn, depend on the generated actuator force managing the mechanical system. Therefore, the control loop is closed [20].

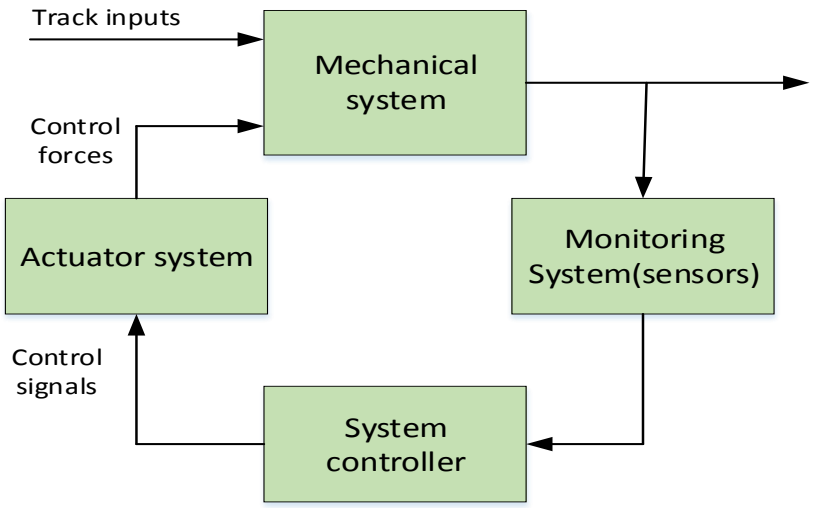

Figure 2.5: Principle of an active suspension system [23]

2.3.3 Dynamic Response of the Actuator for a Full-Active Suspension

The ideal actuator generates precisely the same force as requested over wide range of bandwidth and without time delay. In real applications, this is not possible and designing with active suspension is always a difficult challenge of balance between different parameters, such as cost and actuator performance. In order to implement a full-active suspension system, it is necessary to have an actuator force controller. Figure 2.6 shows the actuator force control, which is a generalised scheme of a force-controlled actuator.

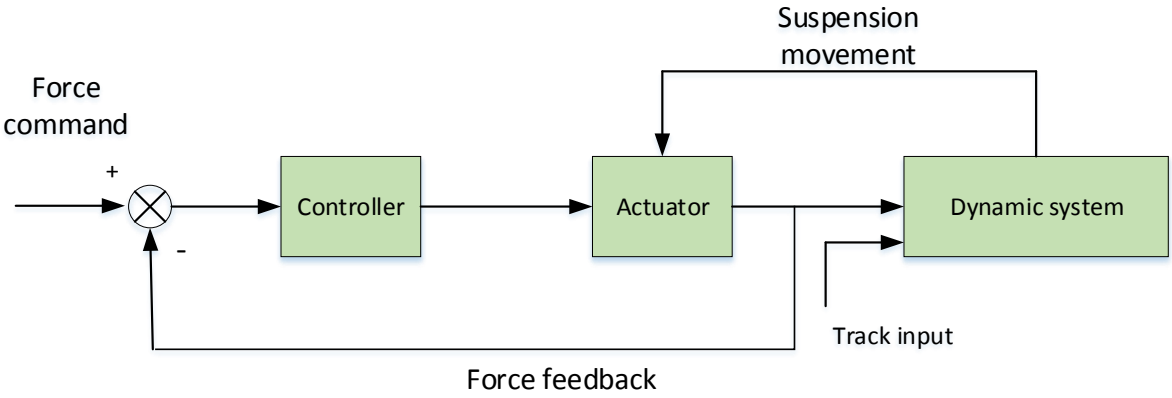

Figure 2.6: Actuator force controller[15]

An active suspension controller generates the command force to the actuator. The track input will impact the dynamic system, which will induce actuator movement. Therefore, the actuator force controller adjusts the control signal to keep the actuator forces as close as possible to the command force[15].

2.3.3.1 Actuator Device

The active suspension system consists of actuators, sensors and a specific control law, which generates the control force demanded for the actuator. The actuator should be able to generate the demanded control force. However, how this is achieved depends on the performance of the actuator. There are various types of actuators that can be used for active vehicle suspension systems, such as electromechanical, hydraulic, electromagnetic[16].

2.3.4 Semi-Active Suspension Systems

Recently, semi-active controlled suspension systems have attracted a great interest by researchers because the semi-active suspension systems only require a low power consumption and can adjust the damping force in real time. Semi-active controlled suspension systems usually use controllable dampers, although the concept is not restricted to the dampers themselves. Semi-active control systems are composed of a system controller and damper controller, as shown in Figure 2.7. The system controller generates the desired damping force according to the feedback signals measured by sensors. The damper controller adjusts the control signal to track the desired damping force.

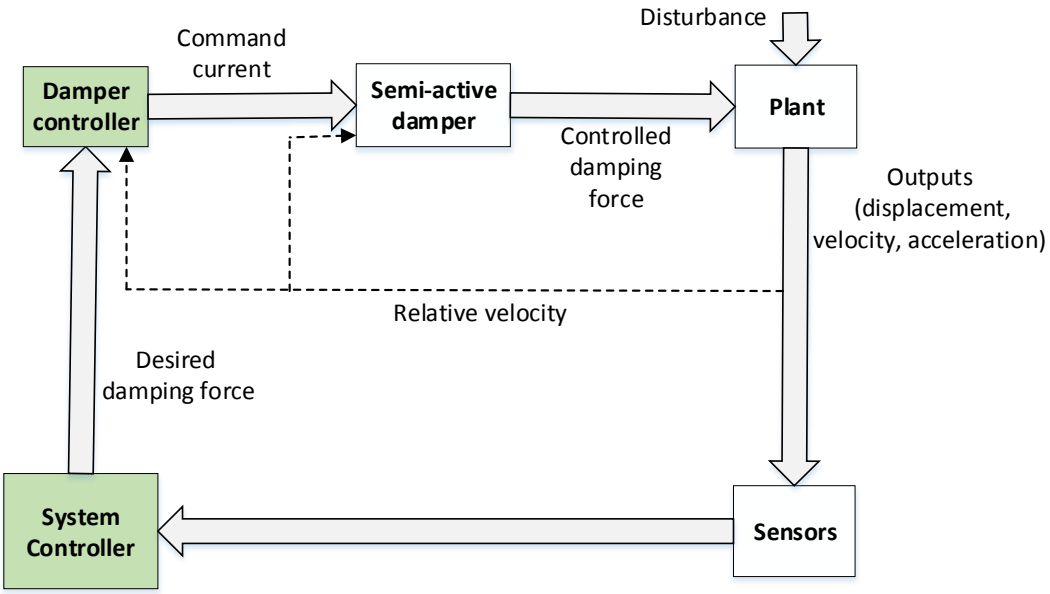

Figure 2.7: Semi-active suspension system

2.3.5 Semi-Active Dampers

Semi-active dampers are passive dampers whose dynamic properties can be varied with time but can only dissipate energy. Although the direction of the damper force in semi-active dampers still depends on the relative velocity of the damper, the magnitude of the damper force is considered to be adjustable.

Semi-active dampers are operated according to semi-active damping control strategies to generate a damping force passively. Semi-active dampers could be of the on-off category or the continuously variable category. Semi-active dampers of the first category are switched, in accordance with a suitable control algorithm, between alternate on and off damping modes, as shown in Figure 2.8(a), which shows the relationship between damping force (F_d) and relative velocity ($\dot{x}$-$\dot{x}_o$) for a semi-active on-off type damper. Continuously variable semi-active dampers are also switched during operation between the on and off modes; however, when continuously variable dampers are in their on-mode, the damping coefficient and corresponding damper force may be changed over a range of magnitudes, as shown in Figure 2.8(b). The damping coefficient of the on-off category is a discontinuous function in the time

domain, as illustrated in Figure 2.9 (a). The damping coefficient of the continuously variable category is a continuous function, as shown in Figure 2.9 (b).

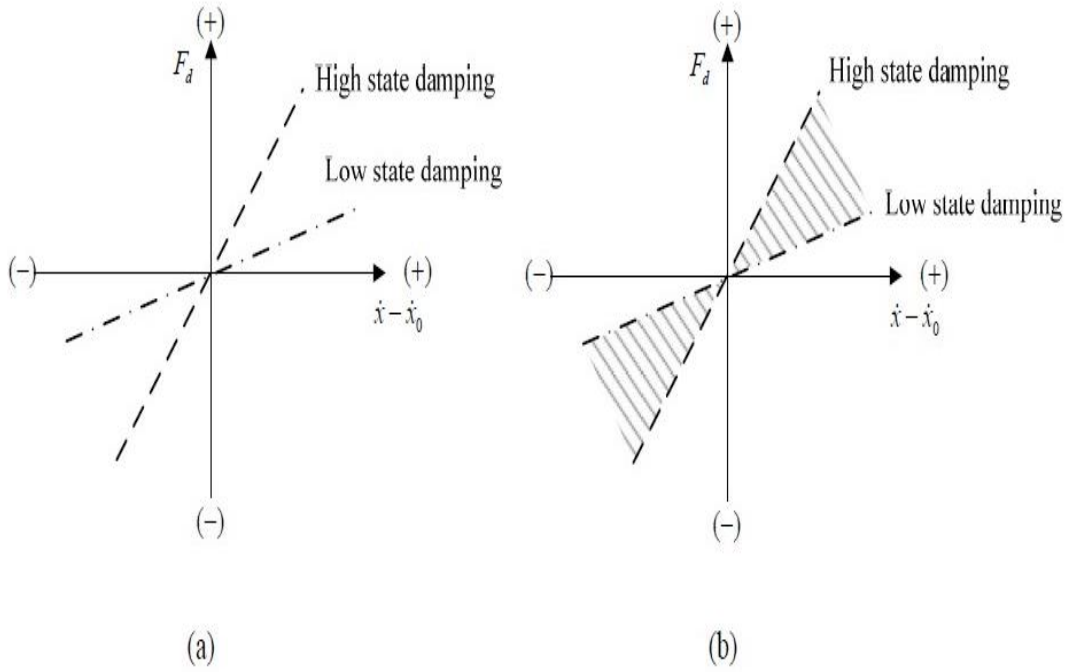

Figure 2.8:Semi-active damper concepts[22] (a) on-off category; (b) continuously variable category

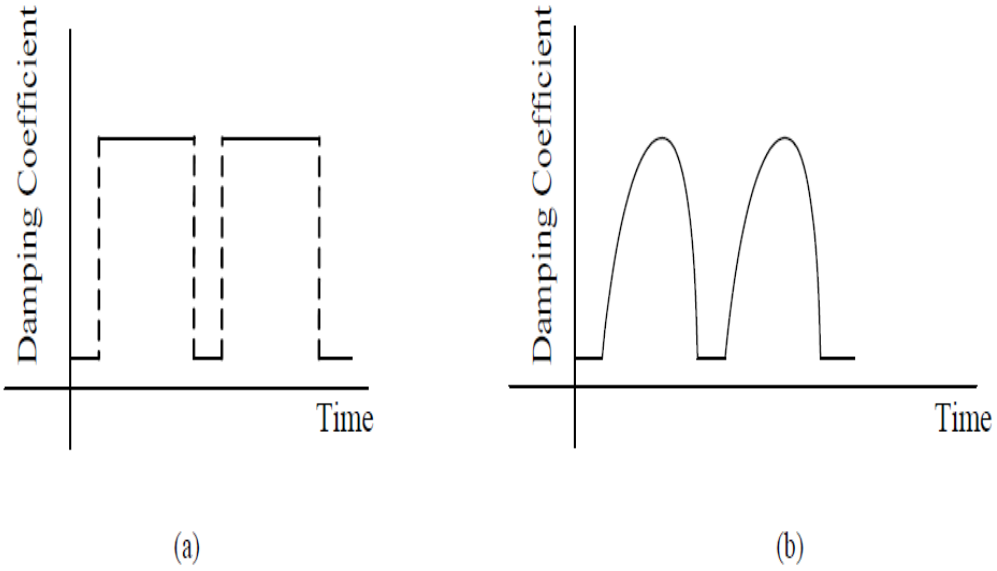

Figure 2.9 :Semi-active damper characteristics in the time domain[22] (a) on-off damper, (b) continuously variable damper

For the purpose of semi-active damping control, various energy-dissipating devices have been used to obtain the desired damping. These devices include hydraulic dampers, Electrorheological (ER) and Magnetorheological (MR) dampers, semi-active friction devices and electromagnetic devices.

In this study, the MR damper used due to the mechanical simplicity, high dynamic range, fast time response, low power consumption, large force capacity, robustness and safe manner operation in case of fail. In addition, the essential characteristic of controllable fluids (MR fluid) of the MR damper is their ability to change from a free-flowing viscous liquid to a semi-solid with a controllable yield strength in milliseconds when exposed to a magnetic field, which changes it is stiffness and damping setting. Therefore, the MR damper has the capability of changing the effective damping force depending on the control current applied to the damper.

2.4 Design Considerations and Requirement

The development of high-velocity railway vehicles has been an interest of many companies because high- velocity railway vehicles have shown to be an economical and efficient transportation means. However, the high velocity of the railway vehicles can induce significant vibrations of a railway vehicle, which cause ride discomfort, wear down wheel and railway profiles, and cost of track maintenance. Another issue is related to the resonance phenomenon where the external disturbance of the vehicle is equal to, or close, to the natural frequency of the whole system, and instability appears at higher velocities as an oscillation in the wheelset and other vehicle components such as the bogie and vehicle body. Therefore, the suspension system of the vehicle has to be modified in order to compensate for the deteriorated dynamic performance. However, the performance improvements possibilities by the mechanism of passive suspension technology have been reached a limit, due to the lack of damping force controllability. Therefore, various active suspension technologies for railway vehicles have

been proposed to overcome the limitations of passive suspension. Active suspension technologies can achieve considerable control performances over the wide bandwidth of the frequency excitations induced by track irregularities. However, full-active actuators consume a considerable amount of power, are more complex, and less reliable than passive systems.

Moreover, the active suspension systems inject mechanical power into the system of the railway vehicle, so the stability of the control system needs to be more inspected. Furthermore, the forces generated by the actuator depending on the performance of the actuator. The ideal actuator generates precisely the same force as demanded over an infinite bandwidth and without time delay. In real applications, this is not applicable, and working with active suspension is usually an issue of trade-offs between different parameters, such as actuator performance and cost[19].

Another issue is related to the multi-objective nature of the design process for any suspension systems(passive or active), as shown in Figure 2.11, which emphasises the difficulty in meeting design parameters that fall within these conflicting constraints. There are varieties of input types and output variables that must be considered, and each output can be affected by different combinations of inputs. The design process will require an optimisation involving conflict constraints. For example, the active secondary suspension design must minimise the accelerations on the vehicle body without exceeding the maximum suspension deflection, whilst the active primary suspension must achieve good curving performance while maintaining acceptable levels of running stability on the straight track. Active control can be used for any or all of the suspension degrees-of-freedom, but, when used in the lateral direction, will necessarily include the yaw mode and in the bounce direction will include the pitching mode[20].

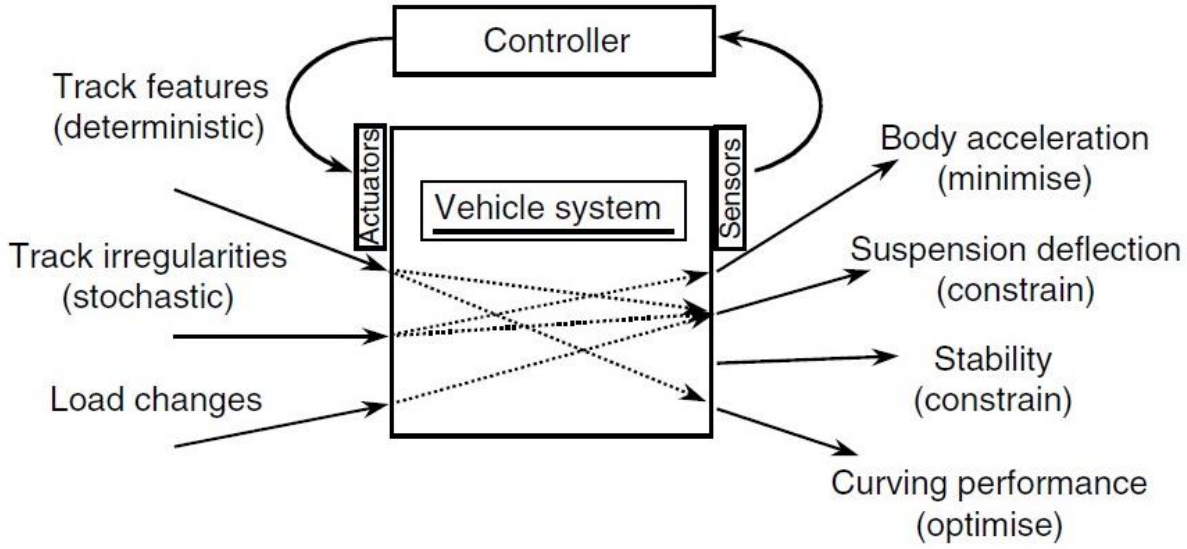

Figure 2.10: Design process [20]

Although full-active suspension systems can provide high control performance over a wide frequency range of vibration, the cost, complexity of this system, and high power requirements of the actuators bring significant obstacles to their commercial adoption. A promising alternative to full-active suspension system is a semi-active suspension.

The advantages of the semi-active approach compared with full active that it is simplicity. They do not require either higher-power actuators or a large power supply. When the control system fails, the semi-active suspension can still work in a passive state. However, the damping force of a semi-active damper remains dependent upon the relative velocity of the damper, which means that larger forces cannot be generated when its relative velocity is low. Another issue is that such systems cannot generate a positive force when the relative velocity reverses because it is only possible to dissipate energy, not inject it. Figure 2.8 illustrates this limitation by showing areas on the force-velocity diagram that are available in a semi-active damper based upon its minimum and maximum levels, whereas the actuator in the full-active suspension system can cover all four quadrants. This limitation restricts the performance of a semi-active suspension to a significant degree.

2.5 Track Inputs

The dynamic behaviour of the railway vehicle is dependent on the wheel-rail interaction. The wheel-rail interaction is affected by both deterministic (low-frequency signals) and random track inputs (high-frequency signals). The deterministic track inputs are things such as curvatures and gradients whilst the random track inputs are due to the track irregularities (in both lateral and vertical directions). The suspension systems of the railway vehicle have to cope with deterministic and random track inputs.

Various studies have been carried out to turn the trade-off between the random and deterministic track input requirements to active suspension. A number of approaches are presented to achieve good curving performance whilst maintaining an adequate level of running straight track; for example, using a linear complementary filter control and non-linear Kalman filter methods [24-26].

However, how the track irregularities influence the wheel-rail interaction is important when studying issues related to ride quality. Track irregularities represent the deviations of the track from its design geometry. The irregularities appear on the track substructure resulting from construction defects or environmental effects. These irregularities are represented by the vertical and lateral displacement of each track.

In the literature review, there are two methods used to represent track irregularities in the computational models for railway vehicle dynamics. The first method considers track irregularities as measured data and is defined as a function of the distance run, which is measured with a railway vehicle that has been specially modified to simulate track defects [1, 27].

The second method considers track irregularities as stochastic inputs and is defined as a function of frequency [28-31]. Many measurements have demonstrated that these track

irregularities represent a stochastic process and they could be described by spectral power density functions [32].

The spatial power spectrum is widely used for this purpose and generally approximated to a fourth-order relationship [33]. The vertical track spectra are approximated as follows:

$$S_t(f_t) = \frac{A_r}{{f_t}^2 + 5.86 f_t^3 + 17.29 f_t^4} \quad \text{---------- (2.1)}$$

Whereas f_t is a spatial frequency in (cycle/m), this can be converted to a temporal frequency using the railway vehicle speed, and A_r is a scalar factor of the track irregularities in (m).

However, for secondary suspension evaluation, the higher-order relationship does not have any significant effect over 14 Hz. Therefore, the random track inputs can be approximated by a simplified power spectrum for the vertical track irregularities, which gives a good representation of the track irregularities in order to study the dynamics of railway vehicles[34].

$$S_t(f_t) = \frac{A_{rv}}{{f_t}^2} \quad \text{---------- (2.2)}$$

Where A_{rv} is the track roughness factor in the vertical direction (2.5 x 10^{-7} m) [26].

For the sake of simplicity, the stochastic track inputs that are used to represent the lateral track irregularities of typical mainlines are generated from a filtered Gaussian white noise function to characterise an approximate spatial spectrum equal to

$$S_t(f_t) = \frac{A_{rl}}{{f_t}^3} \quad \text{---------- (2.3)}$$

Where A_{rl} is the lateral track roughness (0.33 x 10^{-8} m) [35-37], which provides a good representation of the track irregularities in the range 0.1–14 Hz, and the velocity as 83.333 m/s, that is, to represent conditions for railway vehicles travelling at 300 km/h. Time delay-dependent velocities are used to provide the inputs to the other axles of the vehicle.

2.6 Performance Assessment Approach

The performance of suspension systems is influenced by many, often conflicting, factors and attributes. For the secondary suspension, there are two conflicting factors that have that most influence on its performance, namely the suspension deflection and the ride quality. In practice, the possible suspension displacement is limited. Therefore, the control design must improve the ride quality on the vehicle body without exceeding the maximum suspension deflection. Many studies in the literature have shown that a good compromise between ride quality and suspension deflection can be achieved by filtering the absolute velocity to remove the low-frequency variations associated with the deterministic input [24-26].

However, the ride quality analysis is essential to evaluate the performance of secondary suspension systems, which is generally performed by considering the track irregularity inputs.

In general, the ride quality evaluation of choice will depend on the context of its usage. One of the most popular ride quality measures is based on the root mean square (RMS) value of vehicle floor acceleration [38-40]. The International Organisation for Standardization (ISO) has developed standard ISO 2631 to measure the ride quality for the frequency dependence of human sensitivity to vibration and the length of time constituting reasonable human expose [40-42]. Many studies have developed a more comprehensive ride quality evaluation that considers the interdependence of various modes/direction of vibration [40, 43, 44]. E. Foo used frequency-weighted accelerations to evaluate vertical ride quality, which includes frequency weighting before the RMS is calculated to allow for human sensitivity to vibration.

However, for comparative studies in which relative levels of ride quality are being evaluated, the frequency weighting can be neglected[33]. The simple RMS approach of measuring ride quality, which is based on calculating the RMS value of vehicle acceleration levels experienced by the vehicle, is used in this study.

For simplicity, the percentage reduction index of the RMS value of vehicle acceleration is used in this study to evaluate the relative ride quality improvement as follows:

$$PRI = \frac{passive(RMS) - semiactive(\text{RMS})}{passive(RMS)}\ 100\ \% \quad \text{---------- (2.4)}$$

Where PRI is the percentage reduction index of the relative ride quality improvement, $passive(RMS)$ is the RMS acceleration value of passive suspension, and $semiactive(\text{RMS})$ is the RMS acceleration value of semi-active suspension.

CHAPTER THREE

3 LITERATURE REVIEW

3.1 Introduction

Increases in railway vehicle velocity is limited by track geometry, and higher velocities usually generate increased forces and accelerations on the vehicle, which negatively affect ride comfort. Moreover, hunting, which is related to the resonance phenomenon where the external disturbance of the vehicle is equal or close to the natural frequency of the whole system, is an instability which appears at higher velocities as an oscillation in the wheelset and other vehicle components such as the bogie and car body. Hunting in a railway vehicle is undesirable since it can wear down wheel and railway profiles and cause ride discomfort[45]. One possible solution to this is to build new high-quality tracks for high-speed passenger railway vehicles. However, this is a costly solution, and another problem is track maintenance, which is also expensive. Therefore, research is being carried out to implement modifications and different configurations of suspension technologies to balance reasonable cost and acceptable performance. Many survey papers have considered basic concepts and requirements for safety and reliability, and the opportunities available with the development of full-active suspension systems [19, 20, 23, 40, 46]. A great variety of possible approaches to the active suspension issue exist for either improving running stability through controlling the primary suspension or improving ride quality through controlling the secondary suspension. This chapter provides an overview of suspension technologies and the semi-active control algorithms and devices proposed in the literature.

3.2 Full-active Suspension Systems

In the last decade, full-active controllable suspension systems have been proposed by using computer-based control devices and controllable actuators [16]. Actuators can replace conventional passive dampers and should actively generate a required control force according to the force requested by the controller. Full-active technology represents one possible solution to improved ride quality through controlling the secondary suspension and improving running stability and wheelset guidance through controlling the primary suspension.

3.2.1 Configurations of Suspension Technologies

The trade-off between curving and stability is a particularly critical problem, which where the most considerable benefits are expected by the implementation of active control solutions. Many studies have suggested control strategies to solve the problematic design of trade-off between the stability and curving performance of railway vehicles[18, 46]. Secondary yaw control strategy has been used for the improvement of railway vehicle stability and curving performance. This configuration is based on the application of a yaw force at the secondary suspension which is used to both raise the critical speed of the vehicle by introducing additional damping, and to improve curving performance by adding a steering torque on the bogie frame [47, 48]. Shen and Goodall have proposed an active yaw relaxation concept for a two-axle bogie for improved bogie performance, which is based on applying control forces to a solid axle wheelset, either in the longitudinal direction or in the lateral direction, to provide a steering and stability torque[49]. Another approach to improving steering performance is to use directly steered wheels in conjunction with the application of independently rotating wheels. According to this concept, the active control strategy is accomplished by guiding independent wheel pairs [50].

Many different configurations have been proposed for suspension technologies to improve the ride comfort without exceeding the maximum suspension deflection, which with a passive

suspension is difficult [1, 16, 23, 51]. Active control can be applied to any of the suspension system's degrees of freedom, and a number of actuator configurations are possible. The secondary suspension is normally controlled in the lateral direction, including the yaw mode, or in the vertical direction, including the pitch mode. Goodall et al. [29] have investigated a comprehensive comparison between full-active and semi-active suspensions based on hydraulic actuation technology in order to improve the vertical ride quality of railway vehicles. In another study, the performance of an electromechanical actuator in an active railway vertical secondary suspension for ride quality improvement was also investigated [52]. In addition, active control can be applied in the roll direction (tilting control) to improve ride quality, in which vehicle body is tilting inwards through curves where high track plane acceleration is applied to allow higher speeds without negatively impacting the ride quality [53, 54].

Another issue is related to bump stop contact during curve passing or due to lateral displacement having a negative impact on ride quality. Mellado et al. [55] proposed a solution based on lateral pneumatic actuators placed between the bogie and car body and connected to the vertical secondary suspension air springs in order to keep lateral displacement of the vehicle within limits. Orvnas et al. [56] investigated the benefits of using a Hold-Off-Device (HOD) function in the lateral secondary suspension. Alfi et al. [57]developed the active air spring based on suitable open and closed loop control strategy to improve ride quality and safety against crosswinds.

In addition, single suspension stage configurations have also been investigated to improve ride quality on the active suspension of the railway. Goodall et al. [58] presented the potential improvements in ride quality using an electromechanical actuator for a two-axle railway vehicle with a single stage of vertical suspension.

Another configuration to improve the ride comfort is an active vibration reduction system of the flexible vehicle body itself [59]. Schandl et al. [60] have presented an active vibration reduction system using piezo-stack actuators to improve the ride quality of the lightweight railway vehicle. It was concluded that a reasonable reduction in vibrations could be achieved using a small number of sensors and actuators. Another study analysed the influences of car body vertical flexibility on railway vehicle ride quality. Here, a vertical model of railway passenger vehicles, which includes the effects of car body flexibility and all rigid vertical modes, has determined lower limits for the bending frequency to avoid deterioration of vehicle ride quality [61].

In contrast, the active suspension system has been shown to allow higher isolation performance than a passive system. However, an actuator requires an external power supply in the active control system. This is one of the drawbacks of active suspension systems. In order to solve the problem, many researchers have presented self-powered active suspension methods. Suda et al. [62] proposed a method of active vibration control system using regenerated vibration energy. Another study on the self-powered active vibration control was proposed by Suda et al. [63]. Singal et al. [64] explored the idea of a zero-energy active suspension using a simulation study of a novel self-powered active suspension system for automobiles. In recent studies, a new design methodology was investigated in terms of energy consumption and regeneration in the lateral secondary active suspension. The study concluded that the performance gain in ride quality from self-powered suspension is dependent upon the internal power losses of the actuator and the efficiency of the energy supply/storage [65, 66].

3.2.2 Control strategies

In the existing literature, a large number of control strategies have been proposed for developing basic configurations and technology options for active suspension in rail vehicles depending on the design objectives.

Selamat et al. [67] presented the design of an active suspension control of a two-axle railway vehicle using an optimised linear quadratic regulator (LQR). The control objective was to minimise the yaw angle and lateral displacement of the wheelsets when the vehicle travels on straight and curved tracks with lateral irregularities, where the active yaw damping replaced the longitudinal springs to provide yaw torque.

Li and Hong[24] investigated the trade-off between the maximum deflection of the damper and acceptable levels of ride quality. Different control methods have been applied to the Skyhook active suspension system in order to optimise the trade-off between the random and deterministic track input requirements. Results showed that improvement of around 20% in ride comfort could be achieved with a linear complementary filter and about 50% by using nonlinear Kalman filter strategies.

Moreover, the dynamic movements of railway vehicles are highly interactive, and the DOF order is usually high. Therefore, some form of dynamic simplification can be applied. Mei et al. [68] performed a modal decomposition using the modal controller approach to active steering of the railway vehicle. The development of a modal control approach was applied to a two-axle railway vehicle to decouple body lateral and yaw motions, which enables the development of independent controllers for the two movements. Results showed a significant improvement in vehicle performance on curves and improved the ride quality by around 25% compared to a passive vehicle on a straight track.

Furthermore, the interaction issue between the vehicle body roll and the lateral dynamics substantially influence the tilting system in a high-velocity railway vehicle, which results in a negative impact on ride quality. Therefore, integrating an active secondary suspension system into the tilting control system is one of the solutions to improving the design trade-off between straight truck ride quality and curving performance. In the study, Zhou et al. [69] presented a novel active suspension integration strategy that combines tilting control with active lateral

secondary suspension, which can enhance tilt control system performance and ride quality. Another study by Zhou et al. [70] investigated H∞ decentralised control compared with a traditional decentralised control for the integrated tilt control with active lateral secondary suspension in high-speed railway vehicles. H∞ decentralised control was used to overcome the control loop interaction in the classical decentralised control and improve the performance of the local integrated suspension control. Zhou et al. [71] applied advanced system state estimation technology, which used the estimated vehicle body lateral acceleration and true cant deficiency to enhance the system performance further.

Further, the hunting phenomenon is a very common instability exhibited by railway vehicles. It is a self-excited lateral oscillation that is produced by the forward speed of the vehicle and wheel-rail interactive force, which results from the conicity of the wheel – railway contours and friction – and the creep characteristic of the wheel – railway geometry.

A theoretical and an experimental study of stabilisation control methods for the hunting problem in a simple wheelset model was proposed by Yabuno et al. [72]. It was concluded that applying a lateral force proportional to yawing motion can increase the critical speed of the railway vehicle. In another study, a controlled electro-mechanical actuator was designed to substitute for a traditional yaw damper that was used to apply a longitudinal force between the vehicle and the bogie. It was concluded that applying longitudinal forces opposite to yawing velocity can maximise the amount of energy dissipation. Mohamadi et al. [73] designed an active control for lateral vibration for a bogie using a variable structure model reference adaptive control. Results showed that using active suspension can be achieved at higher velocities. Pearson et al. [74] presented a comparison of control algorithms for an actively stabilised wheelset on a high-speed railway vehicle; this was applied to yaw torque to provide a bogie which is stable at high speed without the need for a heavy secondary yaw damper.

Model predictive control based on a mixed H2/H∞ control method has been compared with a classical skyhook controller. This control approach achieved good ride quality while keeping the suspension deflection to its minimum limits, and it is concluded that the proposed controller has the advantage of being multi-objective [75].

3.3 Semi-Active Suspension Systems

Among the many different types of controlled suspensions, semi-active suspension systems have received considerable attention since they achieve the best compromise between cost and performance[15, 40]. The concept of the semi-active suspension system is to apply a controllable device which does not need significant external power to work. The semi-active controllable device is able to respond to feedback control signal from a semi-active control system to control undesired vibrations. The performance of the semi-active suspension system is highly dependent on the selection of an appropriate control strategy and characteristics of the semi-active damper, such as the lower and the upper limits of the damping setting and how fast it can be switched, are particularly important [76].

3.3.1 Control Strategies

During the past decade, various semi-active control strategies have been proposed for improving the performance of semi-active suspension systems for railway vehicles, automotive and vibration control applications [77, 78]. The initial semi-active suspension system was proposed by Karnopp et al. [7]using the skyhook control strategy. The skyhook strategy improves the ride quality with a virtual damping term proportional to the sprung mass velocity by setting an imaginary damper between the vehicle body and the imaginary sky. The skyhook strategy is the simplest control, but very effective in a semi-active control system.

Recently, the on-off skyhook control strategy (which is a kind of clipped-optimal control) have been studied for railway vehicles and automotive applications. Stribersky et al. [79] have

been presented the development of semi-active damping based on the hydraulic damper system used on railway vehicles. By applying the skyhook control strategy, an improvement of up to 15% in ride quality, as measured by the RMS acceleration, can be achieved.

Gao et al.[80] used an on-off skyhook control strategy in order to study the control of the vibration of suspension system based on an MR damper for a railway vehicle suspension system tested over random excitations.

In studies performed by Cristiano et al. [81], a skyhook (SH) control, acceleration drive damping (ADD) control, Mixed SH-ADD control , with the electro-hydraulic damper on lateral secondary suspension, were all investigated. Results illustrated that the Mixed SH-ADD control has the effectiveness of semi-active control with respect to passive suspension. The Mixed SH-ADD control provides up to a 34% reduction of the acceleration experienced by the vehicle body. Khisbullah et al. [82]investigated the performance of semi-active control of the lateral suspension system using a body based on skyhook and a bogie-based skyhook for the purpose of attenuating the effects of track irregularities on body lateral displacement.

In addition to the above control strategies, there are many other control strategies developed for improving the ride quality, such as that of Lu-Hang Zong et al. [28], who investigated semi-active H∞ control with an MR damper for railway vehicle suspension systems to improve the lateral ride quality. They concluded that the MR damper-based semi-active suspension system used for the railway vehicles attenuate the lateral, yaw, and roll accelerations of the car body significantly (about 30%).

Liao and Wang [83]applied Linear-quadratic-Gaussian (LQG) semi-active control integrated with an MR damper to improve ride quality in vertical secondary suspension. Results have proven that applying LQG semi-active control can achieve an improvement of up to 29% in ride quality.

The semi-active adaptive control based air spring suspension that works at both low and high frequencies was proposed by Liang et al.[3]. It adopted an adaptive feedforward control law in operation, and it was concluded that the semi-active air spring suspension has the ability to isolate the vibration and noise across a wide range of frequencies.

Bideleh et al.presented different on-off switching control strategies (various combinations of displacement and velocity) based on an MR damper and applied this to the primary suspension of railway vehicle in order to investigate the effects on wear.

Liao et al. [76] presented a study demonstrating the feasibility of improving the ride quality of railway vehicles with semi-active vertical secondary suspension systems using MR dampers.

Lau et al. [84] proposed a novel MR damper for a semi-active railway vehicle suspension systems. It was developed through the design, fabrication, and tests to ensure the suitability for the railway vehicle suspension. A scaled half railway vehicle model was set up that included a modified Bouc-Wen model of the MR damper in a suspension system that used a semi-active control strategy to improve ride quality [80].

Another study by D. H. Wang et al. [85] used a 17–degrees of freedom full-scale model of a railway vehicle that adopted a semi-active MR damper in its secondary suspension, which was used to control lateral and yaw vibration.

Allotta, Pugi[86] investigated different control strategies for semi-active suspension using an MR damper for the secondary suspension system, demonstrating that the skyhook approach was suitable for railway vehicle using MR damper suspension.

In a study by Sun, Deng [21], a 15- DOF high-speed railway vehicle was developed, and the damping ratio used to investigate the sensitivity of the critical speed with respect to the suspension parameters. It was concluded that the secondary lateral damping rate is the most sensitive parameter impacting the critical speed. It was verified that semi-active secondary

lateral suspension installed with the MR damper had the ability to improve the railway vehicle stability and critical speed.

In recent years, fuzzy logic control and neural network strategies have been introduced into semi-active control suspension systems. SH Ha et al. [87] evaluated the control performance of a railway vehicle MR suspension using fuzzy sky-ground hook control. This controller takes into account both the vibration control of the car body and increases the stability of bogie by adopting a weighting parameter between two performance requirements. Another study performed by Zhiqiang et al. [4] used a PID controller based on BP neural network with a semi-active suspension of a quarter model of a railway vehicle to improve lateral ride comfort.

Another class of semi-active devices used controllable fluids. The essential characteristic of controllable fluids is their ability to reversibly change from a free-flowing viscous fluid to a semi-solid with a controllable yield strength in milliseconds when exposed to an electric or magnetic field. Therefore, semi-active suspension integrated with an MR damper for the railway vehicle was proposed to overcome the drawbacks of other systems. Compared with the semi-active dampers mentioned in the previous paragraph, an advantage of the controllable fluid devices is that they contain no moving parts other than the pistons of the dampers, which makes them simple and potentially highly reliable. Semi-active control integrated with an MR damper can achieve high performance with low power requirements while the system is fail-safe and stable.

Liao and Wang [83] applied semi-active control integrated with an MR damper in the vertical secondary suspension to improve ride quality. They used semi-active control via an MR damper to attenuate the lateral and yaw vibration of the railway vehicle.

Lau and Liao [84] proposed a novel MR damper for a semi-active railway vehicle suspension system. It was developed through the design, fabrication, and tests to ensure its suitability for railway vehicle suspension.

A scaled half railway vehicle model was set up including the modified Bouc-Wen model of the MR damper in a suspension system that applied a semi-active control strategy to improve ride quality [80].

Allotta, Pugi [86] investigated skyhook damping and slide mode strategies for semi-active with MR damper for the secondary suspension system. Results have proven that skyhook approach to be suitable for MR damper suspension systems.

In general, the performance of a semi-active control system is highly dependent on the control strategy, which is the core of the system controller. Various control strategies, such as classical control strategies include a skyhook controller, advanced model control strategies include an adaptive controller and hybrid controller strategies combining more than two different control strategies such as the adaptive fuzzy sliding mode controller have been proposed to improve the performance of semi-active vibration control system. A wide range of semi-active control strategies have been experimentally tested for the semi-active suspension to improve the ride quality of railway vehicles. However, the findings published so far indicate that there appears to be a ceiling on performance improvements with the control strategies that have been proposed, which is about the half of what could be achieved with the full active control. This is mostly because the main constraint for the semi-active suspensions is that the variable dampers are only possible to dissipate energy and they cannot develop a positive force when the damper velocity reverses because it would require a negative damper setting. In this case, the semi-active controller will simply employ a minimum damping setting hence a semi-active damper cannot create the necessary forces in the same way as the full active control in such conditions.

Based on the analysis of limitations of different contributions in the area of full active and semi-active damping control, a new control algorithm is proposed in this study. The motivation of this control strategy is to provide a better comprehensive performance.

The proposed design of the control strategy is focused on minimising the use of the minimum damper setting by using gain-scheduling control.

3.4 Summary

In this chapter, an overview of different contributions in the area of full active and semi-active damping control are presented. The advantages and limitations are briefly discussed, mainly focusing on the secondary suspension to improve ride quality, and the motivation behind semi-active damping control for vibration isolation is also presented in this chapter. From the literature review, it can be concluded that:

- The full-active control suspension system has been used to obtain levels of dynamic performance that are not possible with a passive suspension system.
- Many practical issues have to be considered in the development of active suspension: controller developed must be robust against parameters variation, some feedback signals are costly and difficult to measure such as relative velocity. Therefore one must use alternative methods that are also cost-effective.
- The dynamic models of railway vehicles are highly interactive, and the DOF order is usually high therefore some form of dynamic simplification should be applied.
- The trade-off between curving and stability is a particularly critical issue, and where most of the considerable benefits from the implementation of semi-active solutions are expected to arise.
- There is a trade-off between the maximum deflection of the suspension and an acceptable level of ride quality.

- In a high-speed railway vehicle, the behaviour of the lateral secondary suspension is more important than in a conventional railway vehicle as this has a significant effect on both comfort and stability.
- In order to improve the ride quality of railway vehicles, there are four parameters that must be acknowledged, which are sprung mass acceleration, sprung mass displacement, unsprung displacement and suspension deflection.
- In most numerical studies, the off-mode damping setting of the semi-active damper is assumed zero. However, the actual damper setting is constrained to be between the minimum and maximum levels of damper setting. This limitation restricts the performance of a semi-active suspension.
- The findings published in the literature indicate that there appears to be a ceiling on performance improvements with the control strategies that have been proposed, which is about the half of what could be achieved with the full active control.
- The challenge to researchers and suspension system designers is to design both an effective and cost reasonable strategy. However, if a control strategy so designed can provide excellent performance at acceptable costs, there is significant potential for future implementation.

CHAPTER FOUR

4 MODELLING AND CONTROL OF THE RAILWAY VEHICLE

4.1 Introduction

The main aim of the proposal for semi-active suspension system on railway vehicles is to improve the ride quality through controlling the secondary suspension. A full-scale railway vehicle with four solid axle wheelsets, two bogies, and primary and secondary suspension is taken as the benchmark model for assessment and comparison of the different control strategies considered in this research. For the performance comparison, three suspension configurations are selected: a full-active suspension system, a conventional semi-active suspension based on skyhook damping control (conventional controller) integrated with MR dampers, and a vehicle with passive suspensions; the latter two represent the benchmark and reference cases, respectively, for the assessment of the proposed design, which is presented in the next chapter.

The outline of this chapter is as follows: firstly, analytical models of railway vehicles will be discussed. Then, both the vertical and lateral dynamic models of railway vehicles will be presented as the benchmark model. The full-active suspension based on the skyhook control strategy will then be designed and integrated with the electromechanical actuator. Finally, the conventional semi-active suspension system combined with MR damper will be adapted to a dynamic vehicle simulator as a benchmark of the control of vibration over track irregularities.

4.2 Analytical Model

The railway vehicle is a dynamically complex multi-body system, where each body within the system has six dynamic degrees of freedom corresponding to three displacements (vertical, lateral and longitudinal) and three rotations (pitch, yaw and roll). In addition, wheel-rail contact

presents a nonlinear dynamic/kinematic problem, adding extra complexity to the already complex system.

In order to apply control over complex systems such as these, it is necessary to recognise the difference between the design model and the simulation model. The design model is a simplified version than the simulation model, and the suspension can be considered to be mainly linear components and used for the design of the control strategy and algorithm. However, the simulation model is a more complicated version used to test the full system performance [36].

In the existing literature, some researchers selected the degree of the dynamic model for railway vehicle depending on the objectives of the control. For example, to study the vertical response, it would be appropriate to include the bounce, pitch and sometimes the roll degrees of freedom of the components, whereas for the lateral response, the lateral, yaw and sometimes roll degrees of freedom are sufficient. Karim [88] used a mathematical dynamic model of railway vehicle with 12 degrees of freedom (DOFs) in the equations of motion to study the hunting phenomenon, whose dynamic model consists of a conventional truck with two single wheelsets in which are equipped with lateral, longitudinal and vertical linear stiffness and damping in the primary and secondary suspensions. Sun[21] adopted a dynamic model of a railway truck with 15 DOFs to investigate the influence of different suspension parameters on the sensitivity of the critical velocity and to investigate the MR damper effects on the railway vehicle's stability and critical velocity. Liao[89] present a dynamic model of railway with 17 DOFs to study semi-active suspension systems using magnetorheological (MR) fluid dampers for improving the ride quality of railway vehicles. Hudha et al. [90]studied the performance of semi-active control of lateral suspension system on 17 DOFs railway vehicle. Another study by D. H. Wang et al. [85], a 17 degree of freedom model of a full-scale railway vehicle was

adopted with a semi-active MR damper in secondary suspension, it is used to investigate the control of lateral and yaw vibration.

Hisbullah et al. [82]used 17 DOFs railway vehicle dynamics model to investigates the performance of semi-active control of lateral suspension system based skyhook control for the purpose of attenuating the effects of track irregularities.

However, for studying some objectives is not necessary to consider all the DOFs, as this will make any mathematical processing more complicated. Furthermore, many studies used the dynamic model of the railway with a small number of DOFs. For instance, Scheffel [91] presented a dynamic model of railway with 8 DOFs to develop self-steering bogies. SH et al. [92] established 9 DOFs for railway vehicles featuring MR dampers to investigate the fuzzy sky-ground hook controller, which includes car body, bogie, and the wheel-set data loaded from the values measured for a railway vehicle. However, railway vehicle dynamic models with fewer DOFs cannot accurately reflect the real-world dynamic performance of such vehicles.

In this study, two case studies (the vertical and the lateral dynamics model of conventional railway vehicle) are used in the simulation for the assessment of the proposed semi-active control because it can adequately characterise the main dynamic performance and contains detailed descriptions of suspension components such as vehicle body, bogie, and wheelsets. Firstly, the vertical dynamics of the railway vehicle is considered in this study, where the vehicle being considered is only the vertical and pitch movement. Secondly, the lateral dynamics of the railway vehicle is considered in this study, where the vehicle being considered is only the lateral and yaw movement. The numerical simulation of the vehicle suspension system under different track irregularities are carried out in Matlab/Simulink for a simulation time of 10 seconds. Three performance criteria are considered in this study; they are

acceleration at the centre of the vehicle, accelerations at front and rear of the vehicle, in addition to the maximum deflation of the suspensions.

4.3 Vertical Dynamic Model

In this section, the vehicle is only considered in terms of the bounce and pitch movements, assuming rigid body motion for the vehicle, whereas track characteristics have been considered as disturbance inputs of the system. To evaluate the performance of the proposed control strategy, three states of the art suspension configurations are chosen for comparison: a vehicle with passive suspensions, a vehicle with full-active suspension, and a vehicle with the semi-active suspension system.

The vehicle with passive suspensions, which consists of spring and damper that means the damping rate is fixed, is used as the benchmark and are used as a reference case for assessment of the proposed design, as shown in Figure 4.1.

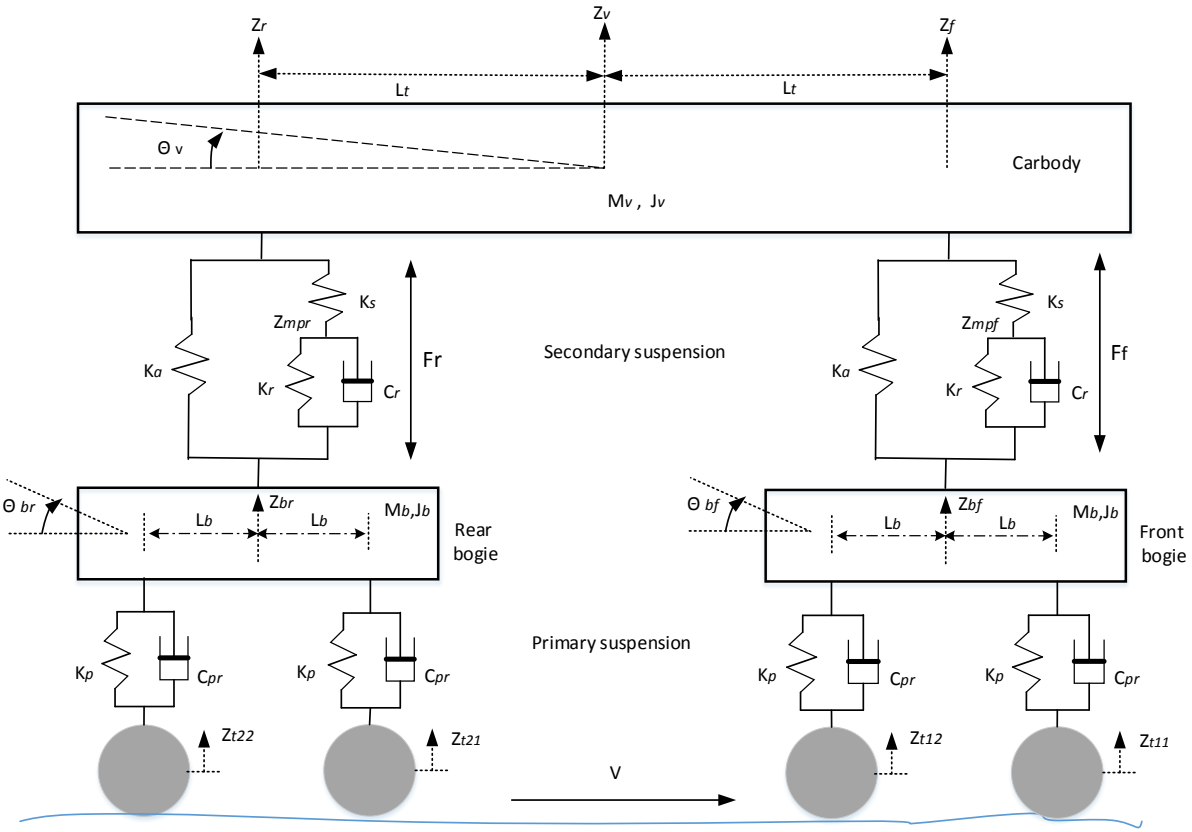

Figure 4.1: Schematic representation of the airspring in vertical secondary suspension of the railway vehicle

The governing equations of motion for the railway vehicle are listed below:

The equation of vehicle motion into the vertical direction is:

$$\ddot{z}_v = \frac{1}{m_v}\left[-k_a(z_f - z_{bf}) - k_s(z_f - z_{mpf}) - k_a(z_r - z_{br}) - k_s(z_r - z_{mpr})\right] \ldots\ldots (4.1)$$

The equation of vehicle motion for pitch is:

$$\ddot{\theta}_v = \frac{1}{J_v}\left[-k_a l_t(z_f - z_{bf}) - k_s l_t(z_f - z_{mpf}) + k_a l_t(z_r - z_{br}) + k_s l_t(z_r - z_{mpr})\right] \ldots\ldots (4.2)$$

From Figure 4.1, the displacements at the front and rear secondary suspension are:

$$z_f = z_v + l_t \,.\sin(\theta_v)$$

$$z_r = z_v - l_t \,.\sin(\theta_v)$$

For simplicity, assuming $\sin(\theta_v)$ approximately equal to θ_v because of the pitch angle (θ_v) is small angle. Under these assumptions, the displacements at the front and rear secondary suspension are given by Equations below:

$$z_f \cong z_v + l_t \,.\, \theta_v$$

$$z_r \cong z_v - l_t \,.\, \theta_v$$

The equations for the bogies can be formulated in a similar way, and similarly for the rear bogie. For the front bogie:

$$\ddot{z}_{bf} = \frac{1}{m_b}\left[k_a\left(z_f - z_{bf}\right) + k_r\left(z_{mpf} - z_{bf}\right) + c_r\left(\dot{z_{mpf}} - \dot{z_{bf}}\right) - c_{pr}\left(\dot{z_{bf1}} - \dot{z_{t11}}\right) - k_p\left(z_{bf1} - z_{t11}\right) - c_{pr}\left(\dot{z_{bf2}} - \dot{z_{t12}}\right) - k_p\left(z_{bf2} - z_{t12}\right)\right] \quad (4.3)$$

$$\ddot{\theta}_{bf} = \frac{1}{J_b}\left[-c_{pr}l_b\left(\dot{z_{bf1}} - \dot{z_{t11}}\right) - k_p l_b\left(z_{bf1} - z_{t11}\right) + c_{pr}l_b\left(\dot{z_{bf2}} - \dot{z_{t12}}\right) + k_p l_b\left(z_{bf2} - z_{t12}\right)\right] \quad (4.4)$$

Whereas the displacements at the front and rear of front bogie are:

$$z_{bf1} \cong z_{bf} + l_b \,.\, \theta_{bf}$$

$$z_{bf2} \cong z_{bf} - l_b \,.\, \theta_{bf}$$

For the rear bogie:

$$\ddot{z}_{br} = \frac{1}{m_b}\left[k_a(z_r - z_{br}) + k_r\left(z_{mpr} - z_{br}\right) + c_r\left(\dot{z_{mpr}} - \dot{z_{br}}\right) - c_{pr}(\dot{z_{br1}} - \dot{z_{t21}}) - k_p(z_{br1} - z_{t21}) - c_{pr}(\dot{z_{br2}} - \dot{z_{t22}}) - k_p(z_{br2} - z_{t22})\right] \quad (4.5)$$

$$\ddot{\theta}_{br} = \frac{1}{J_b}\left[-c_{pr}l_b(\dot{z_{br1}} - \dot{z_{t21}}) - k_p l_b(z_{br1} - z_{t21}) + c_{pr}l_b(\dot{z_{br2}} - \dot{z_{t22}}) + k_p l_b(z_{br2} - z_{t22})\right] \quad (4.6)$$

Whereas the displacements at the front and rear of rear bogie are:

$$z_{br1} \cong z_{br} + l_b \,.\, \theta_{br}$$

$z_{br2} \cong z_{br} - l_b \,.\, \theta_{br}$

The internal dynamics of the front air spring are shown in equation 4.7. The change of area stiffness (k_a), which is usually small, has been assumed to be zero.

$$\ddot{z}_{mpf} = \frac{1}{m_{mpf}}\left[k_s\left(z_f - z_{mpf}\right) - c_r\left(\dot{z_{mpf}} - \dot{z_{bf}}\right) - k_r\left(z_{mpf} - z_{bf}\right)\right] \quad \ldots\ldots (4.7)$$

Similarly, the internal dynamics of the rear air spring are shown in equation 4.8.

$$\ddot{z}_{mpr} = \frac{1}{m_{mpr}}\left[k_s\left(z_r - z_{mpr}\right) - c_r\left(\dot{z_{mpr}} - \dot{z_{br}}\right) - k_r\left(z_{mpr} - z_{br}\right)\right] \quad \ldots\ldots (4.8)$$

Equation (4.1- 4.8) describes the system shown in Figure 4.1, and parameters are defined in Table 4.1[34]. In these equations, $z_{t11,}z_{t12}$, z_{t21}, and z_{t22} are the vertical movements of leading and trailing wheelsets, which are also the track inputs to the system.

Table 4.1: Vehicle parameters of the vertical model

Symbols	Description	Symbols	Description
m_v	Mass of the vehicle (38000kg)	k_{rz}	Secondary reservoir stiffness per bogie (508 kNm^{-1})
J_v	Body pitch inertia (2310000 kgm^2)	k_S	Secondary damping stiffness per bogie (1.116 MNm^{-1})
m_b	Mass of the bogie Frame (2500kg)	c_{rz}	Secondary passive damping per bogie (50000 Nsm^{-1})
i_b	Bogie frame pitch inertia (2000 kgm^2)	k_a	Airspring change of area stiffness (0 Nm^{-1})
m_{mp}	Air spring mass (5 Kg)	k_P	Primary spring stiffness per axle (4.935 MNm^{-1})
l_t	The semi-longitudinal spacing of the secondary suspension (9.5 m)	c_{Pr}	Primary passive damping per axle (50.74 kNsm^{-1})
l_b	The semi-longitudinal spacing of the wheelsets (1.25 m)		

For the simulation of the full-active suspension in the comparative assessment, the damping force of the actuator replaces the passive damper forces in the model, as shown in Figure 4.2.

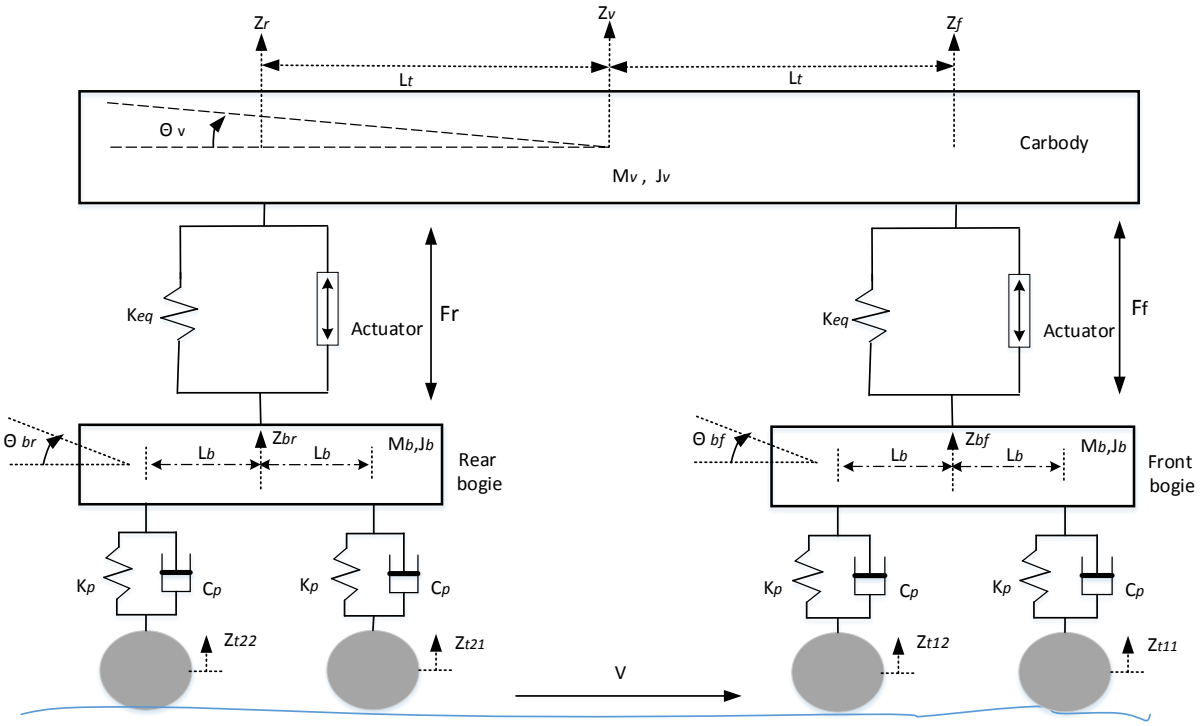

Figure 4.2: Schematic representation of the actuator in vertical secondary suspension of the railway vehicle

Equations (4.9 - 4.14) describe the system representation of the actuator in vertical secondary suspension of the railway vehicle, as listed below:

The equation of vehicle motion into the vertical direction is:

$$\ddot{z}_v = \frac{1}{m_v}\left[-k_{eq}(z_f - z_{bf}) - f_{act.f} - k_{eq}(z_r - z_{br}) - f_{act.r}\right] \quad \text{(4.9)}$$

The equation of vehicle motion for pitch is:

$$\ddot{\theta}_v = \frac{1}{J_v}\left[-k_{eq}l_t(z_f - z_{bf}) - l_t f_{act.f} + k_{eq}l_t(z_r - z_{br}) + l_t f_{act.r}\right] \quad \text{(4.10)}$$

The equations for the bogies can be formulated in a similar way, and similarly for the rear bogie. The equation of front bogie motion for vertical direction is:

$$\ddot{z}_{bf} = \frac{1}{m_b}\left[k_{eq}\left(z_f - z_{bf}\right) + f_{act.f} - c_{pr}\left(\dot{z_{bf1}} - \dot{z_{t11}}\right) - k_p\left(z_{bf1} - z_{t11}\right) - c_{pr}\left(\dot{z_{bf2}} - \dot{z_{t12}}\right) - k_p\left(z_{bf2} - z_{t12}\right)\right] \quad (4.11)$$

The equation of front bogie motion for pitch direction is:

$$\ddot{\theta}_{bf} = \frac{1}{J_b}\left[-c_{pr}l_b\left(\dot{z_{bf1}} - \dot{z_{t11}}\right) - k_p l_b\left(z_{bf1} - z_{t11}\right) + c_{pr}l_b\left(\dot{z_{bf2}} - \dot{z_{t12}}\right) + k_p l_b\left(z_{bf2} - z_{t12}\right)\right] \quad (4.12)$$

The equation of rear bogie motion for vertical direction is:

$$\ddot{z}_{br} = \frac{1}{m_b}\left[k_{eq}(z_r - z_{br}) + f_{act.r} - c_{pr}(\dot{z_{br1}} - \dot{z_{t21}}) - k_p(z_{br1} - z_{t21}) - c_{pr}(\dot{z_{br2}} - \dot{z_{t22}}) - k_p(z_{br2} - z_{t22})\right] \quad (4.13)$$

The equation of rear bogie motion for pitch direction is:

$$\ddot{\theta}_{br} = \frac{1}{J_b}\left[-c_{pr}l_b(\dot{z_{br1}} - \dot{z_{t21}}) - k_p l_b(z_{br1} - z_{t21}) + c_{pr}l_b(\dot{z_{br2}} - \dot{z_{t22}}) + k_p l_b(z_{br2} - z_{t22})\right] \quad (4.14)$$

Whereas k_{eq} is secondary damping stiffness per bogie, which represented the equivalent stiffness per bogie for reservoir stiffness and damping stiffness of air spring($k_{eq} = \frac{k_s.k_r}{k_s+k_r}$), $f_{act.f}$ and $f_{act.r}$ are full active damping forces at front and rear actuators which are electro-mechanical actuators, respectively.

For the simulation of the semi-active suspension system in the comparative assessment, the damping force of the MR damper replaces the passive damper forces in the model, as shown in Figure 4.3.

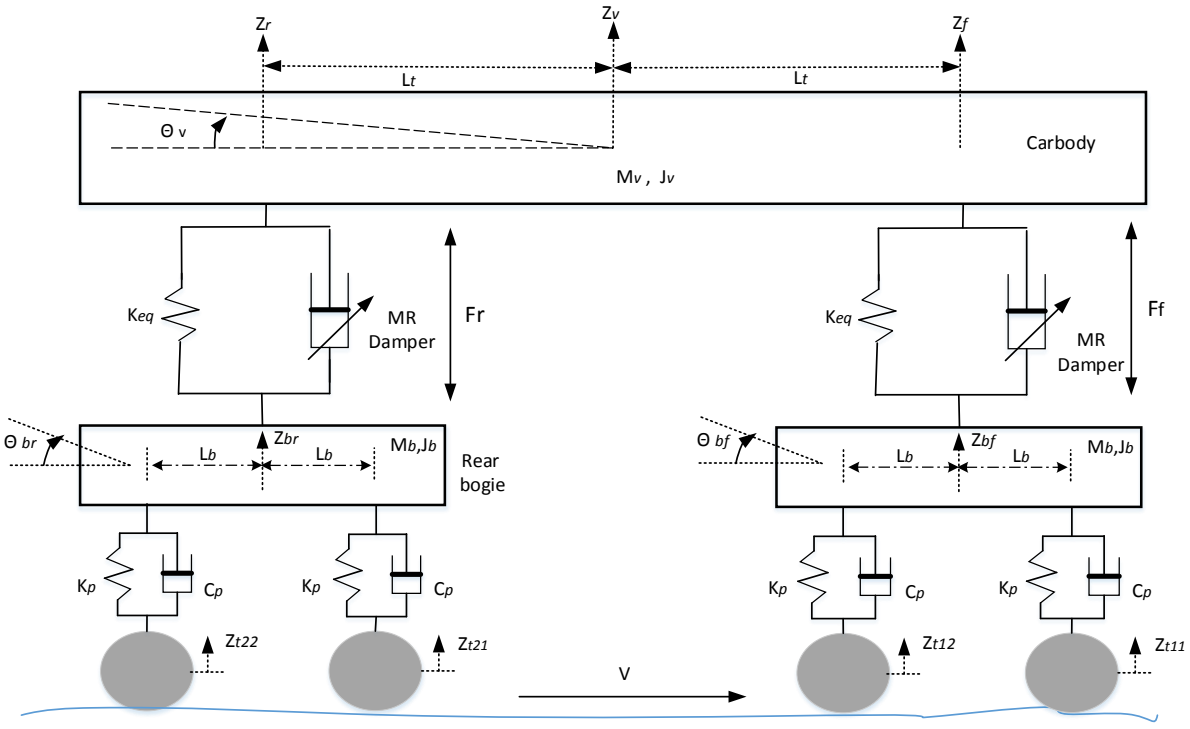

Figure 4.3: Schematic representation of the MR damper in vertical secondary suspension of the railway vehicle

Equations (4.15 - 4.20) describe the system representation of the MR damper in vertical secondary suspension of the railway vehicle, as listed below:

The equation of vehicle motion into the vertical direction is:

$$\ddot{z}_v = \frac{1}{m_v}\left[-k_{eq}(z_f - z_{bf}) - f_{MR.f} - k_{eq}(z_r - z_{br}) - f_{MR.r}\right] \quad (4.15)$$

The equation of vehicle motion for pitch is:

$$\ddot{\theta}_v = \frac{1}{J_v}\left[-k_{eq}l_t(z_f - z_{bf}) - l_t f_{MR.f} + k_{eq}l_t(z_r - z_{br}) + l_t f_{MR.r}\right] \quad (4.16)$$

The equations for the bogies can be formulated in a similar way, and similarly for the rear bogie. For the front bogie:

$$\ddot{z}_{bf} = \frac{1}{m_b}\left[k_{eq}(z_f - z_{bf}) + f_{MR.f} - c_{pr}(\dot{z_{bf1}} - \dot{z_{t11}}) - k_p(z_{bf1} - z_{t11}) - c_{pr}(\dot{z_{bf2}} - \dot{z_{t12}}) - k_p(z_{bf2} - z_{t12})\right] \quad (4.17)$$

$$\ddot{\theta}_{bf} = \frac{1}{J_b}\left[-c_{pr}l_b\left(\dot{z_{bf1}} - \dot{z_{t11}}\right) - k_p l_b\left(z_{bf1} - z_{t11}\right) + c_{pr}l_b\left(\dot{z_{bf2}} - \dot{z_{t12}}\right) + k_p l_b\left(z_{bf2} - z_{t12}\right)\right] \quad (4.18)$$

For the rear bogie:

$$\ddot{z}_{br} = \frac{1}{m_b}\left[k_{eq}(z_r - z_{br}) + f_{MR.r} - c_{pr}(\dot{z_{br1}} - \dot{z_{t21}}) - k_p(z_{br1} - z_{t21}) - c_{pr}(\dot{z_{br2}} - \dot{z_{t22}}) - k_p(z_{br2} - z_{t22})\right] \quad (4.19)$$

$$\ddot{\theta}_{br} = \frac{1}{J_b}\left[-c_{pr}l_b(\dot{z_{br1}} - \dot{z_{t21}}) - k_p l_b(z_{br1} - z_{t21}) + c_{pr}l_b(\dot{z_{br2}} - \dot{z_{t22}}) + k_p l_b(z_{br2} - z_{t22})\right] \quad (4.20)$$

Where $f_{MR.f}$ and $f_{MR.r}$ are semi-active damping forces at the front and rear of rear bogie which are MR dampers, respectively.

4.4 Lateral Dynamic Model

As mentioned in the preview section, for performance comparison, full-active and semi-active suspensions and the vehicle with passive suspensions are used as the benchmark and are used as a reference case for assessment of the proposed design. In this section, the dynamics of the railway vehicle are only considered in terms of the lateral and yaw movement. A plan view diagram of the railway vehicle with passive suspensions is shown in Figure 4.4.

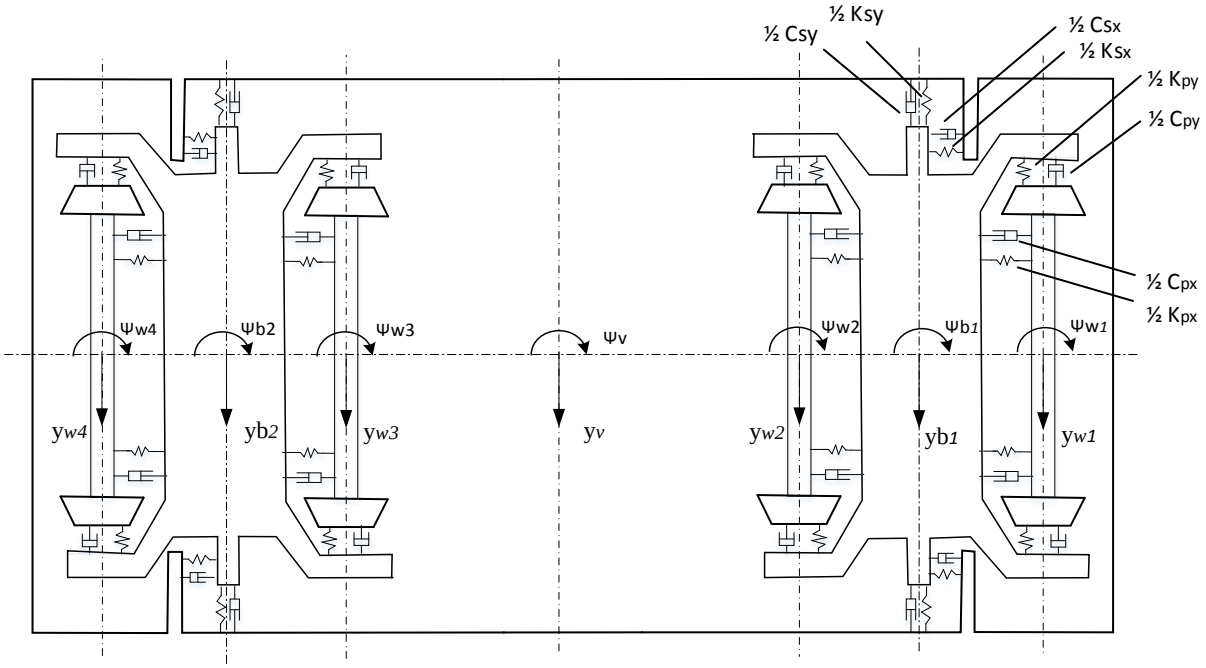

Figure 4.4: Schematic representation of the passive damper in lateral secondary suspension of the railway vehicle

From Figure 4.4, the governing equations of motion for the railway vehicle are listed as follows: $\ddot{y}_v + l\ddot{\psi}_v$

The equation of vehicle motion into the lateral direction is:

$$M_v\ddot{y}_v = -K_{sy}\left[y_v + l\psi_v - y_{b1}\right] - C_{sy}\left[\dot{y}_v + l\dot{\psi}_v - \dot{y}_{b1}\right] - K_{sy}\left[y_v - l\psi_v - y_{b2}\right] - C_{sy}\left[\dot{y}_v - l\dot{\psi}_v - \dot{y}_{b2}\right] \quad (4.21)$$

The equation of vehicle motion into the yaw direction is:

$$I_v\ddot{\psi}_v = -K_{sy}l\left[y_v + l\psi_v - y_{b1}\right] - C_{sy}l\left[\dot{y}_v + l\dot{\psi}_v - \dot{y}_{b1}\right] + K_{sy}l\left[y_v - l\psi_v - y_{b2}\right] + C_{sy}l\left[\dot{y}_v - l\dot{\psi}_v - \dot{y}_{b2}\right] - K_{sx}{b_2}^2\left(\psi_v - \psi_{b1}\right) - K_{sx}{b_2}^2\left(\psi_v - \psi_{b2}\right) - C_{sx}{b_2}^2\left(\dot{\psi}_v - \dot{\psi}_{b1}\right) - C_{sx}{b_2}^2\left(\dot{\psi}_v - \dot{\psi}_{b2}\right) \quad (4.22)$$

The equation of front bogie dynamics into the lateral direction is:

$$M_b\ddot{y}_{b1} = K_{sy}[y_v + l\psi_v - y_{b1}] + C_{sy}[\dot{y}_v + l\dot{\psi}_v - \dot{y}_{b1}] - K_{py}[y_{b1} + a\psi_{b1} - y_{w1}] - C_{py}[\dot{y}_{b1} + a\dot{\psi}_{b1} - \dot{y}_{w1}] - K_{py}[y_{b1} - a\psi_{b1} - y_{w2}] - C_{py}[\dot{y}_{b1} - a\dot{\psi}_{b1} - \dot{y}_{w2}] \quad \text{..... (4.23)}$$

The equation of front bogie dynamics into the yaw direction is:

$$I_b\ddot{\psi}_{b1} = K_{sx}{b_2}^2(\psi_v - \psi_{b1}) + C_{sx}{b_2}^2(\dot{\psi}_v - \dot{\psi}_{b1}) - K_{py}a[y_{bi} + a\psi_{b1} - y_{w1}] - C_{py}a[\dot{y}_{b1} + a\dot{\psi}_{b1} - \dot{y}_{w1}] + K_{py}a[y_{b1} - a\psi_{b1} - y_{w2}] + C_{py}a[\dot{y}_{b1} - a\dot{\psi}_{b1} - \dot{y}_{w2}] - K_{px}{b_1}^2(\psi_{b1} - \psi_{w1}) - C_{px}{b_1}^2(\dot{\psi}_{b1} - \dot{\psi}_{w1}) - K_{px}{b_1}^2(\psi_{b1} - \psi_{w2}) - C_{px}{b_1}^2(\dot{\psi}_{b1} - \dot{\psi}_{w2}) \quad \text{..... (4.24)}$$

The equation of rear bogie dynamics into the lateral direction is:

$$M_b\ddot{y}_{b2} = K_{sy}[y_v - l\psi_v - y_{b2}] + C_{sy}[\dot{y}_v - l\dot{\psi}_v - \dot{y}_{b2}] - K_{py}[y_{b2} + a\psi_{b2} - y_{w3}] - C_{py}[\dot{y}_{b2} + a\dot{\psi}_{b2} - \dot{y}_{w3}] - K_{py}[y_{b2} - a\psi_{b2} - y_{w4}] - C_{py}[\dot{y}_{b2} - a\dot{\psi}_{b2} - \dot{y}_{w4}] \quad \text{..... (4.25)}$$

The equation of rear bogie dynamics into the yaw direction is:

$$I_b\ddot{\psi}_{b2} = K_{sx}{b_2}^2(\psi_v - \psi_{b2}) + C_{sx}{b_2}^2(\dot{\psi}_v - \dot{\psi}_{b2}) - K_{py}a[y_{b2} + a\psi_{b2} - y_{w3}] - C_{py}a[\dot{y}_{b2} + a\dot{\psi}_{b2} - \dot{y}_{w3}] + K_{py}a[y_{b2} - a\psi_{b2} - y_{w4}] + C_{py}a[\dot{y}_{b2} - a\dot{\psi}_{b2} - \dot{y}_{w4}] - K_{px}{b_1}^2(\psi_{b2} - \psi_{w3}) - C_{px}{b_1}^2(\dot{\psi}_{b2} - \dot{\psi}_{w3}) - K_{px}{b_1}^2(\psi_{b2} - \psi_{w4}) - C_{px}{b_1}^2(\dot{\psi}_{b2} - \dot{\psi}_{w4}) \quad \text{..... (4.26)}$$

For the leading wheelset dynamics of the front bogie, the governing equation are given by:

$$M_w\ddot{y}_{w1} = K_{py}[y_{b1} + a\psi_{b1} - y_{w1}] + C_{py}[\dot{y}_{b1} + a\dot{\psi}_{b1} - \dot{y}_{w1}] - \frac{2f_{22}}{v}\dot{y}_{w1} + 2f_{22}\psi_{w1} \quad \text{..... (4.27)}$$

$$I_w\ddot{\psi}_{w1} = K_{px}{b_1}^2(\psi_{b1} - \psi_{w1}) + C_{px}{b_1}^2(\dot{\psi}_{b1} - \dot{\psi}_{w1}) - \frac{2f_{11}b^2}{v}\dot{\psi}_{w1} - \frac{2f_{11}\lambda b}{r_0}(y_{w1} - y_{r1}) \quad \text{..... (4.28)}$$

For the trailing wheelset dynamics of the front bogie, the governing equation are given by:

$$M_w\ddot{y}_{w2} = K_{py}[y_{b1} - a\psi_{b1} - y_{w2}] + C_{py}\left[\dot{y}_{b1} - a\dot{\psi}_{b1} - \dot{y}_{w2}\right] - \frac{2f_{22}}{v}\dot{y}_{w2} + 2f_{22}\psi_{w2}$$

..... (4.29)

$$I_w\ddot{\psi}_{w2} = K_{px}{b_1}^2(\psi_{b1} - \psi_{w2}) + C_{px}{b_1}^2\left(\dot{\psi}_{b1} - \dot{\psi}_{w2}\right) - \frac{2f_{11}b^2}{v}\dot{\psi}_{w2} - \frac{2f_{11}\lambda b}{r_0}(y_{w2} - y_{r2})$$

..... (4.30)

For the leading wheelset dynamics of the rear bogie, the governing equations are given by:

$$M_w\ddot{y}_{w3} = K_{py}[y_{b2} + a\psi_{b2} - y_{w3}] + C_{py}\left[\dot{y}_{b2} + a\dot{\psi}_{b2} - \dot{y}_{w3}\right] - \frac{2f_{22}}{v}\dot{y}_{w3} + 2f_{22}\psi_{w3}$$

..... (4.31)

$$I_w\ddot{\psi}_{w3} = K_{px}{b_1}^2(\psi_{b2} - \psi_{w3}) + C_{px}{b_1}^2\left(\dot{\psi}_{b2} - \dot{\psi}_{w3}\right) - \frac{2f_{11}b^2}{v}\dot{\psi}_{w3} - \frac{2f_{11}\lambda b}{r_0}(y_{w3} - y_{r3})$$

..... (4.32)

For the trailing wheelset dynamics of the rear bogie, the governing equations are given by:

$$M_w\ddot{y}_{w4} = K_{py}\left[y_{bj} - a\psi_{b2} - y_{w4}\right] + C_{py}\left[\dot{y}_{b2} - a\dot{\psi}_{b2} - \dot{y}_{w4}\right] - \frac{2f_{22}}{v}\dot{y}_{w4} + 2f_{22}\psi_{w4}$$

..... (4.33)

$$I_w\ddot{\psi}_{w4} = K_{px}{b_1}^2(\psi_{b2} - \psi_{w4}) + C_{px}{b_1}^2\left(\dot{\psi}_{b2} - \dot{\psi}_{w4}\right) - \frac{2f_{11}b^2}{v}\dot{\psi}_{w4} - \frac{2f_{11}\lambda b}{r_0}(y_{w4} - y_{r4})$$

..... (4.34)

Equations (4.21-4.34) describe the system shown in Figure 4.4, whose parameters are listed in Table 4.2.

Table 4.2:Vehicle parameters of the lateral model [28, 65]

Symbols		Symbols	
y_v,y_{b1},y_{b2}	Lateral displacement of the vehicle, front bogie, rear bogie	K_{sx}	Double of secondary longitudinal stiffness (3.4x10^5 N/m)
y_{w1},y_{w2},y_{w3},y_{w4}	Lateral displacement of the wheelset	K_{sy}	Double of secondary lateral stiffness (3.5x10^5 N/m)
ψ_v, ψ_{b1}, ψ_{b2}	Yaw angle of the vehicle, front bogie, rear bogie	C_{px}	Double of primary longitudinal damping (0 Ns/m)
ψ_{w1},ψ_{w2},ψ_{w3},ψ_{w4}	Yaw angle of the wheelset	C_{py}	Double of primary lateral damping (0 N/m)
y_{r1},y_{r2},y_{r3},y_{r4}	Track lateral displacement (irregularities)	C_{sx}, C_{sy}	Double of secondary longitudinal damping (5x10^5 Ns/m), lateral damping (5.2x10^5 Ns/m)
M_w	Wheelset mass(1750 Kg)	l	Half of the bogie centre pin spacing (9 m)
M_b	Bogie mass(3296kg)	a	Half of the wheelbase (1.25m)
M_v	Vehicle mass(32000kg)	b	Half of wheelset contact distance (0.7465 m)
I_w	Wheelset yaw inertia (1400kg.m^2)	b_1,b_2	Half of the primary longitudinal and secondary longitudinal(1 m)
I_b	Bogie yaw inertia (2100 kg.m^2)	v	Vehicle speed(83.33 m/s)

I_v	Vehicle yaw inertia (2.24x10^6 kg.m^2)	r_o	Wheel rolling radius (0.4575 m)
K_{px}	Double of primary longitudinal stiffness (2.9x10^7 N/m)	f_{11}, f_{22}	Longitudinal creep coefficient (1.12x10^7) and lateral creep coefficient (9.98x10^7)
K_{py}	Double of primary lateral stiffness (1.5x10^7 N/m)	λ	Effective wheel conicity(0.05)

Note in this study, to achieve a comparative assessment, the secondary lateral passive dampers are replaced by the actuators to study the full-active controlled suspensions, as shown in Figure 4.5.

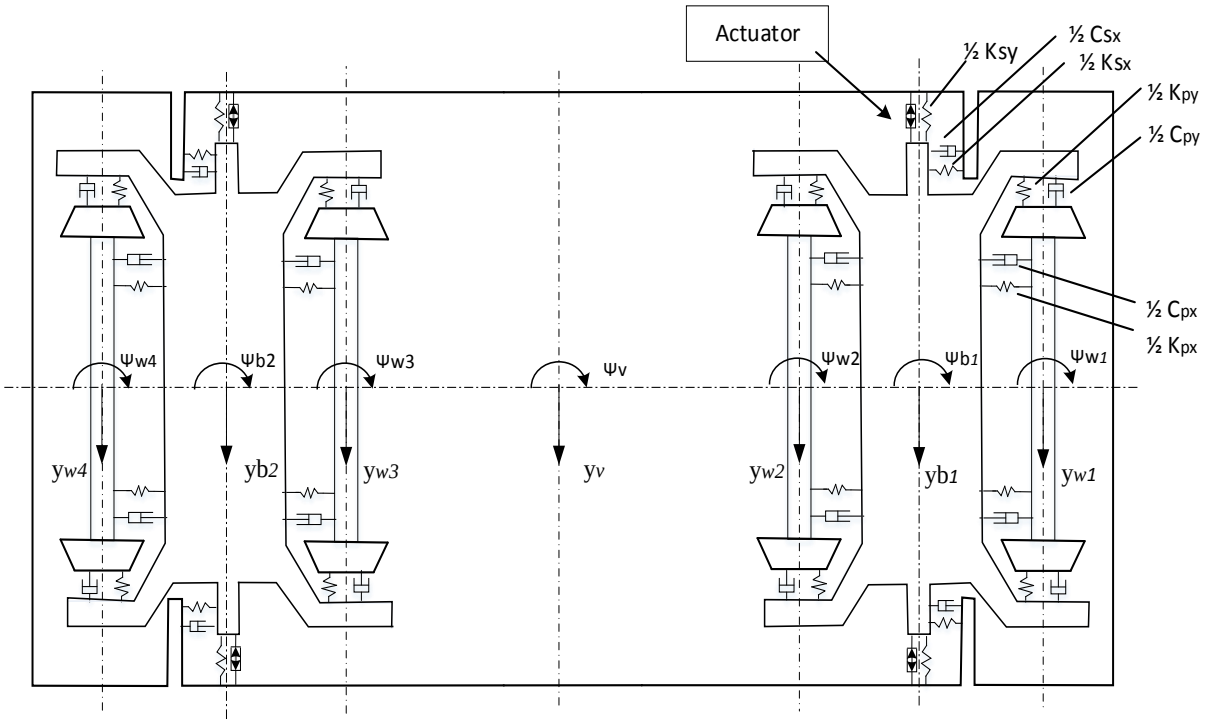

Figure 4.5: Schematic representation of the actuator in lateral secondary suspension of the railway vehicle

From Figure 4.5, the governing equations of motion for the railway vehicle are listed as follows:

The equation of vehicle motion into the lateral direction is:

$$M_v\ddot{y}_v = -K_{sy}[y_v + l\psi_v - y_{b1}] - f_{act.f} - K_{sy}[y_v - l\psi_v - y_{b2}] - f_{act.r} \quad \text{..... (4.35)}$$

The equation of vehicle motion into the yaw direction is:

$$I_v\ddot{\psi}_v = -K_{sy}l[y_v + l\psi_v - y_{b1}] + K_{sy}l[y_v - l\psi_v - y_{b2}] - lf_{act.f} + lf_{act.r} - K_{sx}{b_2}^2(\psi_v - \psi_{b1}) - K_{sx}{b_2}^2(\psi_v - \psi_{b2}) - C_{sx}{b_2}^2(\dot{\psi}_v - \dot{\psi}_{b1}) - C_{sx}{b_2}^2(\dot{\psi}_v - \dot{\psi}_{b2}) \quad \text{..... (4.36)}$$

The equation of front bogie dynamics into the lateral direction is:

$$M_b\ddot{y}_{b1} = K_{sy}[y_v + l\psi_v - y_{b1}] + f_{act.f} - K_{py}[y_{b1} + a\psi_{b1} - y_{w1}] - C_{py}[\dot{y}_{b1} + a\dot{\psi}_{b1} - \dot{y}_{w1}] - K_{py}[y_{b1} - a\psi_{b1} - y_{w2}] - C_{py}[\dot{y}_{b1} - a\dot{\psi}_{b1} - \dot{y}_{w2}] \quad \text{..... (4.37)}$$

The equation of front bogie dynamics into the yaw direction is:

$$I_b\ddot{\psi}_{b1} = K_{sx}{b_2}^2(\psi_v - \psi_{b1}) + C_{sx}{b_2}^2(\dot{\psi}_v - \dot{\psi}_{b1}) - K_{py}a[y_{bi} + a\psi_{b1} - y_{w1}] - C_{py}a[\dot{y}_{b1} + a\dot{\psi}_{b1} - \dot{y}_{w1}] + K_{py}a[y_{b1} - a\psi_{b1} - y_{w2}] + C_{py}a[\dot{y}_{b1} - a\dot{\psi}_{b1} - \dot{y}_{w2}] - K_{px}{b_1}^2(\psi_{b1} - \psi_{w1}) - C_{px}{b_1}^2(\dot{\psi}_{b1} - \dot{\psi}_{w1}) - K_{px}{b_1}^2(\psi_{b1} - \psi_{w2}) - C_{px}{b_1}^2(\dot{\psi}_{b1} - \dot{\psi}_{w2}) \quad \text{..... (4.38)}$$

The equation of rear bogie dynamics into the lateral direction is:

$$M_b\ddot{y}_{b2} = K_{sy}[y_v - l\psi_v - y_{b2}] + f_{act.r} - K_{py}[y_{b2} + a\psi_{b2} - y_{w3}] - C_{py}[\dot{y}_{b2} + a\dot{\psi}_{b2} - \dot{y}_{w3}] - K_{py}[y_{b2} - a\psi_{b2} - y_{w4}] - C_{py}[\dot{y}_{b2} - a\dot{\psi}_{b2} - \dot{y}_{w4}] \quad \text{..... (4.39)}$$

The equation of rear bogie dynamics into the yaw direction is:

$$I_b\ddot{\psi}_{b2} = K_{sx}{b_2}^2(\psi_v - \psi_{b2}) + C_{sx}{b_2}^2(\dot{\psi}_v - \dot{\psi}_{b2}) - K_{py}a[y_{b2} + a\psi_{b2} - y_{w3}] - C_{py}a[\dot{y}_{b2} + a\dot{\psi}_{b2} - \dot{y}_{w3}] + K_{py}a[y_{b2} - a\psi_{b2} - y_{w4}] + C_{py}a[\dot{y}_{b2} - a\dot{\psi}_{b2} - \dot{y}_{w4}] - K_{px}{b_1}^2(\psi_{b2} - \psi_{w3}) - C_{px}{b_1}^2(\dot{\psi}_{b2} - \dot{\psi}_{w3}) - K_{px}{b_1}^2(\psi_{b2} - \psi_{w4}) - C_{px}{b_1}^2(\dot{\psi}_{b2} - \dot{\psi}_{w4}) \quad \text{..... (4.40)}$$

For the leading wheelset dynamics of the front bogie, the governing equation are given by:

$$M_w\ddot{y}_{w1} = K_{py}[y_{b1} + a\psi_{b1} - y_{w1}] + C_{py}\left[\dot{y}_{b1} + a\dot{\psi}_{b1} - \dot{y}_{w1}\right] - \frac{2f_{22}}{v}\dot{y}_{w1} + 2f_{22}\psi_{w1}$$

…… (4.41)

$$I_w\ddot{\psi}_{w1} = K_{px}{b_1}^2(\psi_{b1} - \psi_{w1}) + C_{px}{b_1}^2\left(\dot{\psi}_{b1} - \dot{\psi}_{w1}\right) - \frac{2f_{11}b^2}{v}\dot{\psi}_{w1} - \frac{2f_{11}\lambda b}{r_0}(y_{w1} - y_{r1})$$

…… (4.42)

For the trailing wheelset dynamics of the front bogie, the governing equation are given by:

$$M_w\ddot{y}_{w2} = K_{py}[y_{b1} - a\psi_{b1} - y_{w2}] + C_{py}\left[\dot{y}_{b1} - a\dot{\psi}_{b1} - \dot{y}_{w2}\right] - \frac{2f_{22}}{v}\dot{y}_{w2} + 2f_{22}\psi_{w2}$$

…… (4.43)

$$I_w\ddot{\psi}_{w2} = K_{px}{b_1}^2(\psi_{b1} - \psi_{w2}) + C_{px}{b_1}^2\left(\dot{\psi}_{b1} - \dot{\psi}_{w2}\right) - \frac{2f_{11}b^2}{v}\dot{\psi}_{w2} - \frac{2f_{11}\lambda b}{r_0}(y_{w2} - y_{r2})$$

…… (4.44)

For the leading wheelset dynamics of the rear bogie, the governing equations are given by:

$$M_w\ddot{y}_{w3} = K_{py}[y_{b2} + a\psi_{b2} - y_{w3}] + C_{py}\left[\dot{y}_{b2} + a\dot{\psi}_{b2} - \dot{y}_{w3}\right] - \frac{2f_{22}}{v}\dot{y}_{w3} + 2f_{22}\psi_{w3}$$

…… (4.45)

$$I_w\ddot{\psi}_{w3} = K_{px}{b_1}^2(\psi_{b2} - \psi_{w3}) + C_{px}{b_1}^2\left(\dot{\psi}_{b2} - \dot{\psi}_{w3}\right) - \frac{2f_{11}b^2}{v}\dot{\psi}_{w3} - \frac{2f_{11}\lambda b}{r_0}(y_{w3} - y_{r3})$$

…… (4.46)

For the trailing wheelset dynamics of the rear bogie, the governing equations are given by:

$$M_w\ddot{y}_{w4} = K_{py}\left[y_{bj} - a\psi_{b2} - y_{w4}\right] + C_{py}\left[\dot{y}_{b2} - a\dot{\psi}_{b2} - \dot{y}_{w4}\right] - \frac{2f_{22}}{v}\dot{y}_{w4} + 2f_{22}\psi_{w4}$$

…… (4.47)

$$I_w\ddot{\psi}_{w4} = K_{px}{b_1}^2(\psi_{b2} - \psi_{w4}) + C_{px}{b_1}^2\left(\dot{\psi}_{b2} - \dot{\psi}_{w4}\right) - \frac{2f_{11}b^2}{v}\dot{\psi}_{w4} - \frac{2f_{11}\lambda b}{r_0}(y_{w4} - y_{r4})$$

…… (4.48)

Equations (4.35-4.48) describe the system shown in Figure 4.5

Equations (4.35 - 4.48) describe the system representation of the actuator in lateral secondary suspension of the railway vehicle, whereas $f_{act.f}$ and $f_{act.r}$ are full-active damping forces at front and rear actuators which are electromechanical actuators, respectively.

For the simulation of the semi-active suspension in the comparative assessment, the damping force of the MR damper replaces the secondary lateral passive damper forces in the model, as shown in Figure 4.6.

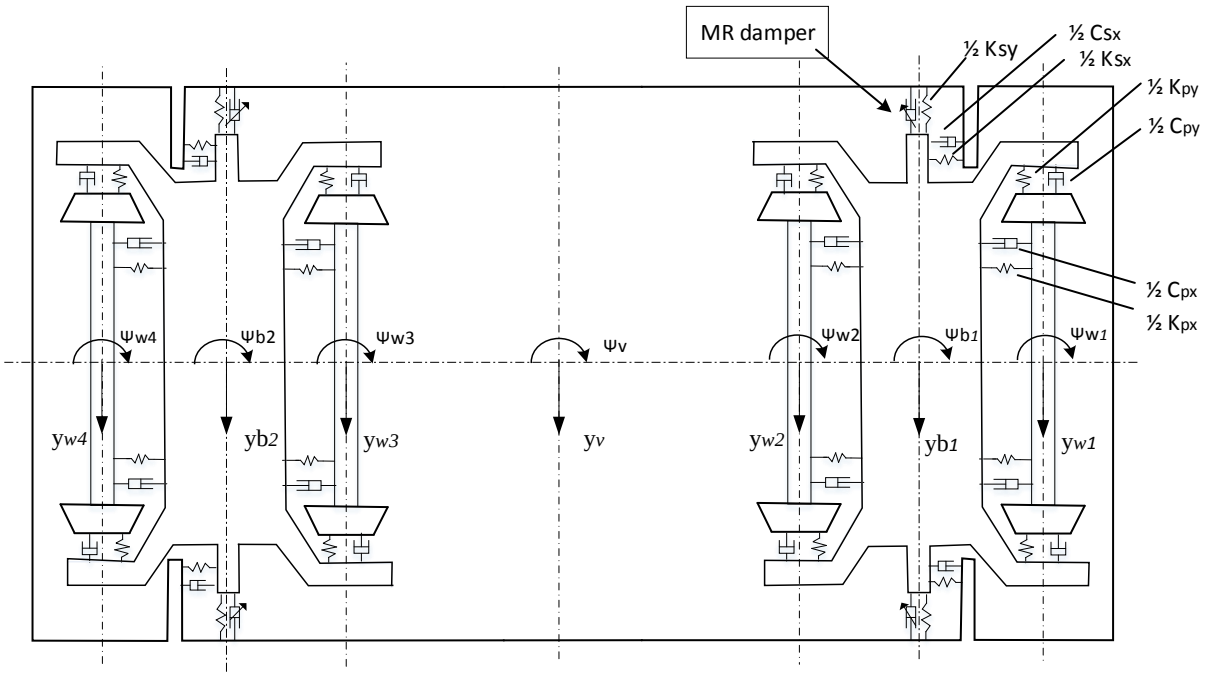

Figure 4.6: Schematic representation of the MR damper in lateral secondary suspension of the railway vehicle

From Figure 4.6, the governing equations of motion for the railway vehicle are listed as follows:

The equation of vehicle motion into the lateral direction is:

$$M_v\ddot{y}_v = -K_{sy}\left[y_v + l\psi_v - y_{b1}\right] - f_{MR.f} - K_{sy}\left[y_v - l\psi_v - y_{b2}\right] - f_{MR.r} \quad \text{..... (4.49)}$$

The equation of vehicle motion into the yaw direction is:

$$I_v\ddot{\psi}_v = -K_{sy}l\left[y_v + l\psi_v - y_{b1}\right] + K_{sy}l\left[y_v - l\psi_v - y_{b2}\right] - lf_{MR.f} + lf_{MR.r} - K_{sx}{b_2}^2\left(\psi_v - \psi_{b1}\right) - K_{sx}{b_2}^2\left(\psi_v - \psi_{b2}\right) - C_{sx}{b_2}^2\left(\dot{\psi}_v - \dot{\psi}_{b1}\right) - C_{sx}{b_2}^2\left(\dot{\psi}_v - \dot{\psi}_{b2}\right) \quad \text{..... (4.50)}$$

The equation of front bogie dynamics into the lateral direction is:

$$M_b\ddot{y}_{b1} = K_{sy}[y_v + l\psi_v - y_{b1}] + f_{MR.f} - K_{py}[y_{b1} + a\psi_{b1} - y_{w1}] - C_{py}\left[\dot{y}_{b1} + a\dot{\psi}_{b1} - \dot{y}_{w1}\right] - K_{py}[y_{b1} - a\psi_{b1} - y_{w2}] - C_{py}\left[\dot{y}_{b1} - a\dot{\psi}_{b1} - \dot{y}_{w2}\right] \text{..... (4.51)}$$

The equation of front bogie dynamics into the yaw direction is:

$$I_b\ddot{\psi}_{b1} = K_{sx}{b_2}^2(\psi_v - \psi_{b1}) + C_{sx}{b_2}^2\left(\dot{\psi}_v - \dot{\psi}_{b1}\right) - K_{py}a[y_{bi} + a\psi_{b1} - y_{w1}] - C_{py}a\left[\dot{y}_{b1} + a\dot{\psi}_{b1} - \dot{y}_{w1}\right] + K_{py}a[y_{b1} - a\psi_{b1} - y_{w2}] + C_{py}a\left[\dot{y}_{b1} - a\dot{\psi}_{b1} - \dot{y}_{w2}\right] - K_{px}{b_1}^2(\psi_{b1} - \psi_{w1}) - C_{px}{b_1}^2\left(\dot{\psi}_{b1} - \dot{\psi}_{w1}\right) - K_{px}{b_1}^2(\psi_{b1} - \psi_{w2}) - C_{px}{b_1}^2\left(\dot{\psi}_{b1} - \dot{\psi}_{w2}\right) \text{..... (4.52)}$$

The equation of rear bogie dynamics into the lateral direction is:

$$M_b\ddot{y}_{b2} = K_{sy}[y_v - l\psi_v - y_{b2}] + f_{MR.r} - K_{py}[y_{b2} + a\psi_{b2} - y_{w3}] - C_{py}\left[\dot{y}_{b2} + a\dot{\psi}_{b2} - \dot{y}_{w3}\right] - K_{py}[y_{b2} - a\psi_{b2} - y_{w4}] - C_{py}\left[\dot{y}_{b2} - a\dot{\psi}_{b2} - \dot{y}_{w4}\right] \text{..... (4.53)}$$

The equation of rear bogie dynamics into the yaw direction is:

$$I_b\ddot{\psi}_{b2} = K_{sx}{b_2}^2(\psi_v - \psi_{b2}) + C_{sx}{b_2}^2\left(\dot{\psi}_v - \dot{\psi}_{b2}\right) - K_{py}a[y_{b2} + a\psi_{b2} - y_{w3}] - C_{py}a\left[\dot{y}_{b2} + a\dot{\psi}_{b2} - \dot{y}_{w3}\right] + K_{py}a[y_{b2} - a\psi_{b2} - y_{w4}] + C_{py}a\left[\dot{y}_{b2} - a\dot{\psi}_{b2} - \dot{y}_{w4}\right] - K_{px}{b_1}^2(\psi_{b2} - \psi_{w3}) - C_{px}{b_1}^2\left(\dot{\psi}_{b2} - \dot{\psi}_{w3}\right) - K_{px}{b_1}^2(\psi_{b2} - \psi_{w4}) - C_{px}{b_1}^2\left(\dot{\psi}_{b2} - \dot{\psi}_{w4}\right) \text{..... (4.54)}$$

For the leading wheelset dynamics of the front bogie, the governing equation are given by:

$$M_w\ddot{y}_{w1} = K_{py}[y_{b1} + a\psi_{b1} - y_{w1}] + C_{py}\left[\dot{y}_{b1} + a\dot{\psi}_{b1} - \dot{y}_{w1}\right] - \frac{2f_{22}}{v}\dot{y}_{w1} + 2f_{22}\psi_{w1}$$

…… (4.55)

$$I_w\ddot{\psi}_{w1} = K_{px}{b_1}^2(\psi_{b1} - \psi_{w1}) + C_{px}{b_1}^2\left(\dot{\psi}_{b1} - \dot{\psi}_{w1}\right) - \frac{2f_{11}b^2}{v}\dot{\psi}_{w1} - \frac{2f_{11}\lambda b}{r_0}(y_{w1} - y_{r1})$$

…… (4.56)

For the trailing wheelset dynamics of the front bogie, the governing equation are given by:

$$M_w\ddot{y}_{w2} = K_{py}[y_{b1} - a\psi_{b1} - y_{w2}] + C_{py}\left[\dot{y}_{b1} - a\dot{\psi}_{b1} - \dot{y}_{w2}\right] - \frac{2f_{22}}{v}\dot{y}_{w2} + 2f_{22}\psi_{w2}$$

…… (4.57)

$$I_w\ddot{\psi}_{w2} = K_{px}{b_1}^2(\psi_{b1} - \psi_{w2}) + C_{px}{b_1}^2\left(\dot{\psi}_{b1} - \dot{\psi}_{w2}\right) - \frac{2f_{11}b^2}{v}\dot{\psi}_{w2} - \frac{2f_{11}\lambda b}{r_0}(y_{w2} - y_{r2})$$

…… (4.58)

For the leading wheelset dynamics of the rear bogie, the governing equations are given by:

$$M_w\ddot{y}_{w3} = K_{py}[y_{b2} + a\psi_{b2} - y_{w3}] + C_{py}\left[\dot{y}_{b2} + a\dot{\psi}_{b2} - \dot{y}_{w3}\right] - \frac{2f_{22}}{v}\dot{y}_{w3} + 2f_{22}\psi_{w3}$$

…… (4.59)

$$I_w\ddot{\psi}_{w3} = K_{px}{b_1}^2(\psi_{b2} - \psi_{w3}) + C_{px}{b_1}^2\left(\dot{\psi}_{b2} - \dot{\psi}_{w3}\right) - \frac{2f_{11}b^2}{v}\dot{\psi}_{w3} - \frac{2f_{11}\lambda b}{r_0}(y_{w3} - y_{r3})$$

…… (4.60)

For the trailing wheelset dynamics of the rear bogie, the governing equations are given by:

$$M_w\ddot{y}_{w4} = K_{py}\left[y_{bj} - a\psi_{b2} - y_{w4}\right] + C_{py}\left[\dot{y}_{b2} - a\dot{\psi}_{b2} - \dot{y}_{w4}\right] - \frac{2f_{22}}{v}\dot{y}_{w4} + 2f_{22}\psi_{w4}$$

…… (4.61)

$$I_w\ddot{\psi}_{w4} = K_{px}{b_1}^2(\psi_{b2} - \psi_{w4}) + C_{px}{b_1}^2\left(\dot{\psi}_{b2} - \dot{\psi}_{w4}\right) - \frac{2f_{11}b^2}{v}\dot{\psi}_{w4} - \frac{2f_{11}\lambda b}{r_0}(y_{w4} - y_{r4})$$

…… (4.62)

Equations (4.49 - 4.62) describe the system representation of the semi-active damper in lateral secondary suspension of the railway vehicle, whereas $f_{MR.f}$ and $f_{MR.r}$ are semi-active damping forces at front and rear MR dampers, respectively.

4.5 Full-Active Suspension System

In the existing literature, a wide variety of control strategies have been proposed for full-active suspension systems. One of the most implemented and analysed over the years is skyhook damping. In order to make performance comparisons between suspension systems, skyhook damping is used as the full-active control strategy, as introduced by Karnopp[7]. Although there are many advanced control methods such as H∞, linear quadratic Gaussian (LQG), that can be used, skyhook is, however, a simple and effective strategy to assess the ride quality in full-active suspension systems. In this section, the skyhook damping control will be used which is known to give excellent improvements in ride quality.

4.5.1 Skyhook Damping

The skyhook damping concept was first introduced by Karnopp in the late 1970s[7]. Many researchers have since investigated and analysed skyhook damping with regards to improved ride quality[93-95]. The absolute velocity damping can be used to improve ride quality by damping to an imaginary sky reference point. The idea of absolute damping is illustrated in Figure 4.7, where a damper is connected between the body mass ad the sky, so, it is called skyhook damping.

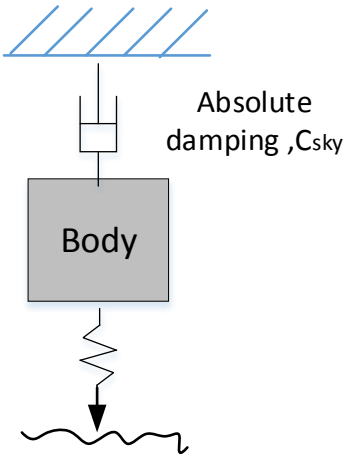

Figure 4.7:The skyhook damping concept [25]

Practically, the absolute velocity measurement is difficult and costly. Therefore, required absolute velocity signal is obtained by integrating the signal measured by a sensor accelerometer on the car body. Then, the velocity signal is high-pass filtered in order to remove integrator drift and then multiplied by the skyhook damping coefficient in order to generate the desired force. Figure 4.8 illustrates the practical implementation of the skyhook damping control system.

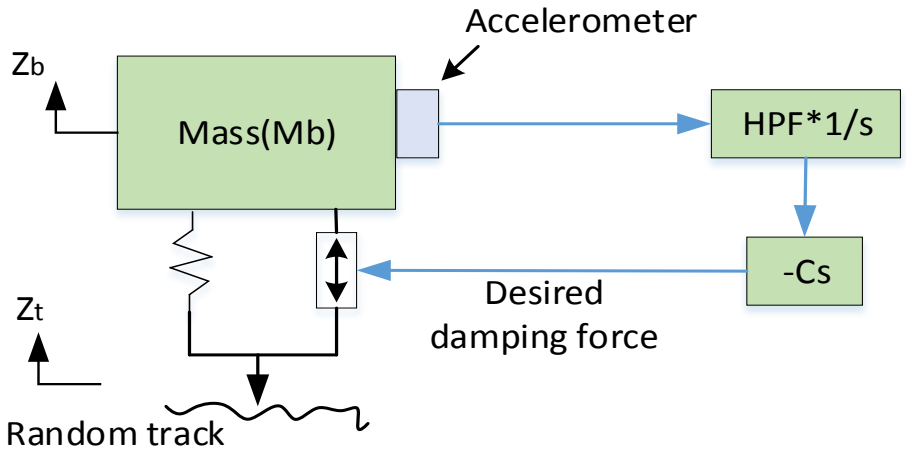

Figure 4.8: Schematic of the skyhook damping control system [25]

Skyhook control strategy gives a significant improvement of ride quality on straight track operation. However, it generates large suspension deflections at deterministic inputs such as curves. A challenge with the full-active skyhook damping is to manage the trade-off between improved ride quality and suspension deflection during curving. There are a number of possible

solutions proposed to overcome the trade-off problem, and considerable results can be achieved by optimising the filtering of the absolute velocity signal. Li and Goodall[25] have investigated three linear and two non-linear approaches to skyhook damping with different filtering methods.

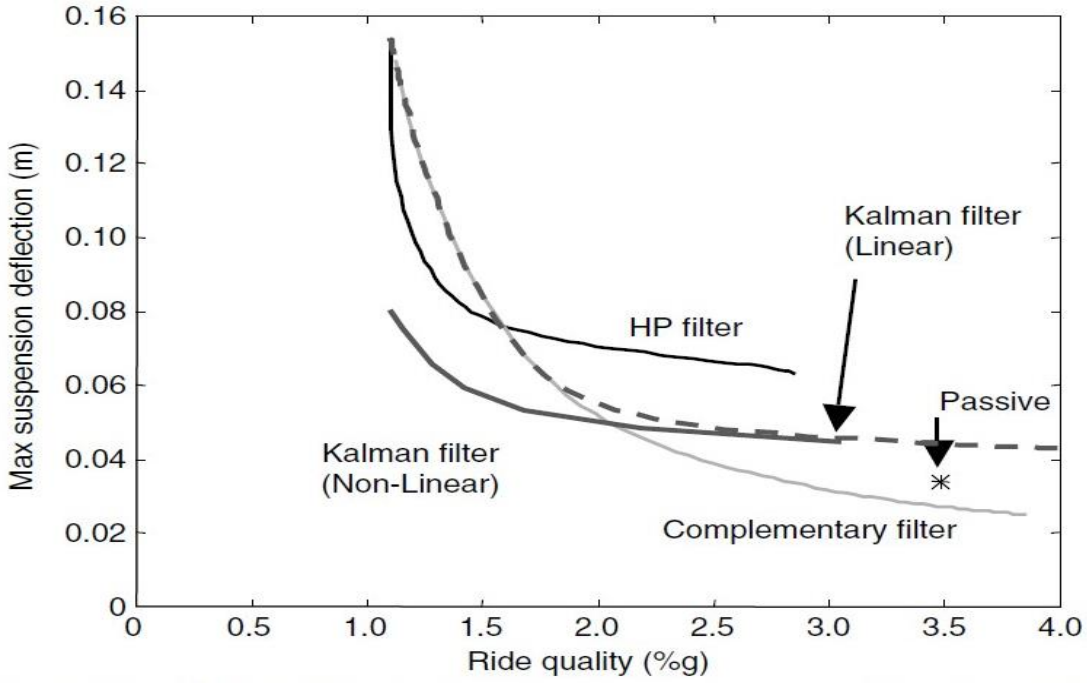

Figure 4.9:Trade-off between ride quality and suspension deflection[15]

Figure 4.9 illustrates typical trade-offs for different control approaches. An improvement of around 23% in ride quality can be achieved with the linear complementary filter control while keeping the defection damper at the same level as for passive suspension and Kalman filtering can result in an improvement of over 50% in ride quality.

4.5.2 Model Decomposition

Model decomposition is used to decouple interconnected motions. It is possible to apply different control strategies to different modes of vibration, enabling different design possibilities for the active system. In this study, a modal control structure is used for the skyhook controller to manage the bounce and pitch modes in the vertical suspension, as shown

in Figure 4.10(a) and to manage lateral and yaw motions in the lateral suspension, as shown in Figure4.10 (b).

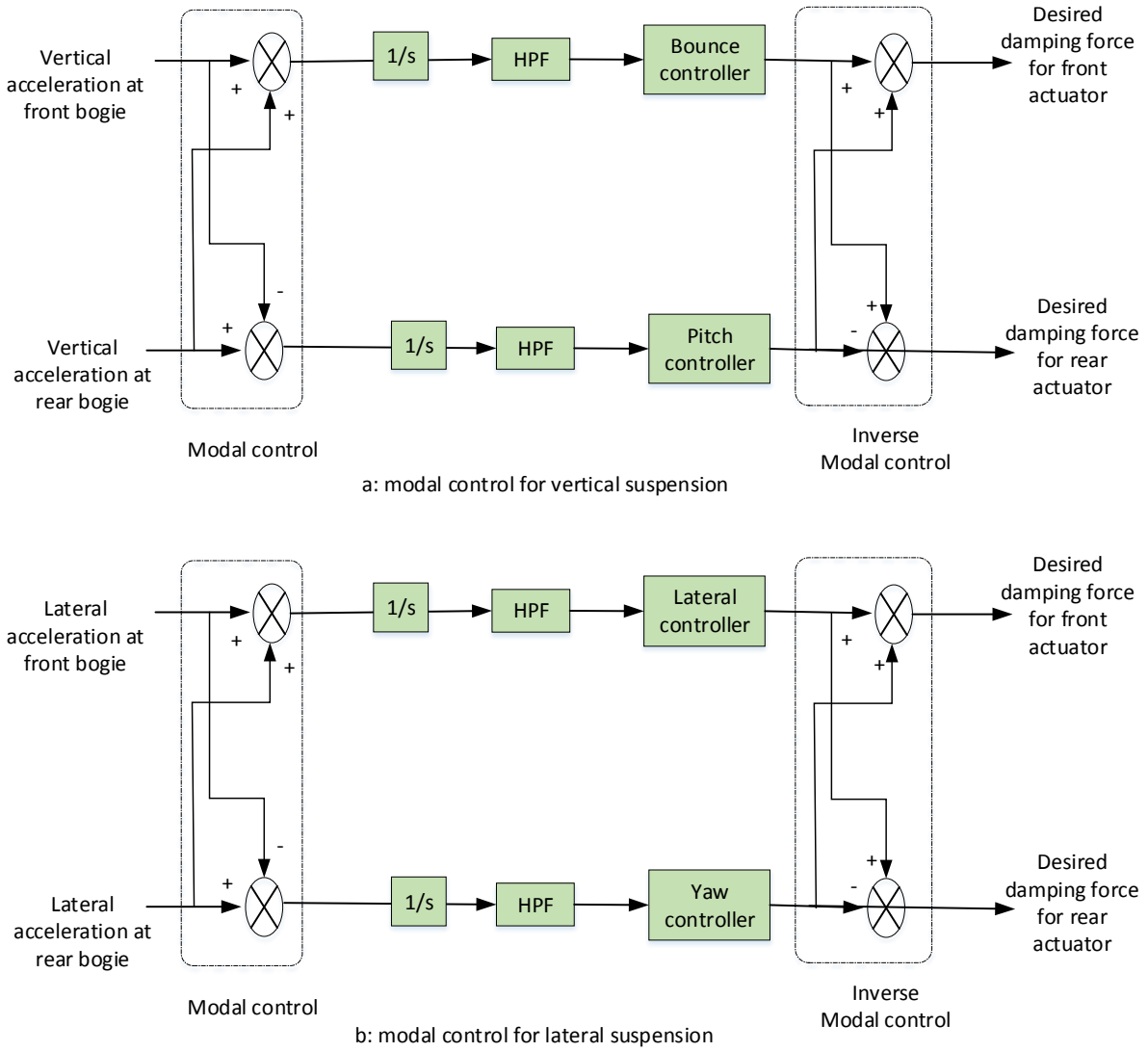

Figure 4.10: Schematic of the modal control diagram

The output measurements from the two bogies are decomposed to give feedback signals required by the skyhook controller to manage the bounce and pitch motion modes for vertical suspension or to manage lateral and yaw motions for lateral suspension, and the output command from the two controllers are then recombined to control the front and rear actuators/dampers accordingly.

4.6 Application of Full-Active Control to Vertical Suspensions

To make a performance comparison between suspension systems, sky-hook damping was used as the full-active control strategy, which is a simple and effective strategy by which to assess ride quality in full-active suspension systems. The modal control structure is used as the skyhook controller to manage the bounce and pitch modes for vertical suspension. These can be handled individually and recombined to drive the actuators. Figure 4.11 shows a full-active suspension system based on the modal control structure, with the relationships between vehicle velocities and actuator forces given by Equation 4.63 and 4.64 [58].

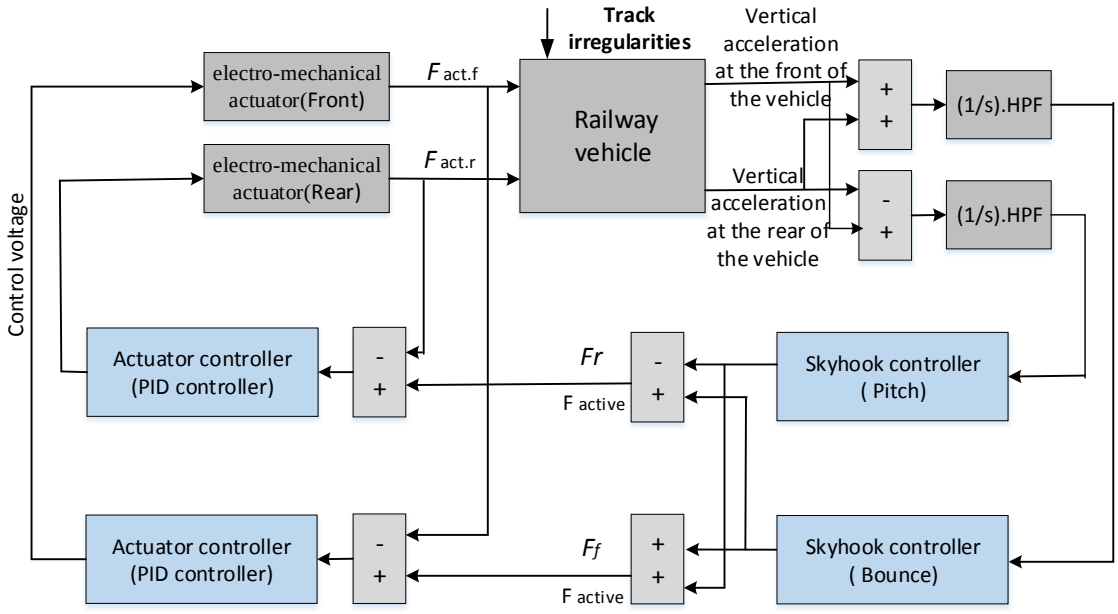

Figure 4.11: Schematic of the full-active of vertical suspension system based on the modal control structure

$$F_f = C_b \dot{z}_v + C_p l_t \,.\, \dot{\theta}_v \quad ----(4.63)$$

$$F_r = C_b \dot{z}_v - C_p l_t \,.\, \dot{\theta}_v \quad ----(4.64)$$

In these equations, $\dot{z}_v$ is bounce velocity of the vehicle, $\dot{\theta}_v$ is pitch angular velocity of the vehicle, and l_t is the half-longitudinal spacing of the secondary suspension, whereas $C_b \dot{z}_v$ and $C_p l_t \,.\, \dot{\theta}_v$ are the skyhook damping forces of bounce and pitch modes, which are these can be

processed individually and recombined to drive the actuators, F_f and F_r are the desired damping forces for the front and rear suspension, respectively. The skyhook damping coefficients of bounce and pitch controller (C_b, C_p) are chosen to give a good ride quality and ensure the suspension deflection does not pass the maximum allowed value of 55 mm.

As mentioned previously, the skyhook damping control provides a force dependent upon the absolute velocity of the vehicle body. Practically, the absolute velocity measurement is obtained by integrating the signal from an accelerometer, and in order to remove integrator drift, it becomes practical to integrate this with a high-pass filter. A high-pass filter (HPF) with a cut-off frequency of 0.16 Hz frequency is used both to dispose of long-term drift in the integrator and to minimise the suspension deflection due to deterministic track input. The electromechanical actuators replace conventional passive dampers between the vehicle and bogies.

Electromechanical actuator is selected as a practical solution achieves the main requirements for the full-active suspension systems, such as required force to size ratio, bandwidth, robustness weight, and maintainability. Figure 4.12 is shown the structure of the actuator [65].

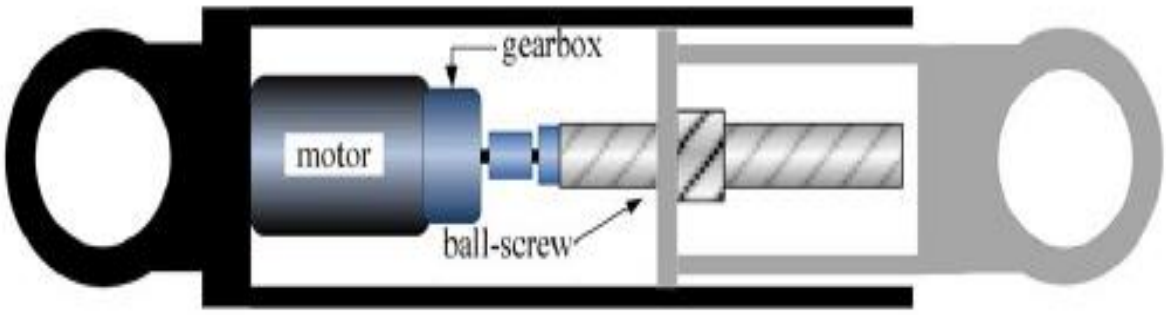

Figure 4.12: Diagrams of the electro-mechanical actuator [65]

The actuator consists of a combination of the direct current (DC) motor and the ball-screw mechanism set. The DC motor generates the required torque, and the ball-screw set converts

the rotation of the DC motor to the linear motion to provide the required damping force that works between the bogie and the vehicle body. For the equivalent electrical model of the DC motor, the governing equation is given by:

$$l_{arm}.\dot{i_a} = -r_{arm}i_a - k_e\dot{\theta_m} + v_a \quad \text{..... (4.65)}$$

Figure 4.13 shown an equivalent mechanical model of the electro-mechanical actuator. The gearing block represents a fixed kinematic ratio between motor shaft rotation and the linear displacement of the screw. Where the connection between the vehicle and the actuator is represented by the springs k_{sc} and k_m, whereas the damper c_{sc} represents the damping effect in the connection. The variable x_m is internal to the actuator, whereas x_{act} represents the relative displacement between the ends.

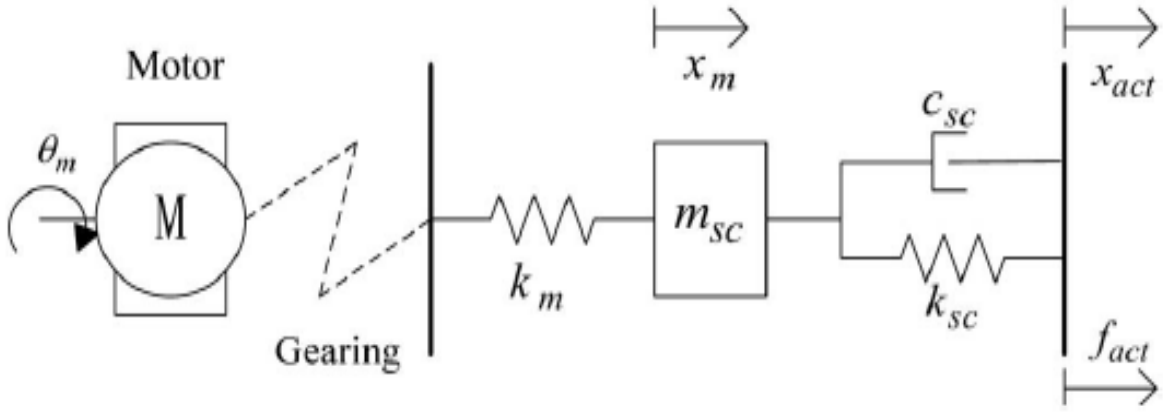

Figure 4.13: The equivalent mechanical model of the electro-mechanical actuator [65]

For the equivalent mechanical model of the electro-mechanical actuator, the governing equations are given by:

$$\ddot{\theta}_m.J_m = k_t.i_a - c_m.\dot{\theta}_m - k_m(n.x_m - n^2.\theta_m)$$

$$\ddot{x}_m.m_{sc} = k_m\,(n.\theta_m - x_m) + k_{sc}(x_{act} - x_m) + c_{sc}(\dot{x}_{act} - \dot{x}_m)$$

$$f_{act} = k_{sc}(x_m - x_{act}) + c_{sc}(\dot{x}_m - \dot{x}_{act}) \quad \text{..... (4.66)}$$

The variables and parameters of the electromechanical actuator are defined in Table 4.3.

Table 4.3:Variables and parameters of the electromechanical actuator[65]

Symbols	Description	Symbols	Description
X_{act}	The relative displacement of the actuator	k_m	Motor series stiffness (1 x 10^7 N/m)
X_m	Displacement of the ball-screw	c_m	Motor damping (8 x 10^{-5} N.m.s/rad
θ_m	The rotation angle of the motor	J_m	Motor inertia (3.67 x 10^{-4} kg.m^2)
f_{act}	Force generated by the actuator	n	Screw pitch (7.96 x 10^{-4} m/rad)
v_a , i_a	Voltage and current of the motor	k_t	Motor torque constant (0.297 N.m/A)
m_{sc}	Screw mass (2 kg)	k_e	Motor back-emf gain (0.297 V/rad/s)
k_{sc}	Screw stiffness (1.8 x 10^5 N/m)	l_{arm}	Winding inductance (3.7 mH)
c_{sc}	Screw damping (1.2 x 10^3Ns/m)	r_{arm}	Winding resistance(1.8Ω)

The full-active suspension controller generates the command damping force to the actuator. The track inputs will influence the dynamic system, which will effect actuator displacement. Therefore, the proportional-integral-derivative (PID) local controller for the electromechanical actuators is used in the study to maintain as close the generated actuator forces to the damping force demand as possible, as shown in Figure 4.14.

The PID controller is a control loop feedback mechanism widely used in industrial control systems. The PID controller is a simple design and offers a robust performance. The governing equation of the PID controller is shown as following[96]:

$$u = K_p e + K_i \int e dt + K_d \frac{de}{dt} \quad \text{..... (4.67)}$$

Where u is the control variable(control voltage), e is the error defined as $e = F_d - F_{act}$, $K_p$is the proportional feedback gain, K_i is the integral feedback gain, K_d is the derivative feedback gain, F_{act} is the generated actuator force and F_d is the desired damping force that generated by the system controller. Control gain for this local controller are tuned to match the out to the input at best possible level for the bandwidth of (0-14Hz) which is considered appropriate for the control of the secondary suspension.

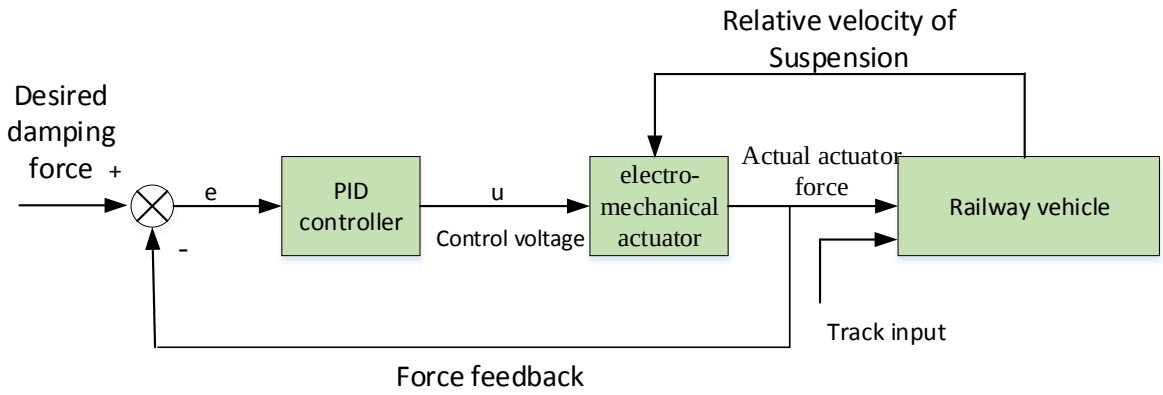

Figure 4.14: The PID local controller for the electromechanical actuator

4.7 Application of Full-active Control to Lateral Suspensions

In this section, the same structure of full-active control system with the electromechanical actuator that shown in Figure 4.11 is used, but the modal control structure is used in the system controller to manage the lateral and yaw modes in the lateral suspension. Figure 4.15 shows schematic of the full-active of lateral suspension system based on the modal control structure, with the relationships between vehicle velocities and full-active damping forces are given by Equation 4.68 and 4.69.

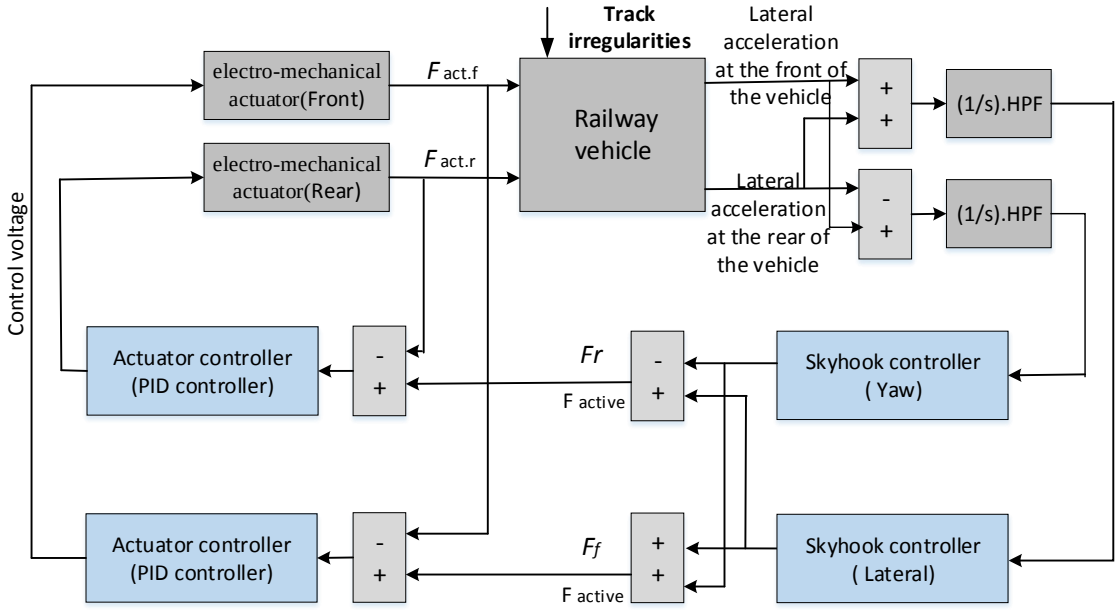

Figure 4.15: Schematic of the full-active of lateral suspension system based on the modal control structure

Equation 4.68 and 4.69 give the full-active forces:

$$F_f = C_l \dot{y}_v + C_y l \,.\, \dot{\varphi}_v \quad ----(4.68)$$

$$F_r = C_l \dot{y}_v - C_y l \,.\, \dot{\varphi}_v \quad ----(4.69)$$

Where F_f and F_r are the desired damping forces for the front and rear suspension, respectively, $\dot{y}_v$ is lateral the velocity of the vehicle, $\dot{\varphi}_v$ is yaw angular velocity of the vehicle, and l is the half-longitudinal spacing of the secondary suspension, C_l is skyhook damping gain of lateral controller, C_y is skyhook damping gain of yaw controller . The terms $C_l \dot{y}_v$ and $C_y l \,.\, \dot{\varphi}_v$ are the skyhook damping forces of lateral and yaw modes, which are these can be optimised individually and recombined to drive the actuators.

In practical, the absolute vehicle velocities that are required for skyhook damping will be obtained by integrating by the acceleration measurement, as shown in Figure 4.14. However, a pure integration will cause drift in the accelerometer. Therefore, a high-pass filter (HPF), which is inserted between the skyhook damping and the integrator, with a cut-off frequency of 0.16 Hz frequency, is used both to deduct of long-term drift in the integrator and to minimise the

suspension defalcation due to deterministic track input. The skyhook damping coefficients (C_l, C_y) for full-active forces (F_f , F_r) is normally determined based on a trial-and-error method by considering the magnitude of required damping force and tuned to achieve the best results by decreasing the RMS values for vehicle body accelerations.

As mentioned in preview section 4.6, the electromechanical actuators replace conventional passive dampers, between the vehicle and bogies. A PID local controller for the electromechanical actuators is used to maintain as close the generated actuator forces to the damping force demand as possible.

4.8 Conventional Semi-Active Suspension System

The semi-active control system integrated with the MR damper consists of a system controller and a damper controller. The system controller calculates the desired damping force according to the measured output. The damper controller then adjusts the command current applied to the MR damper to track the desired control force. Finally, the desired damping forces are approximately realised by the MR damper. Figure 4.16 shows the semi-active control system with the MR fluid damper.

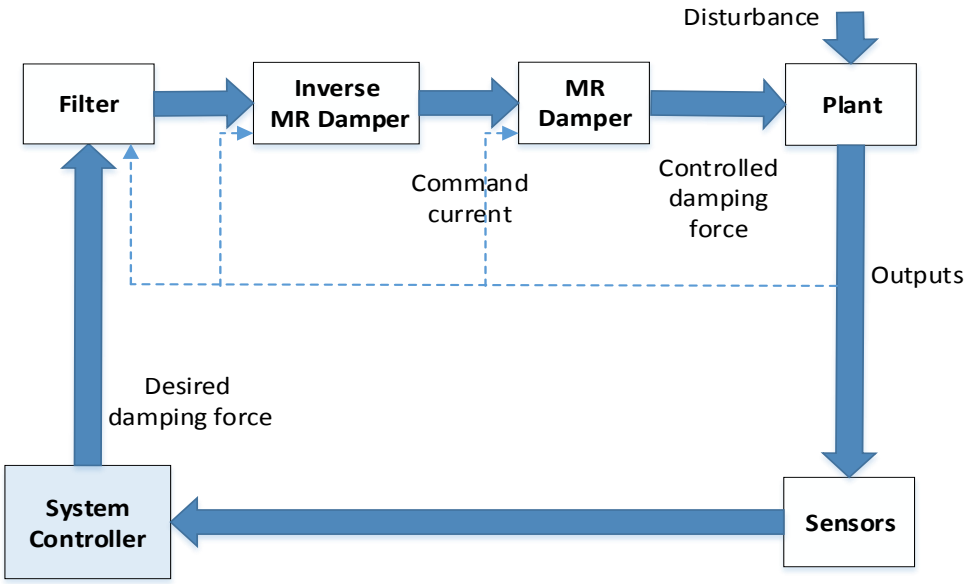

Figure 4.16: Schematic of the semi-active control system with the MR damper

As a classical semi-active control strategy, the skyhook damping control approach has been widely adopted to control semi-active suspension studies and is used in this study for performance comparison. The semi-active skyhook strategy can be described by the equations below[7]:

$$F_{sa.front} = \begin{cases} F_f\ , & F_f.\Delta V_f \geq 0 \\ C_{min}\ \Delta V_f\ , & F_f.\Delta V_f < 0 \end{cases} \quad ---(4.70)$$

$$F_{sa.rear} = \begin{cases} F_r\ , & F_r\Delta V_r \geq 0 \\ C_{min}\ \Delta V_r\ , & F_r.\Delta V_r < 0 \end{cases} \quad -----(4.71)$$

where $F_{sa.front}$ and $F_{sa.rear}$ are the desired semi-active damping forces at the front and rear dampers that can be tracked by the MR dampers, F_f and F_r are full-active damping forces, ΔV_f and ΔV_r are MR damper front and rear relative velocities, and C_{min} is minimum damping setting when the control current is minimum (I_{min}). The switching policy turns on the minimum damper setting when velocity reverses because this would otherwise require a

negative damper setting. In this case, the semi-active controller will simply employ a minimum damping setting.

4.9 Summary

In this chapter, the modelling of the conventional railway vehicle in vertical and lateral directions are presented. Vehicles with passive suspension, full-active and conventional semi-active controls are introduced as benchmarks and are used for comparative assessment of the proposed semi-active controlled suspension design.

In this study, a model decomposition is used to decouple interconnected motions, which is used for the full-active controller to manage the bounce and pitch modes in the vertical suspension and to manage lateral and yaw motions in the lateral suspension. In order to make performance comparisons between suspension systems, the skyhook damping control strategy is used as the full-active control strategy, which is a simple and effective strategy to assess the ride quality in full-active suspension systems.

The conventional semi-active control system integrated with the MR damper, which consists of a system controller and a damper controller, is presented as a benchmark. As a classical semi-active control strategy, the skyhook damping control strategy is adopted to control semi-active suspension and is used in this study for performance comparison.

In semi-active control, the tracking of the desired force is the main issue. In particular, the semi-active damper cannot develop a positive force when the relative velocity reverses because it is only possible to dissipate energy. The force that is available for a semi-active damper is based upon its minimum and maximum levels of damping setting. This limitation upon controllability restricts the performance of a semi-active suspension system.

CHAPTER FIVE

5 DYNAMICS OF THE MR DAMPER

5.1 Introduction

The magnetorheological (MR) damper is a semi-active control device that has recently received a great deal of attention from the vibration control community. The MR damper is a device that uses the MR fluid to adapt its mechanical properties. The unique characteristics of MR dampers such as low power consumption, large damping force range, consistent efficacy across temperature variations, fast response time, essential system stability (no active forces generated), and safe-mode operation in case of failure are have made them attractive devices for semi-active control in suspension applications[97].

5.2 MR Fluid

The MR fluid consists of micro-sized ferromagnetic particles such as iron particles that are suspended in a carrier fluid. In the absence of a magnetic field, the particles are randomly distributed, and the MR fluid will be free-flowing with a solidity similar to liquid oil, and the particles are in a formless state, as shown in Figure 5.1(a). When the magnetic field is applied, the particles are polarised and attract each other in accordance with the magnetic field path, as shown in Figure 5.1(b), and the particles form chains, as shown in Figure 5.1(c). This results in chains of particles within the fluid which increase its viscosity. The MR fluid accordingly changes from liquid to that of semi-solid behaviour on a fast timescale [98-100].

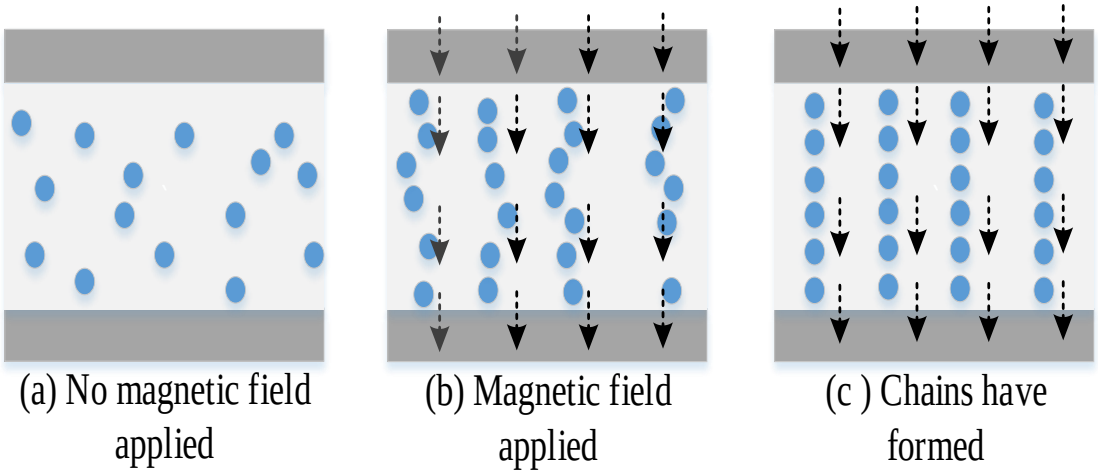

Figure 5.1: Changes to ferromagnetic particles in an MR fluid

As a result, MR fluids can reversibly and rapidly change from a liquid type behaviour to a semi-solid in a millisecond with controllable yield strength when subjected to a known magnetic field[101].

5.3 MR Damper

The MR damper consists of MR fluid belonging to the type of controllable fluids that show the ability to change from liquid-type behaviour to that of semi-solid when subjected to an external magnetic field. The MR damper achieves the essential performance criteria such as continuous controllability of dynamic range and fast response, low power consumption, and temperature stability. The unique characteristics of MR dampers have made them suitable for semi-active energy-dissipating applications in suspension applications [99, 102, 103]. In MR dampers, varying the control current flow to coils seated on the piston allow the dynamical properties of the MR fluid to be modified and, as a result, change the viscous damping coefficient. MR dampers typically consist of a piston, magnetic coils, seal, bearing, accumulator, and a damper chamber filled with the MR fluid. Figure 5.2 shows a Lord RD-1005-3 MR fluid damper[104].

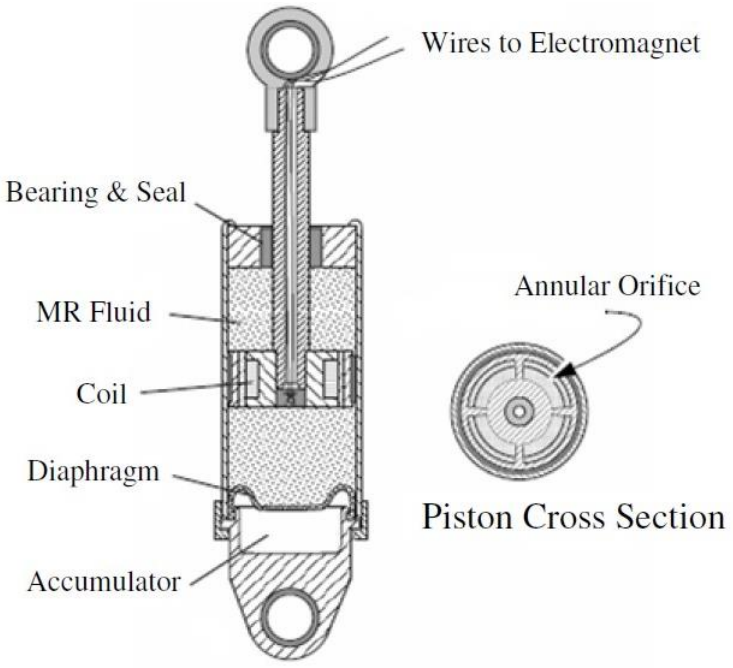

Figure 5.2: Cross-section of typical MR fluid damper[104]

5.4 Modelling of the MR Fluid Damper

There is a considerable body of the literature that has considered MR damper modelling, and various models have been developed based on sets of well-suited functions [105]. Spencer et al.[106] successfully developed a phenomenological model to simulate the dynamic behaviour of the damper. The model is capable of predicting the response of the MR damper over a wide range of loading while under a constant or variable voltage signal. The model proposed by Spencer et al. is governed by seven simultaneous differential equations containing 14 parameters. The parameters are obtained according to a constrained nonlinear optimization technique such that the model closely emulates the behavioural data of the damper as obtained experimentally. A novel MR damper designed by Lau and Liao [84] was developed through the design, fabrication, and testing stages to ensure suitability for railway vehicle suspension in order to improve ride comfort. Wang and Liao [89]used phenomenological model proposed by into to integrate the MR damper dynamics with the secondary suspension of the railway vehicle to improve ride quality. Bideleh, Milad used a

Bouc-Wen model to integrate the MR damper dynamics with the primary suspension of a railway vehicle to investigate the effects of semi-active control on wear, safety and ride comfort.

In this study, a modified Bouc-Wen model was used to represent the dynamic behaviour of prototype MR damper developed by Zong and Gong[28]. It has been specifically designed for railway vehicles. The modified Bouc-Wen model, which is described by the equations and the parameters are explained in the next section.

5.4.1 Modified Bouc–Wen Model for MR Damper

In this section, the dynamic phenomenological model is introduced to describe the dynamic performance of a prototype MR damper designed for railway vehicles by Zong and Gong [28]. The mechanical equivalent model is shown in Figure 5.3.

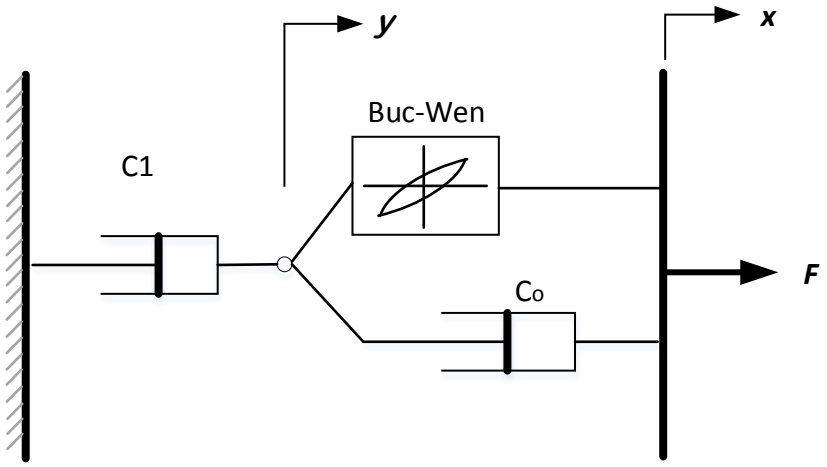

Figure 5.3: The modified Bouc–Wen model for the MR damper

A modified Bouc–Wen model is based on the phenomenological model, which is represented by the following equations (5.1) – (5.6):

$$F = c_1\dot{y} \quad \text{..... (5.1)}$$

$$\dot{y} = \frac{1}{c_0+c_1}\left[\alpha z + c_0\dot{x}\right] \quad \text{..... (5.2)}$$

$$\dot{z} = -\gamma|\dot{x} - \dot{y}|z|z|^{n-1} - \beta(\dot{x} - \dot{y})|z|^{n} + A(\dot{x} - \dot{y})$$..... (5.3)

Where F is the damping force, c_1 is represents the viscous damping at low velocities, the parameters c_0 represents the viscous damping at high velocities, x is the piston relative displacement, y is the internal displacement of the damper and z is the evolutionary variable, and α is a scaling value for the Bouc–Wen model. The parameters γ, β, A, *n* are parameters used to adjust the scale and shape of the hysteresis loop, respectively.

In order to determine the MR damper model that is valid for fluctuating magnetic fields, it is necessary to determine the functional dependence of the parameters on the applied current. The viscous damping constant (c_0) and yield stress of the MR fluid ($\propto$) is directly dependent on the magnetic field strength[28, 106], therefore the parameters c_0 and α are assumed to be a functions of the applied current (I), as shown in equation (5.5) and (5.6).

$$\propto = \propto_a + \propto_b I + \propto_c I^2$$..... (5.4)

$$c_0 = c_{0a} + c_{0b} I$$ ..... (5.5)

Consequently, experimentally validated results for the MR damper with application in railway vehicle given in [28] are chosen for analysis here. The optimum values of parameters for the MR damper model are listed in Table 5.1[28]

Table 5.1:MR damper parameters[28]

Symbols	Description
C_{oa}	8.4 N s mm^{-1}
C_{ob}	11.23 N s mm^{-1}A^{-1}
$\propto_a$	40 N mm^{-1}
$\propto_b$	2036.8 N s mm^{-1}A^{-1}
$\propto_c$	-535.95 N s mm^{-1}A^{-2}
C_1	the viscous damping at low velocities (91.6 Ns mm^{-1})
β	parameters used to adjust the scale and shape of the hysteresis loop (0.15 mm^{-2})
A	parameters used to adjust the scale and shape of the hysteresis loop (0.45)
γ	parameters used to adjust the scale and shape of the hysteresis loop (0.15 mm^{-2})
n	parameters used to adjust the scale and shape of the hysteresis loop (2)

Finally, to assure that the modified Bouc–Wen model accurately predicts the MR damper behaviour is given in [28], the damping force versus velocity are introduced as shown in Figure 5.4 and Figure 5.5, where I is the control current ,which can be changed from 0~1.2A, and the excitation inputs (sinewave) applied across the MR damper were 1 Hz frequency, ±20 mm amplitude and 2 Hz frequency, ±15 mm amplitude, respectively.

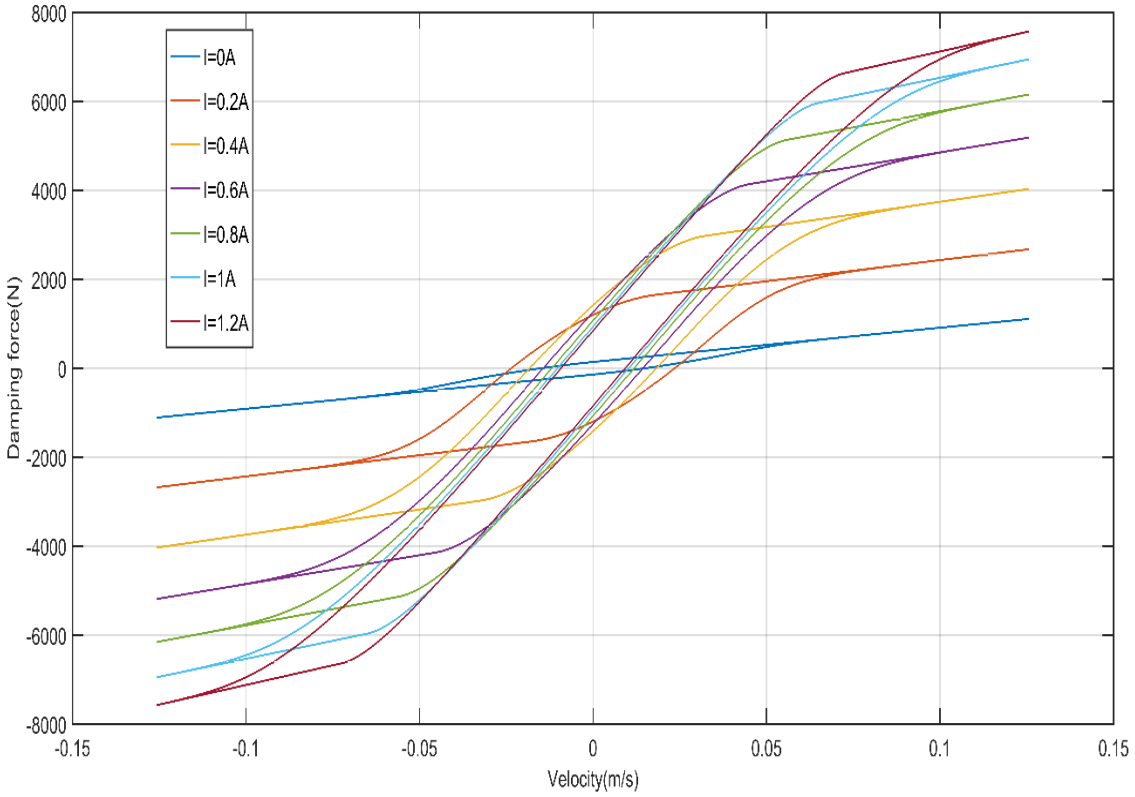

Figure 5.4: The damping force versus velocity (1 Hz, ±20 mm/s)

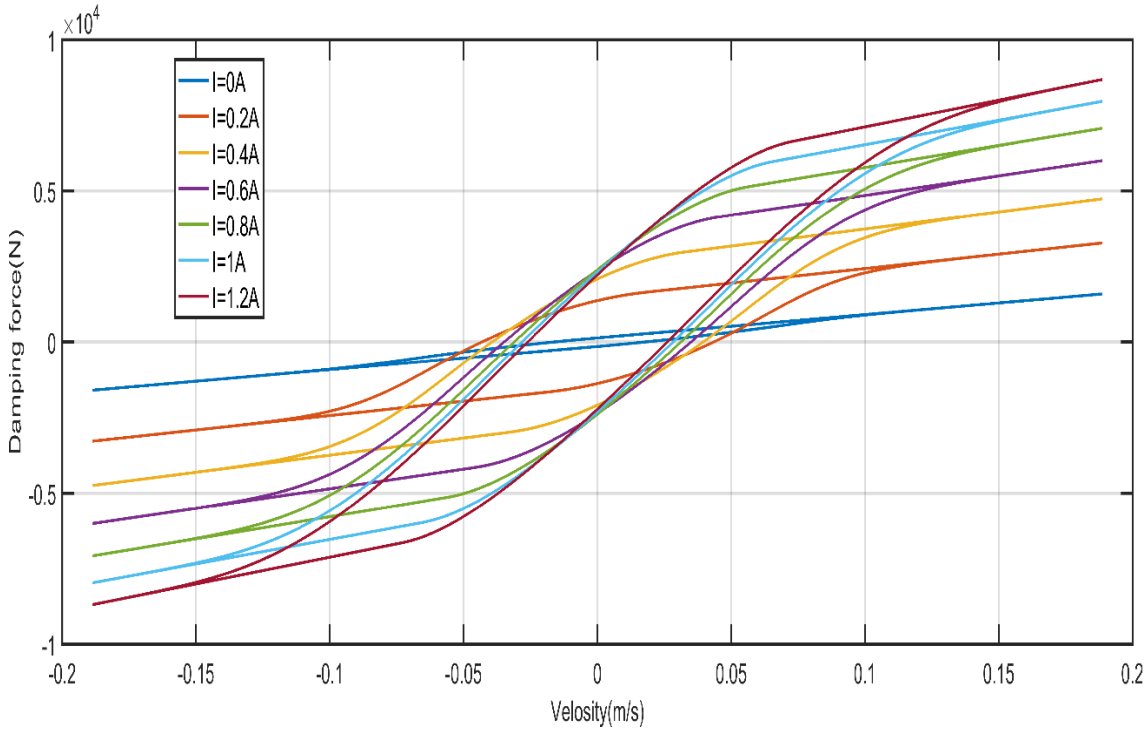

Figure 5.5: The damping force versus velocity (2 Hz, ±15 mm/s)

From Figure 5.4 and Figure 5.5, it is observed that the damping force is not centred at zero. This behaviour in the damping force is due to the stiffness associated with the accumulator in the MR damper (see Figure 5.2), which acts as a spring in the MR damper. The accumulator is necessary to prevent cavitation in the MR fluids during normal operations. In addition, from Figure 5.4 and Figure 5.5, it observed that for large velocity, the force in the damper varies linearly with velocity. However, as the velocity decrease and before it becomes zero, the force-velocity relationship is no longer linear. This type of behaviour in the force at small velocity is due to bleed of MR fluid between the cylinder and the piston, which is necessary to eliminate harshness of the MR damper.

5.5 Local Controller for MR Damper Based Semi-Active Systems

MR dampers are favourable semi-active devices in which the viscosity of an MR fluid can be controlled depending on a control current. In order to use the MR damper to control vibrations efficiently, the necessary control current to the MR damper to generate the required damping force should be determined.

The MR damper control current is determined based on the semi-active control strategy in use. One of the most popular strategies is the on-off swathing control law [107]. The MR damper is set to a relatively low damping rate by applying the minimum current control as the passive on low mode (off swathing). When swathing control law is on, the MR damper will be set to a relatively high damping rate by applying a maximum current control as the passive on high mode. The applied current for the MR damper can vary between a minimum and maximum current control, but the MR damper with too low or too high damping is not favourable in a suspension system [84].

However, there are several alternative methods to specify the relationship between the desired damping force for the MR damper and control current. Wang et al.[85] used a Signum function as the damper controller to generate the desired control current for the MR damper.

Because of the highly nonlinear features of the MR damper, as well as the complexity of a mathematical description of its behaviour, the nonlinear technique are used as a local controller for MR damper. The inverse MR damper models are used to obtain the control current according to the desired force in actual application, for which suitable model relating the force generated by the damper to the piston velocity and current driving the coil has to be identified based on data derived from specially designed experiments. The adaptive neuro-fuzzy inference system (ANFIS) technique has been investigated to build the inverse MR damper model [28, 85, 108]. Neural network and system identification technique have been investigated to build the inverse MR damper model[109]. Wang and Hu [110] presented a novel technique to the model inverse model of the MR damper by using the universal approximation of neuro-fuzzy systems in which two different neuron-fuzzy systems are designed to identify the inverse models on the basis of the ANFIS.

In this study, the inverse MR damper model using a lookup table is introduced to obtain the control current according to the desired damping force, which is illustrated in the following section.

5.6 Inverse Model of MR Damper

The inverse MR damper model was used to obtain the command current according to the desired force in the actual application. The lookup table technique, which possesses universal approximations to the nonlinear system was used to build the inverse MR damper model. Figure 5.6 illustrates the lookup table for the inverse model of the MR damper.

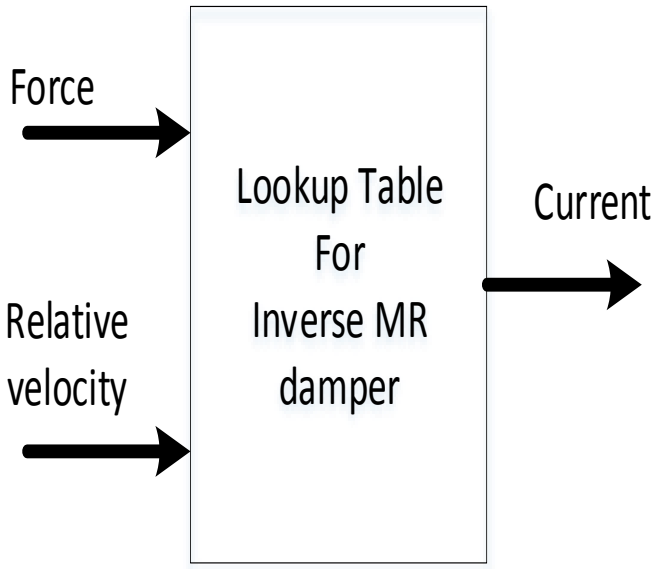

Figure 5.6: Lookup table for the inverse model of MR Damper

The lookup table for the inverse model of the MR damper generates the command current by using the damping force and relative velocity as inputs. For building lookup table, the desired damping force is recorded according to the particular velocity and specific current inputs applied to the MR damper. Then, the recorded data are used to build the lookup table for the inverse model of the MR damper, as shown in Table 5.1.

Table 5.1 shows the lookup table of the command current that is used to control the positive damping force of the MR damper, where (I) is the control current which can be changed from 0~1.6A dependence on desired damping force (F) and relative velocity(ΔV). In order to control the reverse damping force of the MR damper, the lookup table of the command current as shown in Table 5.1 is used, with changes the inputs direction for the reverse.

Table 5.2: Lookup table for the inverse model of MR damper

	F1=F_{min}	F2= 799N	F3= 920N	F4= 1373N	...	...	F_{max}
ΔV1=0.01	I_{min}	0.080645A	0.13226A	0.2A	…	I_{max}	I_{max}
ΔV2=0.03	I_{min}	0.06A	0.09354A	0.1406A	…	I_{max}	I_{max}
ΔV3=0.06	I_{min}	0.028A	0.045A	0.1A	…	…	I_{max}
ΔV4=0.09	I_{min}	0.005A	0.013A	0.07A	…	…	I_{max}
…	I_{min}	…	…	…	…	…	I_{max}
…	I_{min}	I_{min}	…	…	…	…	I_{max}
ΔV_{max}	I_{min}	I_{min}	I_{min}	…	…	…	I_{max}

In order to validate the inverse model, the single mass model with semi-active skyhook controller is used as a benchmark as shown in Figure 5.7.

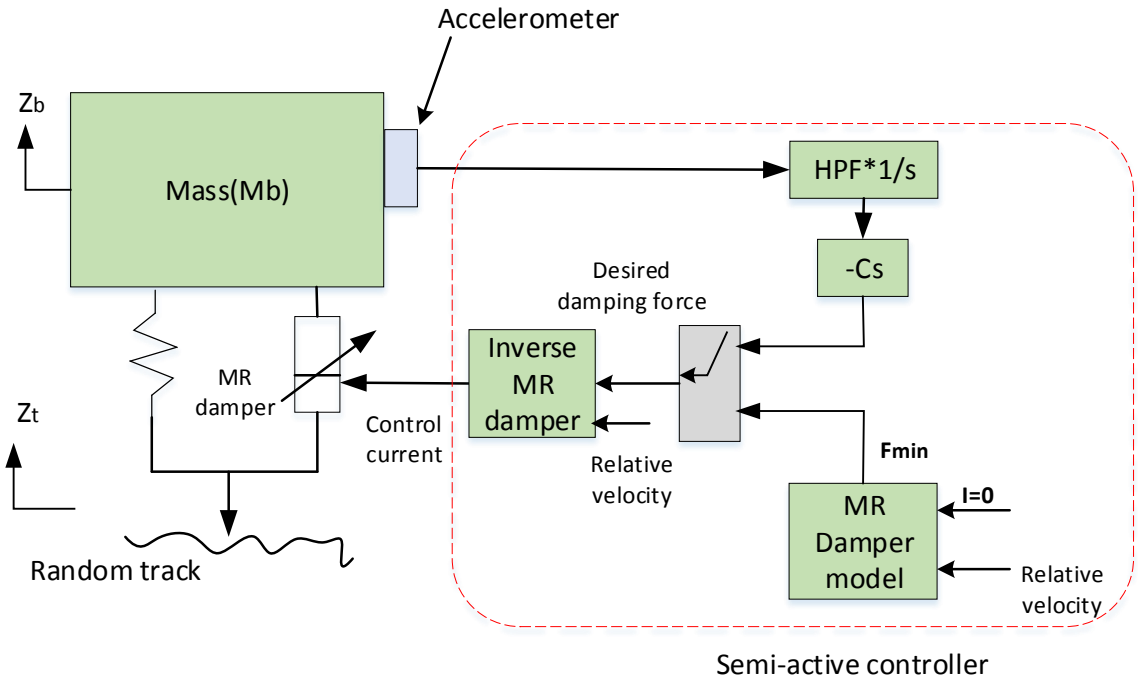

Figure 5.7: Single mass model with semi-active controller

The governing equation of motion for the single mass model is shown below:

$$m_{b.}\ddot{z}_b = -F_{MR} - k(z_b - z_t) \ldots\ldots\ldots \quad (5.6)$$

Whereas z_b is the displacement of body, z_t is the track inputs to the system, $m_{b.}$ is the mass of the body (7500kg), k is damping stiffness (1022 kNm-1), and F_{MR} is the MR damper force.

For simplicity and investigating MR damper dynamics in the suspension system, a skyhook damping is used a semi-active control strategy. The semi-active skyhook strategy can be described by the equations below:

$$F_{sa} = \begin{cases} c_s.\dot{z}_b\ , & (c_s.\dot{z}_b).(\dot{z}_b - \dot{z}_t) \geq 0 \\ F_{min}\ , & (c_s.\dot{z}_b).(\dot{z}_b - \dot{z}_t)\ < 0 \end{cases} \quad \ldots\ldots\ldots\ldots\ldots\ldots \quad (5.7)$$

Whereas F_{sa} is the desired semi-active damping force, c_s is skyhook damping gain, ($c_s.\dot{z}_b$)is the active control forces, F_{min} is the minimum damping force.

When the relative velocity across the MR damper is in the same direction of the velocity of the sprung mass, a control current is applied to the MR damper by using the lookup table inverse model. Otherwise, no damping force is required. However, for MR damper it is impossible to provide a zero force. Therefore, we should minimise the semi-active damping force by setting the input current at zero. In this study, the operating range for the damping force between F_{min}, which gives the minimum damping coefficient (C_{min}) when $I_{min} = 0\ A$, and F_{max} which gives the maximum damping coefficient (C_{max}) when $I_{max} = 1.6\ A$.

The damping forces are generated and compared under various excitation conditions as shown in Figure 5.8.

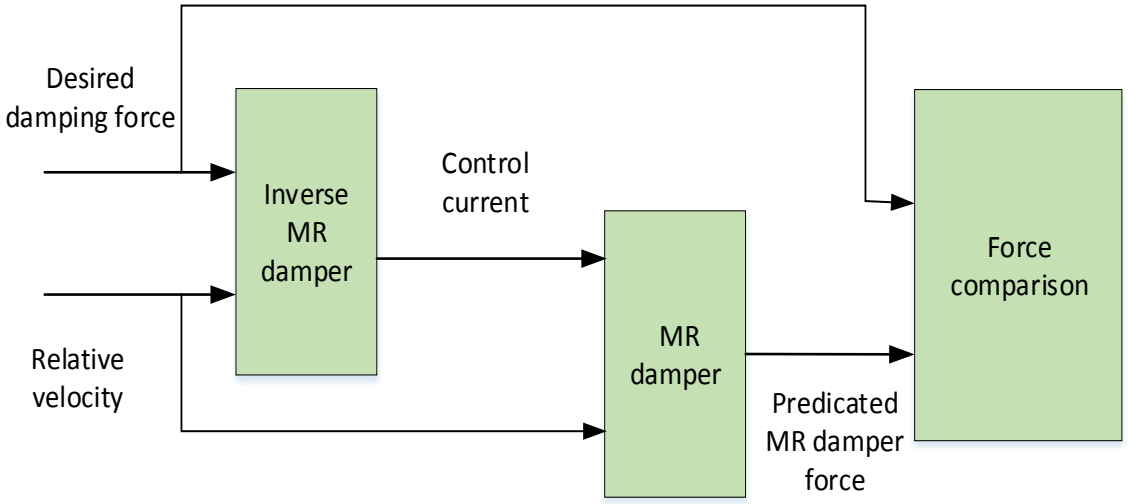

Figure 5.8: Validation of the inverse model

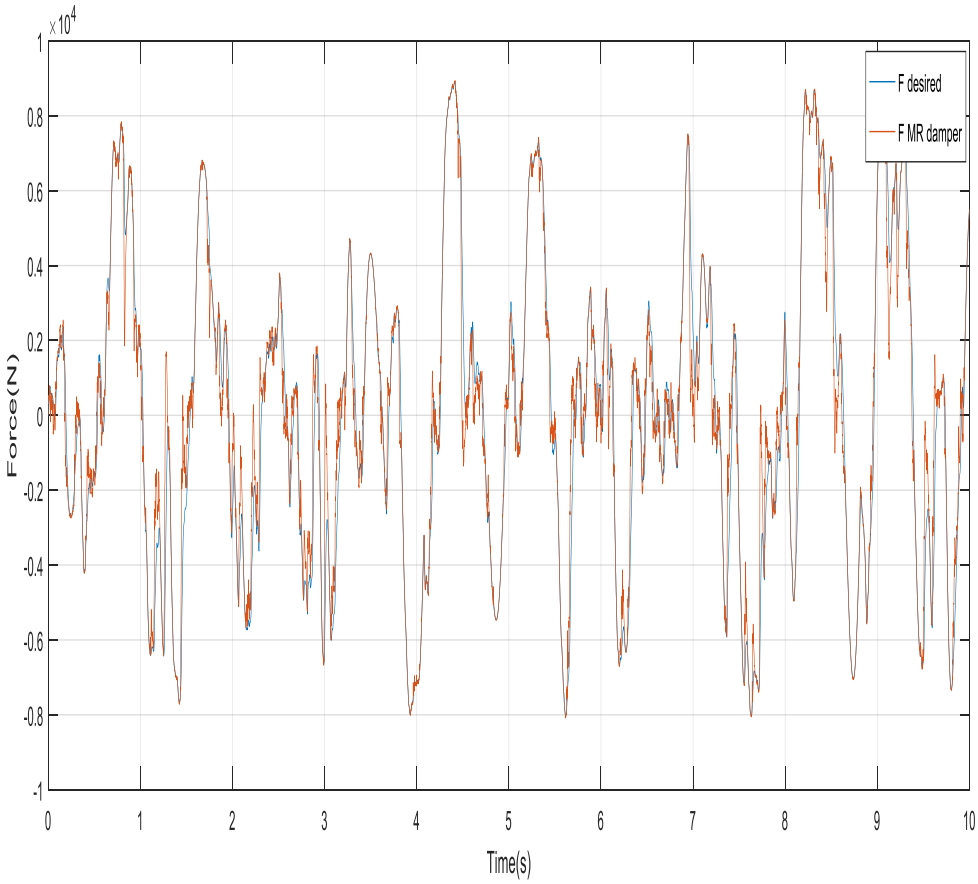

Figure 5.9: Comparison of MR damper forces under the random track

Figure 5.9 shows the desired damping force generated by the semi-active controller synchronises with the damping force generated by the control current. It can be seen from Figure 5.9 that when using the lookup table inverse model of MR damper, the MR damper force closely follow the desired damping force, which indicates that the lookup table inverse model of MR damper can satisfy the needs of semi-active control requirements, with which the inverse model is used to track the desired damping force.

5.7 Summary

In this chapter, magnetorheological (MR) dampers, which can change the damping ratio by suitable magnetic fields, have been studied for semi-active suspensions. The unique characteristics of MR dampers such as fast response time, large damping force range, low power consumption, consistent efficacy across temperature variations, essential system stability, and safe-mode operation in case of failure are have made them attractive devices for semi-active control in suspension applications.

The dynamic phenomenological model is introduced to describe the dynamic performance of a prototype MR damper. The modified Bouc-Wen model was used to represent the dynamic behaviour of prototype MR damper. The simulation results show that the model is capable of predicting the response of the MR damper over a wide range of excitation inputs while under a constant or variable current signal.

Then, in order to use the MR damper to efficiently control vibrations, the control current to the MR damper to generate the required damping force is introduced. Because of the highly nonlinear features of the MR damper, as well as the complexity of a mathematical description of its behaviour, the inverse model technique is used as a local controller for MR damper. In this study, the inverse MR damper model using a lookup table is introduced to obtain the control current according to the desired damping force. The simulation results show that the

lookup table inverse model of MR damper can satisfy the needs of semi-active control requirements.

CHAPTER SIX

6 SEMI-ACTIVE SUSPENSIONS BASED ON GAIN-SCHEDULING CONTROL

6.1 Introduction

In recent years, various control strategies have been presented for the semi-active suspension systems to achieve a competitive level of performance. A wide range of semi-active control strategies have been experimentally tested for semi-active suspension systems to improve the ride quality of railway vehicles.

However, the findings published so far indicate that there appears to be a ceiling on performance improvements with the control strategies that have been proposed, which is approximately the half of what can be achieved with the full active control. This is mostly due to semi-active devices such as MR dampers being essentially passive components that are only capable of providing active control forces by dissipating energy, as they switch to work as passive dampers when the control laws demand energy injection. In this case, the semi-active controller will simply employ a minimum damping setting, and hence cannot generate the necessary forces in the same way as the full-active control in such conditions.

In this study, a semi-active control strategy based on gain-scheduling control is presented to overcome the constraints of the conventional semi-active control strategies and to control the dynamics of semi-active suspensions to achieve a ride quality close to that of full-active control suspensions. Gain scheduling is an approach to the control of non-linear systems that employs a group of linear controllers, where each controller provides satisfactory performance control for a different operating condition of the system. The gain-scheduling strategy is realised using a set of controllers whose gains are adjusted as a function of scheduling variables that represent the current operating conditions. The gain-scheduling approach has been

successfully and widely applied in fields ranging from process control to aerospace [111-113]. The gain-scheduling strategy, which has a form of adaptive ability, is used to design the nonlinear semi-active controller. This kind of adaptive capability with gains that are automatically adjusted as a function of the operating condition is used for adaptive adjustment (gain scheduling) of controller parameters depending on the working state of the system.

6.2 Semi-Active Controller based on Gain-Scheduling

In order to achieve the semi-active constraint and performance requirement, a generalised control scheme is designed as shown in Figure 6.1.

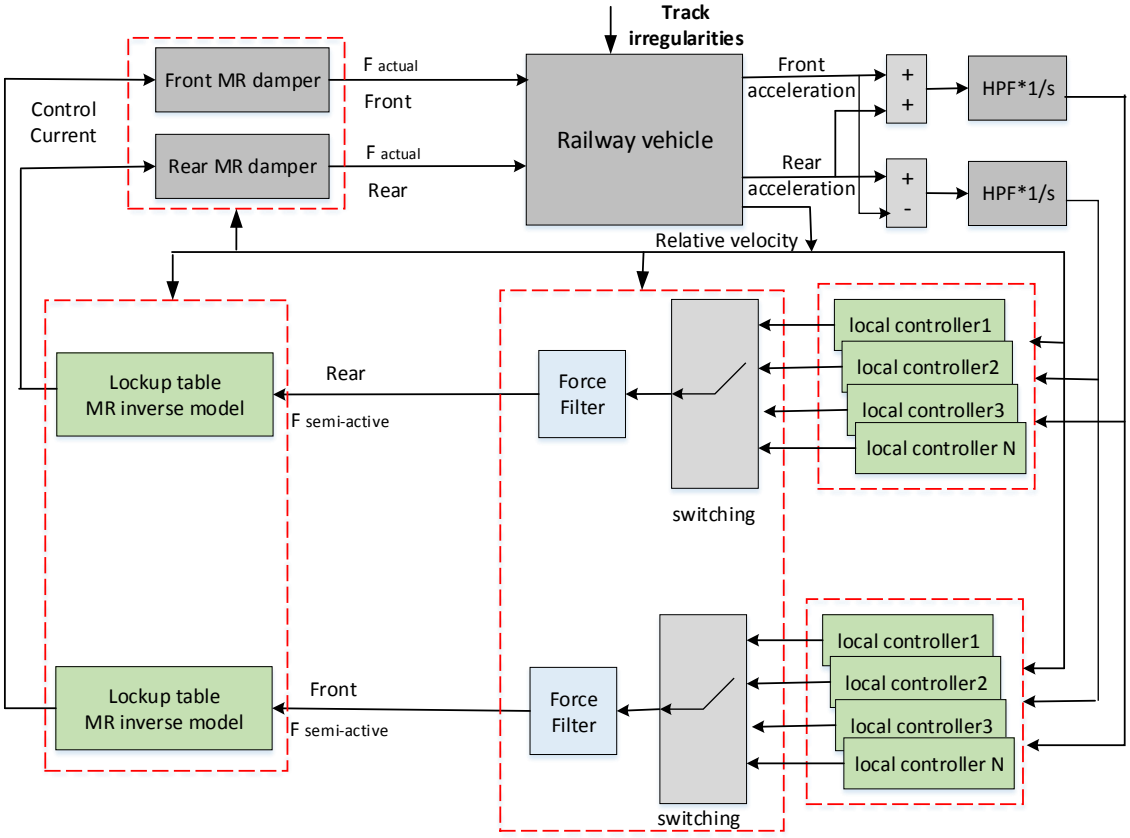

Figure 6.1: Semi-active suspension based on gain scheduling

In this configuration, the required absolute velocity signals are obtained by integrating the signal measured by a sensor accelerometer on the front and rear suspensions. Then, the velocity signal is high-pass filtered in order to remove integrator drift and then used to generate the

desired force. The system controller generates the desired damping force depending on the operating condition by using a group of linear controllers, where each linear controller generates the desired damping force by using the skyhook control structure with a set of gain scheduling of different stiffnesses and damping coefficients. Then, the decision maker (the switching process) in the control algorithm will select the desired damping force that satisfies the performance control and the passive constraints. Then, the force filter is used to make the frequency of the desired force concentrate in the frequency range of the railway vehicle system and remove high frequency harmonic the impact of rapid switching between controllers.

Then, the lookup table inverse model of the MR damper (the damper controller) is used to generate the control current to track the desired damping force. Finally, the desired damping forces are approximately realised by MR damper.

6.3 Control Strategies

The proposed design of the control strategy is focussed on minimising the use of the minimum damper setting by using a gain-scheduling structure control. The gain-scheduling structure controller is used to generate the desired damping forces in order to achieve the appropriate conditions to keep the dampers within their normal working range as much as possible. The desired damping force is generated using the control structure with a set of different stiffness and damping parameters that provides forces dependent upon the absolute velocity of the vehicle body and relative displacement of the suspension.

In the proposed gain-scheduling strategy, the desired damping force for each controller is generated using the skyhook control as per a set of different damping and stiffness parameters that provides desired forces dependent upon the absolute velocity of the vehicle and the relative displacement of the damper. Using a variable stiffness parameter and a variable damping coefficient, a semi-active controller can adapt to different running conditions.

A decision-making procedure in the control algorithms will then determine and select the desired damping force that satisfies the passive constraints. Finally, the damper controller adjusts the command current applied to the MR damper to track the desired control force.

Equations (6.1-6.2) describes the use of variable damper settings with a variable stiffness in order to generate the desired forces to minimise the using minimum damper setting for front and rear damper of the vertical suspension, as shown in Figure 6.2.

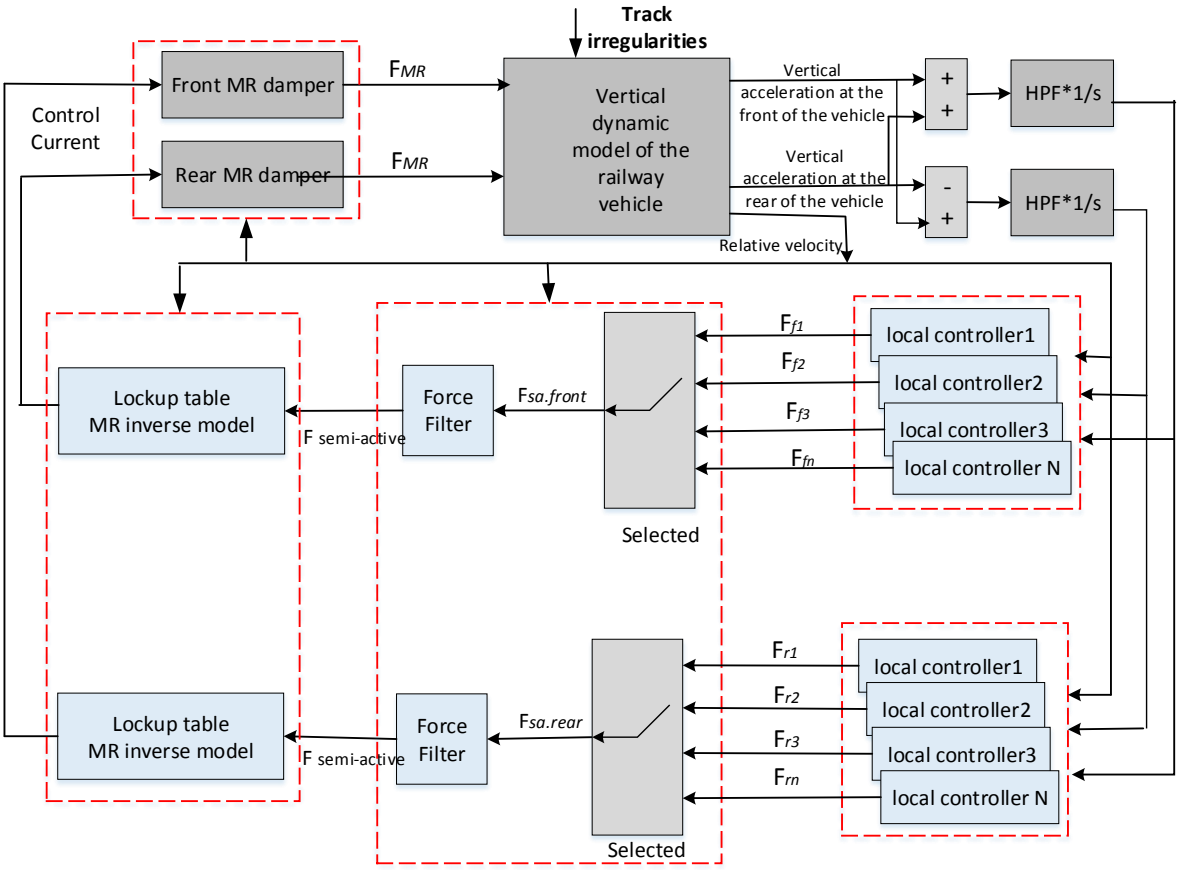

Figure 6.2: Semi-active control based on gain scheduling for vertical suspension model

The desired damping force for front damper of the vertical suspension:

$$F_{f1} = C_{b1}\dot{z}_v + C_{p1}l_t\,.\,\dot{\theta}_v + k_{vs1}\,(Z_f - Z_{bf})$$

$$if \quad F_{f1}(\dot{Z}_f - \dot{Z}_{bf}) \geq 0 \quad \overset{select}{\longrightarrow} \quad F_{sa.front} = F_{f1}$$

Otherwise

$$F_{f2} = C_{b2}\dot{z}_v + C_{p2}l_t\,.\,\dot{\theta}_v + k_{vs2}\,(Z_f - Z_{bf})$$

$$if \quad F_{f2}(\dot{Z}_f - \dot{Z}_{bf}) \geq 0 \quad \overset{select}{\longrightarrow} \quad F_{sa.front} = F_{f2}$$

Otherwise

$$F_{f3} = C_{b3}\dot{z}_v + C_{p3}l_t\,.\,\dot{\theta}_v + k_{vs3}\,(Z_f - Z_{bf})$$

$$if \quad F_{f3}(\dot{Z}_f - \dot{Z}_{bf}) \geq 0 \quad \overset{select}{\longrightarrow} \quad F_{sa.front} = F_{f3}$$

Otherwise

$$F_{fn} = C_{bn}\dot{z}_v + C_{pn}l_t\,.\,\dot{\theta}_v + k_{vsn}\,(Z_f - Z_{bf})$$

$$if \quad F_{fn}(\dot{Z}_f - \dot{Z}_{bf}) \geq 0 \quad \overset{select}{\longrightarrow} \quad F_{sa.front} = F_{fn}$$

Otherwise

$$if \quad F_{fn}(\dot{Z}_f - \dot{Z}_{bf}) < 0 \quad \overset{select}{\longrightarrow} F_{sa.front} = C_{min}\ (\dot{Z}_f - \dot{Z}_{bf}) \text{ -------- (6.1)}$$

Where F_{f1} , F_{f2} , F_{f3} , and F_{fn} are a set of different full-active damping forces. $F_{sa.front}$ is the desired semi-active damping force at the front suspension that can be tracked by the MR damper.

The desired damping force for rear damper of the vertical suspension:

$$F_{r1} = C_{b1}\dot{z}_v - C_{p1}l_t\,.\,\dot{\theta}_v + k_{vs1}\,(Z_r - Z_{br})$$

$$if \quad F_{r1}(\dot{Z}_r - \dot{Z}_{br}) \geq 0 \quad \overset{select}{\longrightarrow} \quad F_{sa.rear} = F_{r1}$$

Otherwise

$$F_{r2} = C_{b2}\dot{z}_v - C_{p2}l_t\,.\,\dot{\theta}_v + k_{vs2}\,(Z_r - Z_{br})$$

$$if \quad F_{r2}(\dot{Z}_r - \dot{Z}_{br}) \geq 0 \quad \overset{select}{\longrightarrow} \quad F_{sa.rear} = F_{r2}$$

Otherwise

$$F_{r3} = C_{b3}\dot{z}_v - C_{p3}l_t\,.\,\dot{\theta}_v + k_{vs3}\,(Z_r - Z_{br})$$

$$if \quad F_{r3}(\dot{Z}_r - \dot{Z}_{br}) \geq 0 \quad \xrightarrow{select} \quad F_{sa.rear} = F_{r3}$$

Otherwise

$$F_{rn} = C_{bn}\dot{z}_v - C_{pn}l_t \,.\dot{\theta}_v + k_{vsn}\,(Z_r - Z_{br})$$

$$if \quad F_{rn}(\dot{Z}_r - \dot{Z}_{br}) \geq 0 \quad \xrightarrow{select} \quad F_{sa.rear} = F_{rn}$$

Otherwise

$$if \quad F_{rn}(\dot{Z}_r - \dot{Z}_{br}) < 0 \quad \xrightarrow{select} F_{sa.rear} = C_{min}\ (\dot{Z}_r - \dot{Z}_{br}) \text{ -------- (6.2)}$$

Where F_{r1} , F_{r2} , F_{r3} , and F_{rn} are a set of different full-active damping forces, (C_b, C_p, k_{vs}) are gain-scheduling controller coefficients, $F_{sa.rear}$ is the desired semi-active damping force at the rear suspension that can be tracked by the MR damper.

The goal of the switching policy is to improve the ride quality level while operating within the constraints of the MR dampers by adjusting the gain control parameters as appropriate. The gain-scheduling controller can minimise the use of the minimum damper setting by selecting skyhook gain (C_b, C_p) and dynamic stiffness (k_{vs}) from a set of different stiffness and damping parameters that provide a damping force which satisfies the passive constraint range of the semi-active damper as far as possible. Otherwise, the switching policy turns on the minimum damper setting when the direction of the damper velocity is not consistent with the direction of the desired damping force.

A similar control strategy was used for generating the desired semi-active damping force for front and rear damper of the lateral suspension as shown in Figure 6.3.

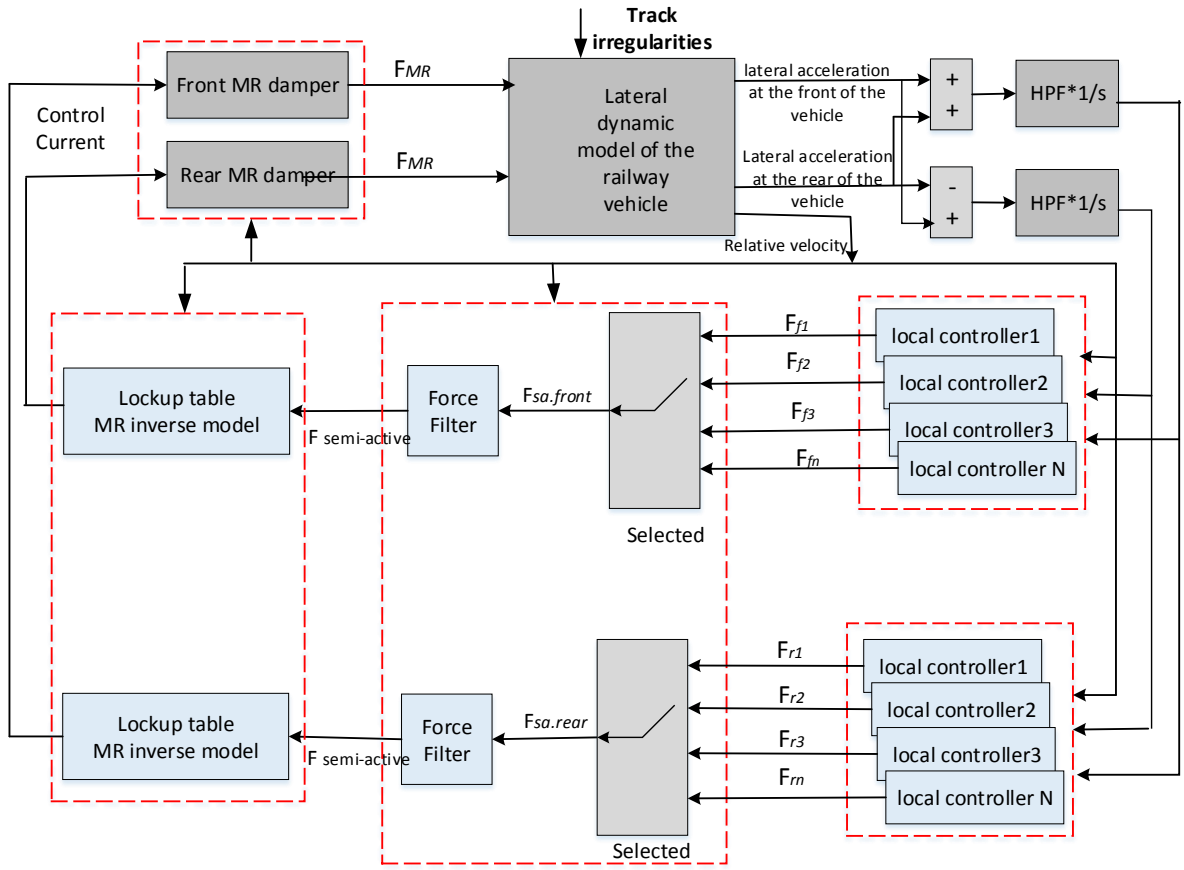

Figure 6.3: Semi-active control based on gain scheduling for lateral suspension model

The desired damping force for front damper of the lateral suspension:

$$F_{f1} = C_{l1}\dot{y}_v + C_{y1}l\,.\,\dot{\varphi}_v + k_{s1}\,(y_f - y_{b1})$$

$$if \quad F_{f1}(\dot{y}_f - \dot{y}_{b1}) \geq 0 \quad \xrightarrow{select} \quad F_{sa.front} = F_{f1}$$

Otherwise

$$F_{f2} = C_{l2}\dot{y}_v + C_{y2}l\,.\,\dot{\varphi}_v + k_{s2}\,(y_f - y_{b1})$$

$$if \quad F_{f2}(\dot{y}_f - \dot{y}_{b1}) \geq 0 \quad \xrightarrow{select} \quad F_{sa.front} = F_{f2}$$

Otherwise

$$F_{f3} = C_{l3}\dot{y}_v + C_{y3}l\,.\,\dot{\varphi}_v + k_{s3}\,(y_f - y_{b1})$$

$$if \quad F_{f3}(\dot{y}_f - \dot{y}_{b1}) \geq 0 \quad \xrightarrow{select} \quad F_{sa.front} = F_{f3}$$

Otherwise

.

$$F_{fn} = C_{ln}\dot{y}_v + C_{yn}l\,.\,\dot{\varphi}_v + k_{sn}\,(y_f - y_{b1})$$

$$if \quad F_{fn}(\dot{y}_f - \dot{y}_{b1}) \geq 0 \quad \xrightarrow{select} \quad F_{sa.front} = F_{fn}$$

Otherwise

$$if \quad F_{fn}(\dot{y}_f - \dot{y}_{b1}) < 0 \quad \xrightarrow{select} F_{sa.front} = C_{min} \ (\dot{y}_f - \dot{y}_{b1}) \text{ -------- (6.3)}$$

Where F_{f1} , F_{f2} , F_{f3} , and F_{fn} are a set of different full-active damping forces. $F_{sa.front}$ is the desired semi-active damping force at the front suspension that can be tracked by the MR damper.

The desired damping force for front damper of the lateral suspension:

$$F_{r1} = C_{l1}\dot{y}_v - C_{y1}l \,.\, \dot{\varphi}_v + k_{ls1}\,(y_r - y_{b2})$$

$$if \quad F_{r1}(\dot{y}_r - \dot{y}_{b2}) \geq 0 \quad \xrightarrow{select} \quad F_{sa.rear} = F_{r1}$$

Otherwise

$$F_{r2} = C_{l2}\dot{y}_v - C_{y2}l \,.\, \dot{\varphi}_v + k_{ls2}\,(y_r - y_{b2})$$

$$if \quad F_{r2}(\dot{y}_r - \dot{y}_{b2}) \geq 0 \quad \xrightarrow{select} \quad F_{sa.rear} = F_{r2}$$

Otherwise

$$F_{r3} = C_{l3}\dot{y}_v - C_{y3}l \,.\, \dot{\varphi}_v + k_{ls3}\,(y_r - y_{b2})$$

$$if \quad F_{r3}(\dot{y}_r - \dot{y}_{b2}) \geq 0 \quad \xrightarrow{select} \quad F_{sa.rear} = F_{r3}$$

Otherwise

.

$$F_{rn} = C_{ln}\dot{y}_v - C_{yn}l \,.\, \dot{\varphi}_v + k_{lsn}\,(y_r - y_{b2})$$

$$if \quad F_{rn}(\dot{y}_r - \dot{y}_{b2}) \geq 0 \quad \xrightarrow{select} \quad F_{sa.rear} = F_{rn}$$

Otherwise

$$if \quad F_{rn}(\dot{y}_r - \dot{y}_{b2}) < 0 \quad \xrightarrow{select} F_{sa.rear} = C_{min} \ (\dot{y}_r - \dot{y}_{b2}) \text{ -------- (6.4)}$$

Where F_{r1} , F_{r2} , F_{r3} , and F_{rn} are a set of different full-active damping forces, (C_l, C_y, k_{ls}) are gain-scheduling controller coefficient, $F_{sa.rear}$ is the desired semi-active damping force at the rear suspension that can be tracked by the MR damper.

6.4 Design Process and Tuning

As mentioned previously, the proposed control strategy aims to improve the performance of a semi-active suspension by using gain-scheduling control structure that dynamically extends the duration of the active mode that satisfies the passive constraints of the MR damper. The gain-scheduling control structure controller is used to generate the desired damping forces to keep the dampers within their normal working range. The desired damping force is generated by using the control structure with a set of different stiffness and damping parameters that provide forces dependent upon the absolute velocity of the vehicle body and the relative displacement of the suspension. Then, a decision-making procedure in the control algorithm will determine and select the desired damping force that satisfies the passive constraints.

The challenge in the gain-scheduling controller design is in the selection of appropriate parameters. There is no standard method for selecting gain parameters. Therefore, gain-scheduling control systems are designed by choosing a small set of operating points and developing a suitable linear controller for each point. In operation, the system switches or interpolates between these controllers according to the current values of the scheduling variables.

For tuning the system controller, the parameters are optimised for each gain-scheduling controller individually to achieve the best results by minimising the RMS values of vehicle body accelerations. Simulink Design Optimization tools in MATLAB® were used to optimise controller parameters to meet design requirements. Simulink Design Optimization is a numerical optimisation tool used to improve designs by estimating and tuning Simulink model parameters using numerical optimisation. Simulink Design Optimization offers a comprehensive interface for setting up and running optimisation problems within Simulink itself. The optimisation process is repeated sequentially and cumulatively for the remaining controllers. Then, the decision-making procedure in the control algorithms will then determine

and select the desired damping force that satisfies the passive constraints. Finally, the damper controller adjusts the command current applied to the MR damper to track the desired control force.

6.5 Application to Vertical suspension (tuning)

Gain-scheduling coefficients (C_b, C_p, k_{vs}) are determined for each gain-scheduling controller individually and tuned to achieve the best results by decreasing the RMS values for vehicle body accelerations. Table 6.1shows controller coefficients of gain-scheduling semi-active control for vertical suspension and ride quality improvement.

Table 6.1: Controller coefficients of gain-scheduling semi-active control for vertical suspension and ride quality improvement

Control	Front (m/s^2)	Centre (m/s^2)	Rear (m/s^2)	Pitch (rad/s^2)	Time use min. damper at damper1	Time use min. damper at damper2
One condition(conventional semi-active) C_{b1}=2.3058 x 10^5 N/m s^{-1} C_{p1}=2.7614 x 10^5 N/m s^{-1} k_{vs1}=0	26.638%	22.366%	23.079%	26.105%	3.999s	3.5313s
Two conditions C_{b2}=2.1615 x 10^5 N/m s^{-1} C_{p2}=2.3257 x 10^5 N/m s^{-1} k_{vs2}=3.6233 x 10^5 N/m	29.87%	24.121%	25.777%	29.769%	3.805s	3.2492s
Three conditions C_{b3}=1.5131 x 10^5 N/m s^{-1} C_{p3}=1.3954 x 10^5 N/m s^{-1} k_{vs3}=9.3316 x 10^4 N/m	35.105%	28.654 %	30.422%	34.919%	1.074s	1.1703 s
Four conditions C_{b4}=1.2969 x 10^5 N/m s^{-1} C_{p4}=1.8605 x 10^5 N/m s^{-1} k_{vs4}=263120 N/m	36.251%	29.341%	30.775%	35.642%	0.593s	0.87081s
Five conditions C_{b5}=7.6463 x 10^4 N/m s^{-1}	36.383%	29.341%	30.789 %	35.734%	0.531s	0.86059 s

C_{p5}=2.0931 x 10^5 N/m s^{-1} k_{vs5}=2.8312 x 10^5 N/m						
six conditions C_{b6}=3.90 x 10^4 N/m s^{-1} C_{p6}=2.00013 x 10^5 N/m s^{-1} k_{vs6}=3.37739 x 10^5 N/m	36.471%	29.451%	30.798%	35.753 %	0.391s	0.75327 s

Whereas $(C_{b1}, C_{p1}, k_{vs1})$, $(C_{b2}, C_{p2}, k_{vs2})$, $(C_{b3}, C_{p3}, k_{vs3})$, $(C_{b4}, C_{p4}, k_{vs4})$, $(C_{b5}, C_{p5}, k_{vs5})$, and $(C_{b6}, C_{p6}, k_{vs6})$ are gain-scheduling coefficients of the first linear controller, the second linear controller, the third linear controller, the fourth linear controller, the fifth linear controller, and the sixth linear controller, respectively.

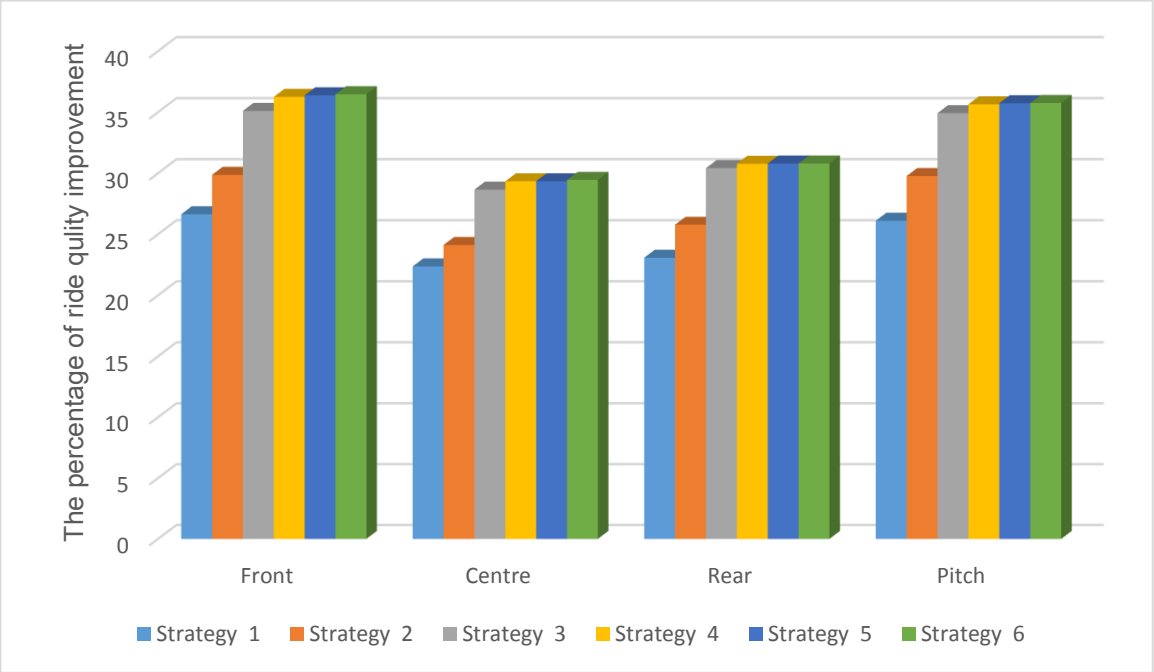

Figure 6.4: Tuning process of gain-scheduling semi-active control for vertical suspension

It is worth noting that the time for the MR damper being set at the minimum damping is significantly reduced (i.e. the suspension is in the passive mode) and the extending duration of the active mode was proximity 9.6 seconds for a simulation time of 10 seconds, as shown in Table 6.1. Moreover, it can also be seen from Table 6.1 and Figure 6.4 that the ride quality improvements using a gain-scheduling semi-active suspension system reached almost the

saturation point after six conditions. Therefore, it is worthless to add extra controllers after the saturation point.

6.6 Application to lateral suspension (tuning)

Gain-scheduling controller coefficient (C_l, C_y, k_{ls}) are determined for each gain-scheduling controller individually and tuned to achieve the best results by decreasing the RMS values for vehicle body accelerations. Table 6.2 shows the controller coefficients of gain-scheduling semi-active control for lateral suspension and ride quality improvement. Figure 6.5 shows the tuning process of gain-scheduling semi-active control for lateral suspension.

Table 6.2: Controller coefficients of gain-scheduling semi-active control for lateral suspension and ride quality improvement

Control	Front (m/s^2)	lateral (m/s^2)	Rear (m/s^2)	yaw (rad/s^2)	Time use min. damper at damper1	Time use min. damper at damper2
One condition C_{l1}=1.6108 x 10^5 N/m s^{-1} C_{y1}=1.4125 x 10^5 N/m s^{-1} k_{ls1}=0	32.755%	30.251%	29.848 %	31.406%	3.962s	3.792s
Two conditions C_{l2}=1.9851 x 10^5 N/m s^{-1} C_{y2}=1.4037 x 10^5 N/m s^{-1} k_{ls2}=1.6077 x 10^5 N/m	38.05%	33.24%	35.01%	37.25%	2.776 s	2.833s
Three conditions C_{l3}=1.1979 x 10^5 N/m s^{-1} C_{y3}=1.9830 x 10^5 N/m s^{-1} k_{ls3}=2.1223 x 10^4 N/m	40.08%	36.73 %	37.08%	38.90%	1.654s	1.554s
Four conditions C_{l4}=4.3599 x 10^4 N/m s^{-1}	41.85 %	38.65%	38.40%	40.31%	0.352s	0.496s

C_{y4}=2.7105 x 10^4 N/m s^{-1} k_{ls4}=1.2710 x 10^5 N/m						
Five conditions C_{l5}=9.5466 x 10^4 N/m s^{-1} C_{y5}=6.3254 x 10^4 N/m s^{-1} k_{ls5}=4.6569 x 10^5 N/m	41.86 %	38.86%	38.66%	40.44 %	0.311s	0.373s

Whereas $(C_{l1}, C_{y1}, k_{ls1})$, $(C_{l2}, C_{y2}, k_{ls2})$, $(C_{l3}, C_{y3}, k_{ls3})$, $(C_{l4}, C_{y4}, k_{ls4})$, and $(C_{l5}, C_{y5}, k_{ls5})$ are gain-scheduling coefficients for the first linear controller, the second linear controller, the third linear controller, the fourth linear controller, and the fifth linear controller, respectively.

Figure 6.5: shows the tuning process of gain-scheduling semi-active control for lateral suspension

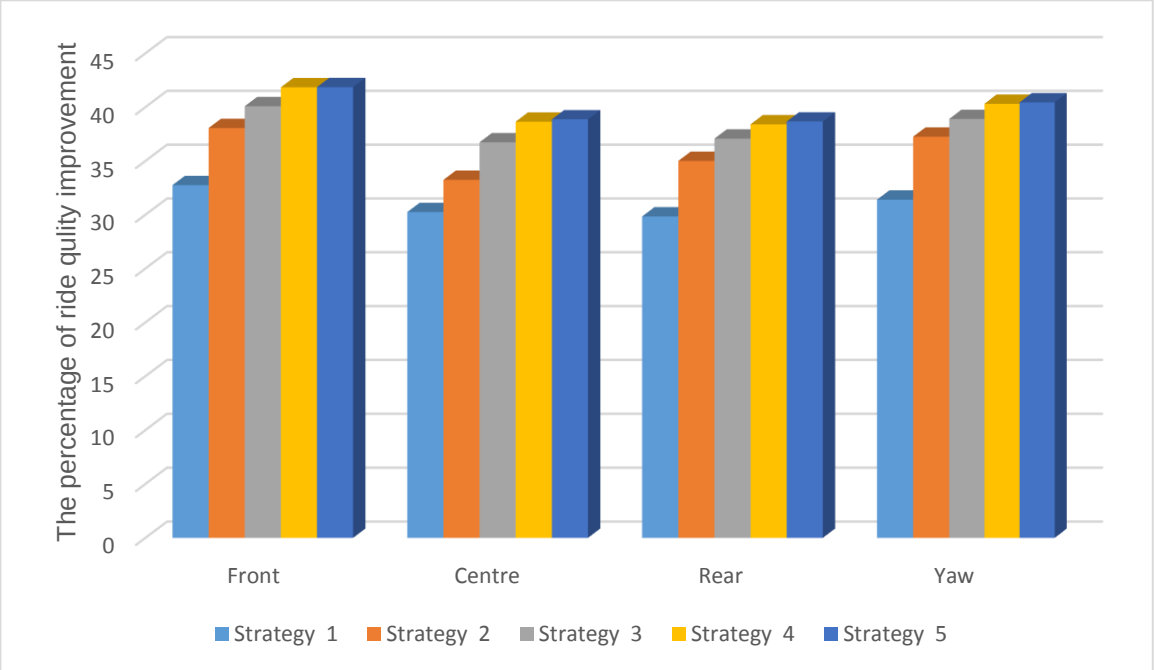

Figure 6.5: Tuning process of gain-scheduling semi-active control for lateral suspension

It can clearly be seen from Figure 6.5 and Table 6.2 that the gain-scheduling semi-active control reached almost the saturation point by using five controllers (five conditions), where the lateral ride quality improvements using gain-scheduling semi-active suspension system was

about 38.66%, and the duration of the passive mode was around 0.31 seconds for a simulation time of 10 seconds.

6.7 Force Filter Tuning

The gain scheduling semi-active suspension is an approach to control nonlinear systems that employs a group of linear controllers, where the decision maker in the control algorithm will select the desired damping force that satisfies performance control and the passive constraints. The drawback of the switching process between the group of linear controllers is that while this controls the vehicle vibration effectively, the rapid switching generates high-frequency harmonics that lead to the creation of unacceptable noise.

As stated previously, the frequency range of the vibration with the most significant impact on the ride quality is between 0.16 to 14 Hz, therefore, a first-order low pass filter (with gain equal to one) is used to make the frequency of desired force concentrate in that the frequency range and remove the impact of high frequency switching between controllers.

$$H(s) = \frac{87.92}{s+87.92} \text{ ---------- (6.5)}$$

Figure 6.6 provides a comparison between desired force without force filter and desired force with force filter.

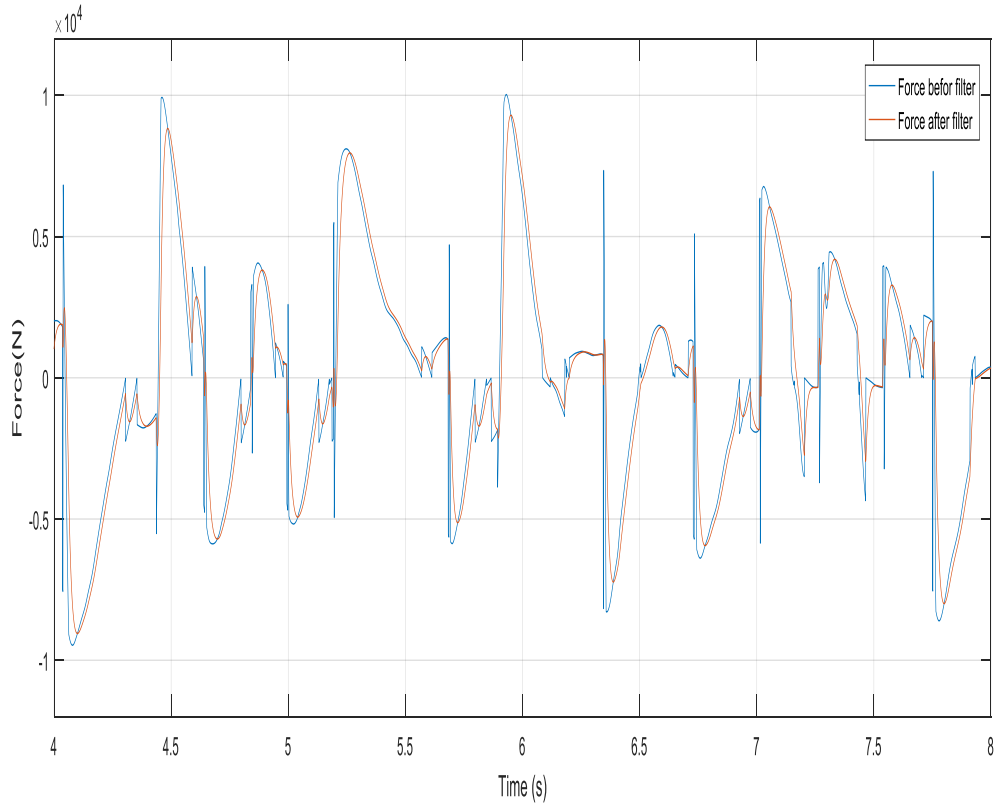

Figure 6.6: Comparison desired force without force filter and desired force filter damping force at the front suspension

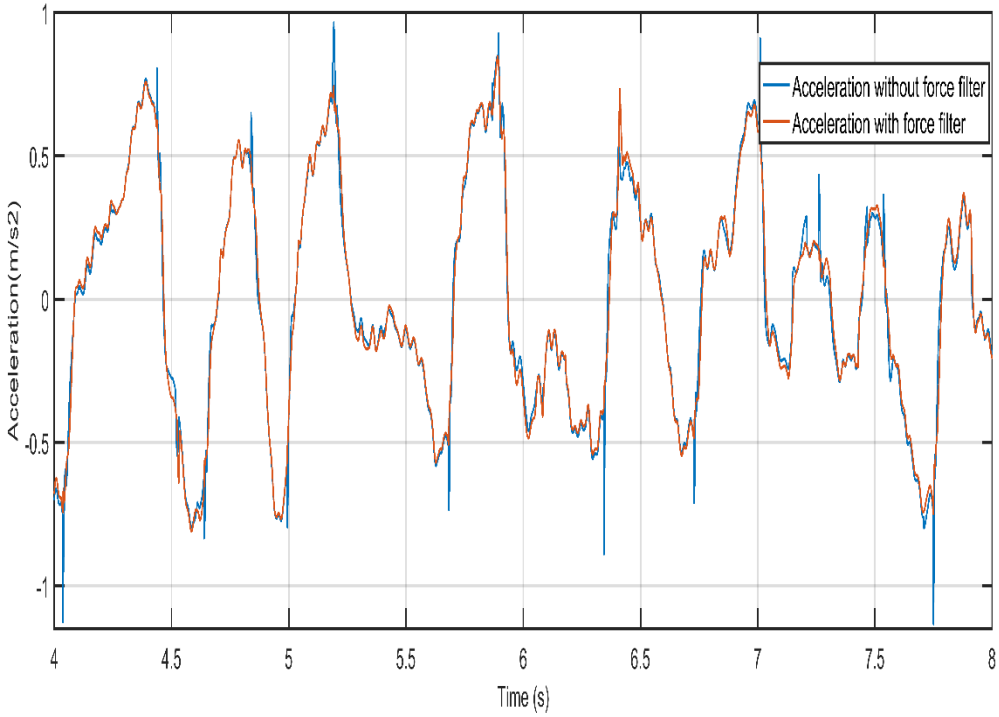

Figure 6.7: Comparison acceleration response at the front suspension

Moreover, the MR damper because of the time delay could not easily track the control force with high frequency. Thus, a lowpass filter would maintain the frequency range of the control force in the range where the influence on the ride quality is most considerable.

6.8 Summary

In this chapter, a gain-scheduling controller is presented to overcome the constraints of the conventional semi-active control strategies and to control the dynamics of semi-active suspensions using controllable/variable dampers such as MR dampers to achieve the ride quality close to that of the full active control suspensions. The proposed control strategy is focused on extending the duration of the active mode for semi-active dampers by using a novel gain-scheduling control structure that dynamically changes the control forces demanded according to the operating conditions.

Conventional railway vehicle vertical and lateral models are used to design and evaluate the performance of the proposed semi-active controlled suspension systems. For a control design and tuning, the numerical simulation of the vehicle suspension system under generalised track irregularities are carried out in Matlab/Simulink for a simulation time of 10 seconds. Three performance criteria are considered in this study; they are acceleration at the centre of the vehicle, accelerations at front and rear of the vehicle, in addition to the maximum deflation of the suspensions.

The obtained simulation results show that a significant improvement of the vehicle ride quality is achieved via the use of gain scheduling control integrated with the MR damper of the secondary suspension. In addition, the results obtained with the use of a gain-scheduling controller show the improvements increased by reducing the use of minimum damper setting.

CHAPTER SEVEN

7 NUMERICAL SIMULATION OF VERTICAL SECONDARY SUSPENSION

The numerical simulations of the vehicle suspension system under different track irregularities were carried out in Matlab/Simulink for a simulation time of 10 seconds. Three performance criteria were considered in this study: acceleration at the centre of the vehicle, accelerations at the front and rear of the vehicle, and the maximum deflection of the suspensions. For control design and tuning, computer-generated random data is used to represent generalised track irregularities[26], which provides a good representation of real-world track irregularities in the range 0.1–12 Hz, and a velocity of 83.333 m/s, that is, to represent conditions for a 300 km/h railway vehicle. Time delay-dependent velocities are used to provide the inputs to the other axles of the vehicle. For assessment, real measured data for different track sections between two Stations in Britain are used to represent track irregularities [65].

7.1 Results of Vertical Secondary Suspension

Computer simulation was used to evaluate the proposed gain scheduling-based semi-active suspension and compared against the benchmarking models, as presented in the preview chapters. For a more comprehensive assessment, real measured data for four different track sections are used to represent track irregularities. The proposed semi-active control using the gain-scheduling approach is applied to the vertical secondary suspensions of a railway and evaluated the passive suspension, full-active suspension, semi-active suspension with skyhook controller again. Table 7.1 gives simulation results for the ride quality, and suspension deflection using computer generated track data as input. A comparison of ride quality

improvements and maximum suspension deflection for three sections of the measured track data are shown in Tables 7.2, 7.3, and 7.4.

Table 7.1: Ride quality and suspension deflection results from time simulation under random track irregularities

Control strategy	Front (m/s^2)	Centre (m/s^2)	Rear (m/s^2)	Pitch (rad/s^2)	Time use min. damper setting at damper1	Time use min. damper setting at damper2	Def. damper 1(mm)	Def. Damper2 (mm)
Passive (RMS value)	0.69836	0.43592	0.7396	0.06357			27.885	29.256
Full-active with actuator	0.17438	0.1199	0.1744	0.01406			52.328	51.852
(%vs passive)	75.01%	72.45%	76.57%	77.99%				
Semi-active with MR damper	0.51183	0.3379	0.5728	0.04724	3.999s	3.5313s	35.494	32.694
(% vs passive)	26.638%	22.36%	23.07%	26.10%				
Gain scheduling with MR damper	0.44323	0.30714	0.5153	0.0410	0.391s	0.75327s	37.895	34.341
(% vs passive)	36.47%	29.45%	30.79%	35.75%				

As can be seen in Table 7.1, the active suspension delivers a better ride quality than passive, conventional semi-active, and gain-scheduling semi-active suspensions. For conventional semi-active, it should be noted that the time uses the minimum damper setting of MR damper (indicating the suspension is in the passive mode) proximity 4 seconds for a simulation time of 10 seconds, and the ride quality improvements are around 30%. However, the time during

which the MR damper is in the minimum setting (indicating the suspension is in the passive mode) in the semi-active suspension with a gain-scheduling controller is significantly decreased. As a result, the gain-scheduling semi-active suspension achieves a much better ride quality than conventional semi-active suspension.

Moreover, Figures 7.1, 7.2, and 7.3 (accelerations comparison at the centre, front, and rear of the vehicle body) show that the gain-scheduling semi-active suspension achieves a much smoother and lower acceleration (and closer to that of the full-active suspension) when compared with the conventional semi-active and passive suspensions.

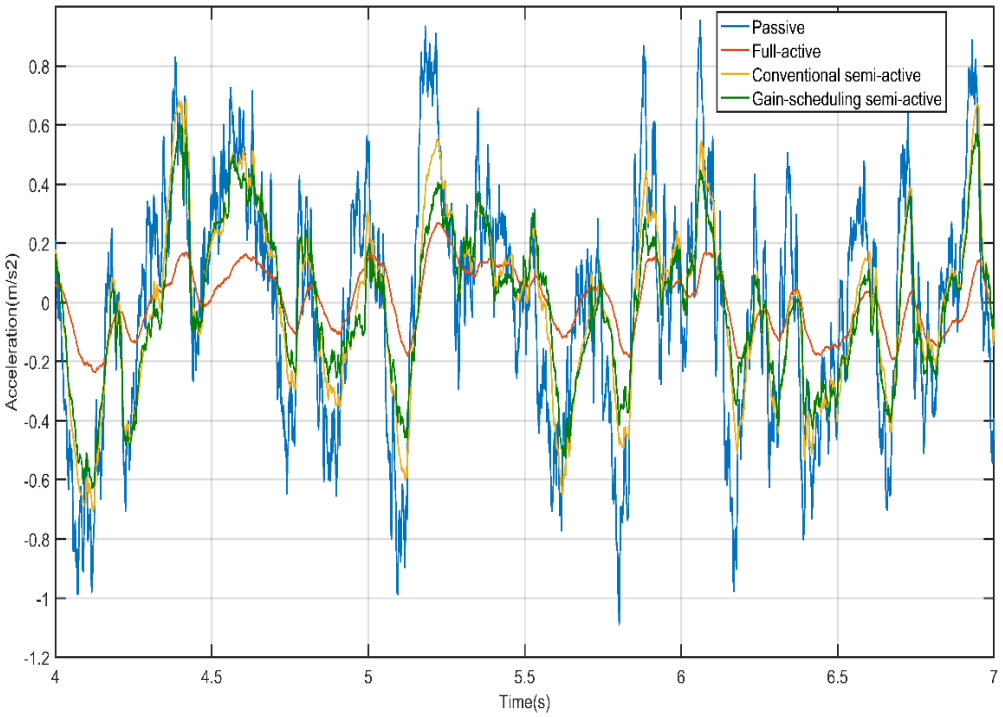

Figure 7.1: Vertical acceleration comparison at the centre of the vehicle body using computer-generated track data input

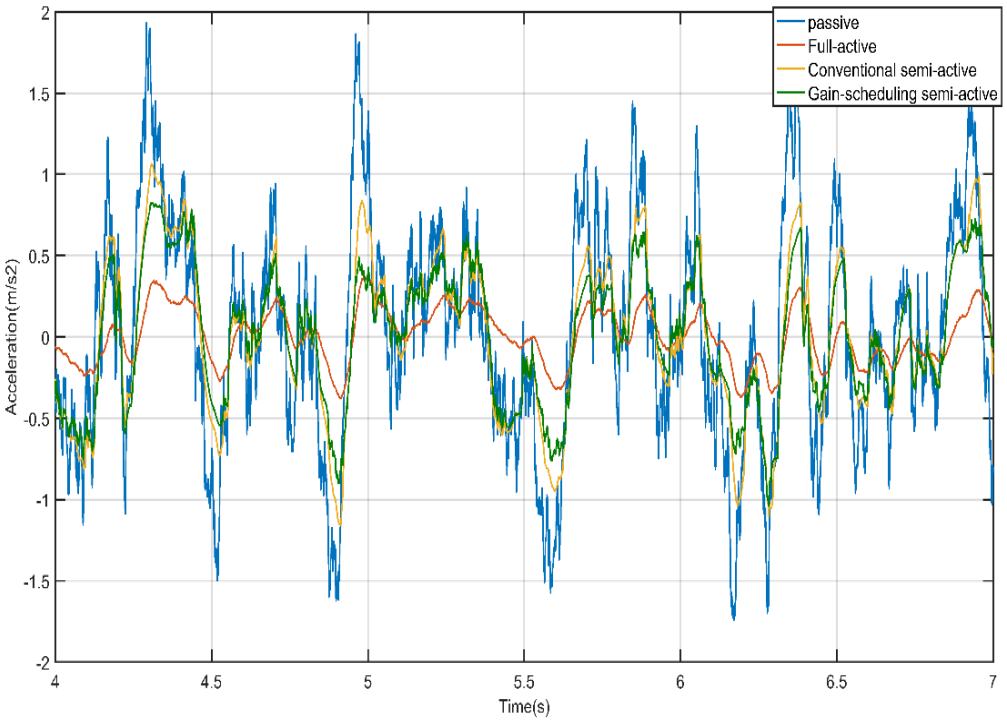

Figure 7.2: Vertical acceleration comparison at the front of the vehicle body using computer-generated track data input

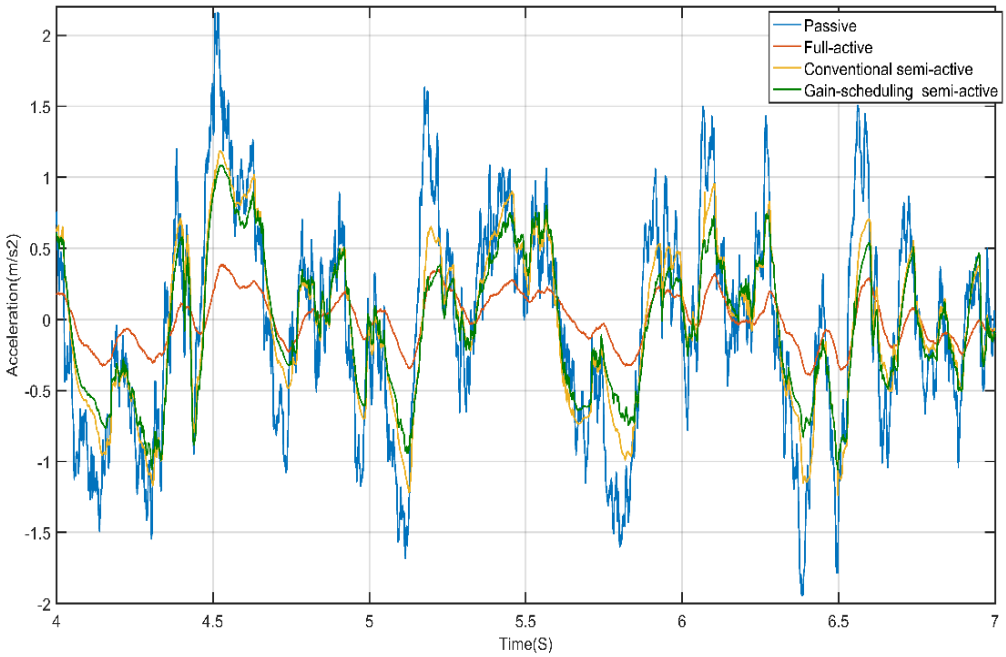

Figure 7.3: Vertical acceleration comparison at the rear of the vehicle body using computer-generated track data input

In order to investigate the effects of the control strategies on the accelerations of the vehicle over frequency, the power spectrum densities (PSD) of the vertical, pitch, front, and rear of the vehicle with the control strategies (under the random track irregularities) are illustrated in Figures 7.4 -7.7. It can be seen that the vertical vibrations of the vehicle body using gain-scheduling semi-active suspension are lower than using conventional semi-active systems.

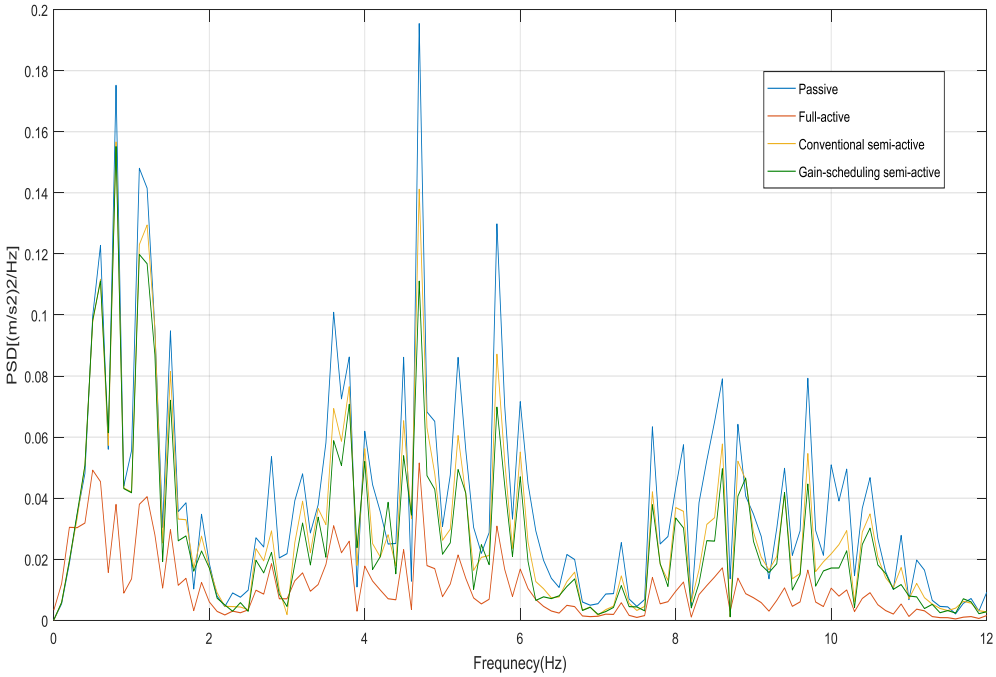

Figure 7.4: PSD of vertical comparison acceleration at the centre of the vehicle body using computer-generated track data

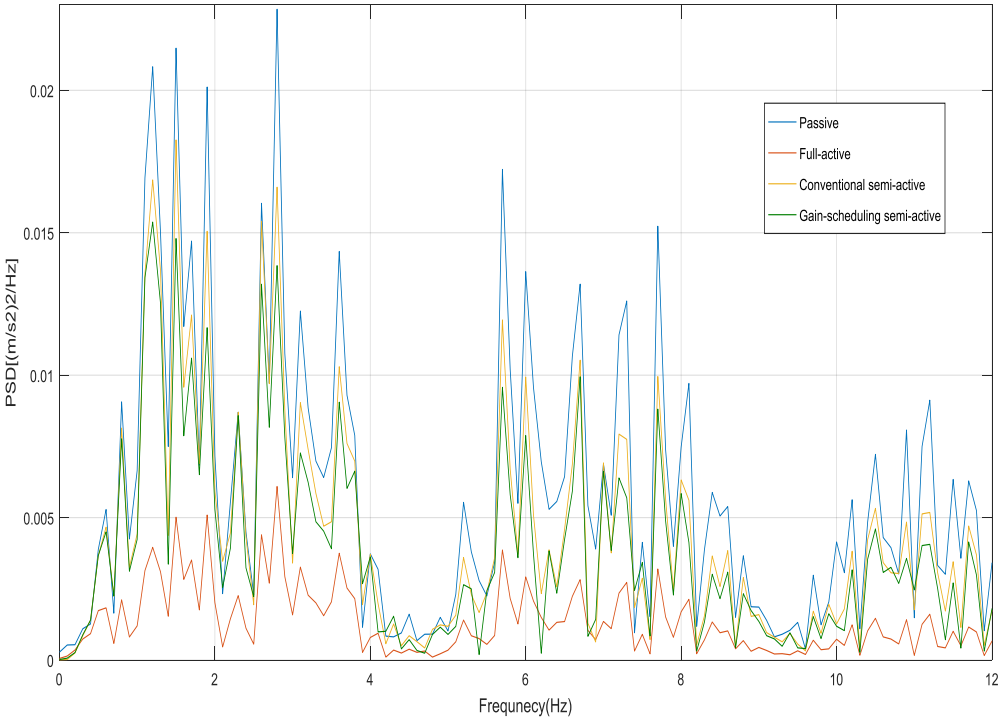

Figure 7.5: PSD of vertical comparison acceleration at the pitch of the vehicle body using computer-generated track data

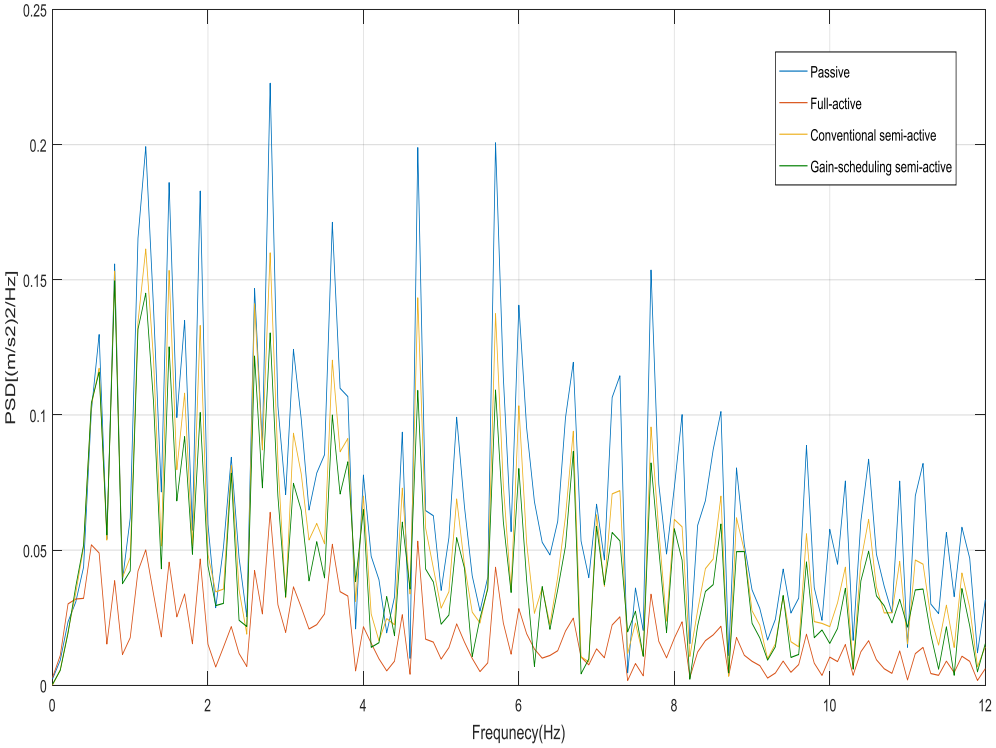

Figure 7.6: PSD of vertical comparison acceleration at the front of the vehicle body using computer data

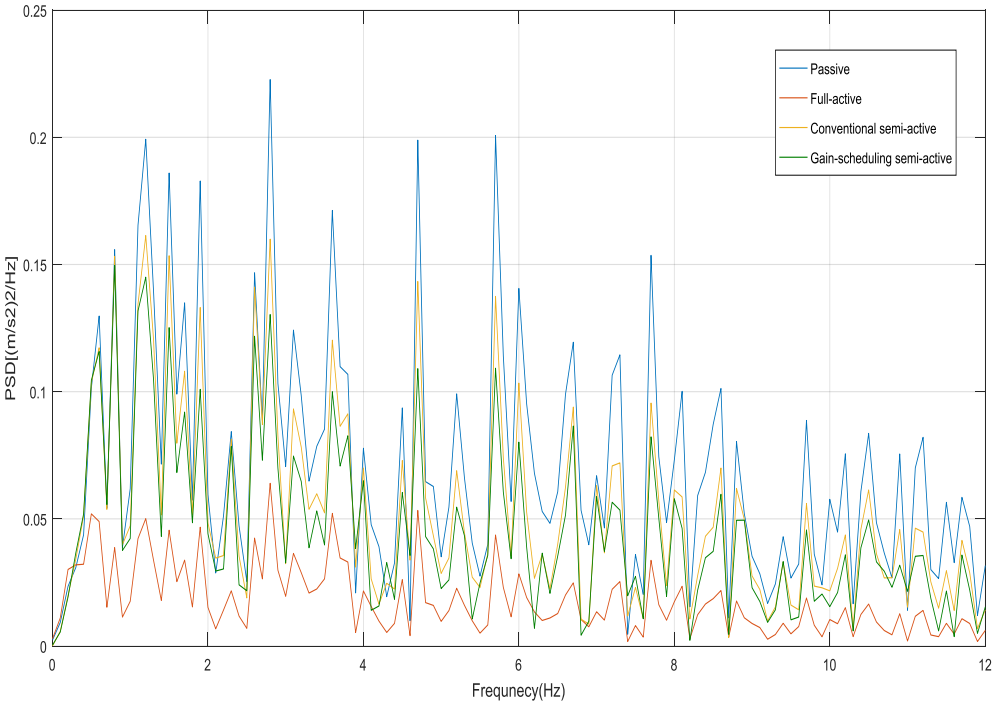

Figure 7.7: PSD of vertical comparison acceleration at the rear of the vehicle body using computer data

For more research assessments, a comparison of ride-quality improvements and maximum suspension deflections for the vertical secondary suspension system under measured track irregularity data for three different sections are shown in Tables 7.2, 7.3, and 7.4.

Table 7.2: Ride-quality improvements and suspension deflection results using measuring track data input (track1)

Control strategy/ track1	Front (m/s^2)	Centre (m/s^2)	Rear (m/s^2)	Pitch (rad/s^2)	Time use min. damping settingr at damper1	Time use min. damping setting at damper2	Def. damper1 (mm)	Def. Damper 2(mm)
Passive(RMS value)	0.87389	0.54561	0.85242	0.07432	-	-	29.697	28
Full-active with actuator	0.24107	0.1519	0.21586	0.01901	-	-	29.06	28.916
(%vs passive)	72.41%	72.15%	74.67%	74.42%				

Semi-active with MR damper (% vs passive)	0.59147	0.3582	0.58107	0.05157	3.041 s	3.4434s	29.3	30.078
	32.31%	34.34%	31.83%	30.61%				
Gain scheduling with MR damper (% vs passive)	0.39908	0.2359	0.39196	0.03527	0.023s	0.085854 s	30.184	30.464
	54.33%	56.76%	54.01%	52.53%				

Table 7.3: Ride-quality improvements and suspension deflection results using measuring track data input (track2)

Control strategy/ track2	Front (m/s2)	Centre (m/s2)	Rear (m/s2)	Pitch (rad/s2)	Time use min. damper at damper1	Time use min. damper at damper1	Def. damper1 (mm)	Def. Damper2 (mm)
Passive(RMS value)	0.77602	0.54941	0.7580	0.05948	-	-	36.889	35.843
Full-active with actuator (%vs passive)	0.20833	0.14932	0.18749	0.01447	-	-	39.818	39.567
	73.15%	72.82%	75.26%	75.66				
Semi-active with MR damper (% vs passive)	0.53084	0.37314	0.52325	0.04135	3.135 s	3.6212s	36.821	35.823
	31.59%	32.08%	30.97%	30.46%				
Gain scheduling with MR damper (% vs passive)	0.33952	0.23262	0.33547	0.02717	0.054 s	0.20033 s	39.695	39.57
	56.24%	57.66%	55.74%	54.32%				

Table 7.4: Ride-quality improvements and suspension deflection results using measuring track data input (track3)

Control/ Track3	Front (m/s^2)	Centre (m/s^2)	Rear (m/s^2)	Pitch (rad/s^2)	Time use min. damper at damper1	Time use min. damper at damper1	Def. damper1 (mm)	Def. Damper2 (mm)
Passive(RMS value)	0.58176	0.36226	0.55359	0.04858	-	-	19.343	19.47
Full-active with actuator	0.14679	0.09594	0.13313	0.01134	-	-	21.694	21.664
(%vs passive)	74.76%	73.51%	75.95%	76.64%				
Semi-active with MR damper(% vs passive)	0.37119	0.22903	0.35616	0.0314	3.138 s	3.1817 s	20.506	20.993
	36.19%	36.77%	35.66%	35.37%				
Gain scheduling with MR damper	0.25596	0.15548	0.2464	0.02192	0.097s	0.11754 s	21.217	22.098
(% vs passive)	56.01%	57.08%	55.49%	54.87%				

The time histories of the accelerations of the vehicle body with the passive, full-active, conventional semi-active, and gain-scheduling semi-active suspension systems under measured track irregularity data for three different track sections are shown in Figures 7.8~7.16. Observing the time histories of the accelerations of the vehicle body in different suspension systems in Figures7.8 ~7.16, it would be noted that the gain-scheduling semi-active suspension system provides better attenuation of the vibration of the vehicle than the conventional semi-active suspension.

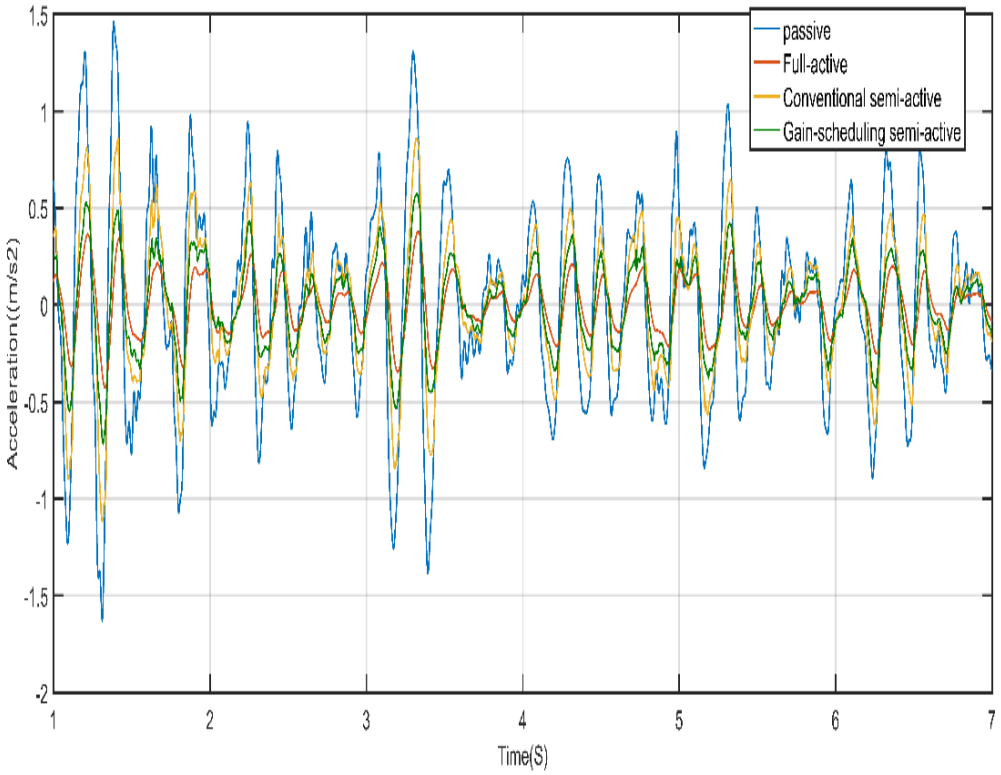

Figure 7.8: Vertical acceleration comparison at the centre of the vehicle body using measured track data input (track1)

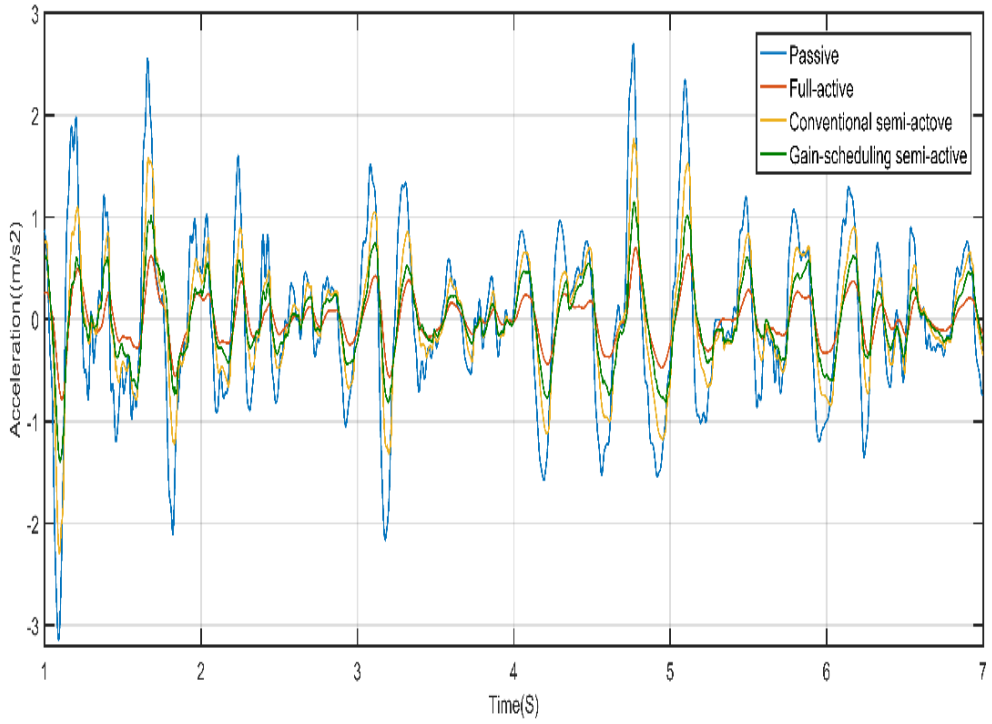

Figure 7.9: Vertical acceleration comparison at the rear of the vehicle body using measured track data input (track1)

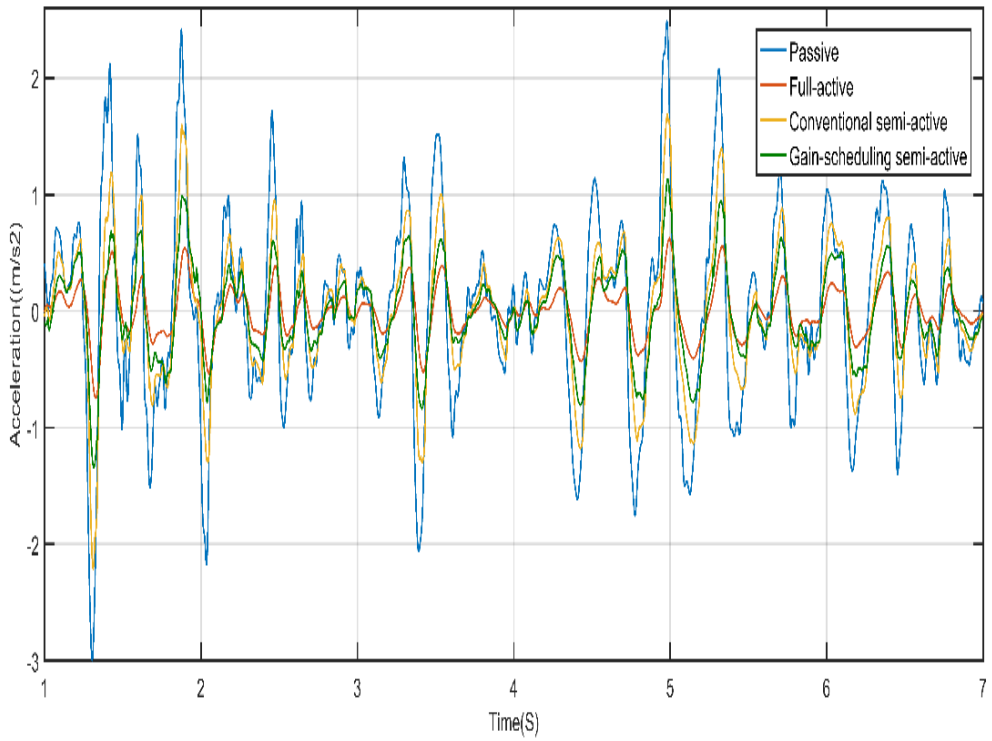

Figure 7.10: Vertical acceleration comparison at the rear of the vehicle body using measured track data input (track1)

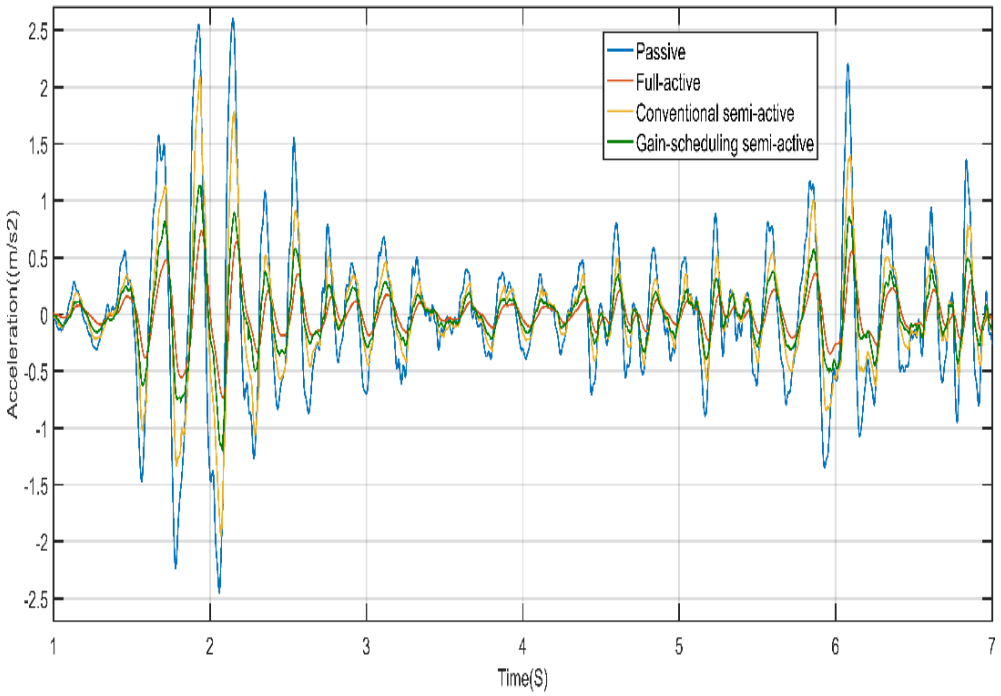

Figure 7.11: Vertical acceleration comparison at the centre of the vehicle body using measured track data input (track2)

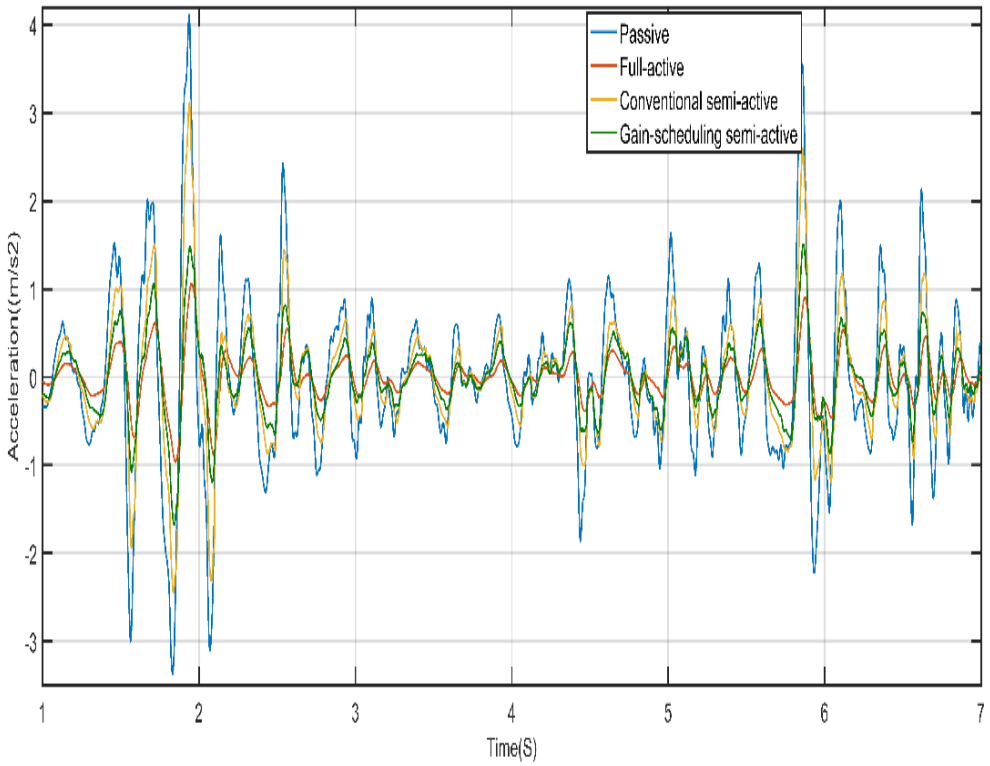

Figure 7.12: Vertical acceleration comparison at the front of the vehicle body using measured track data input (track2)

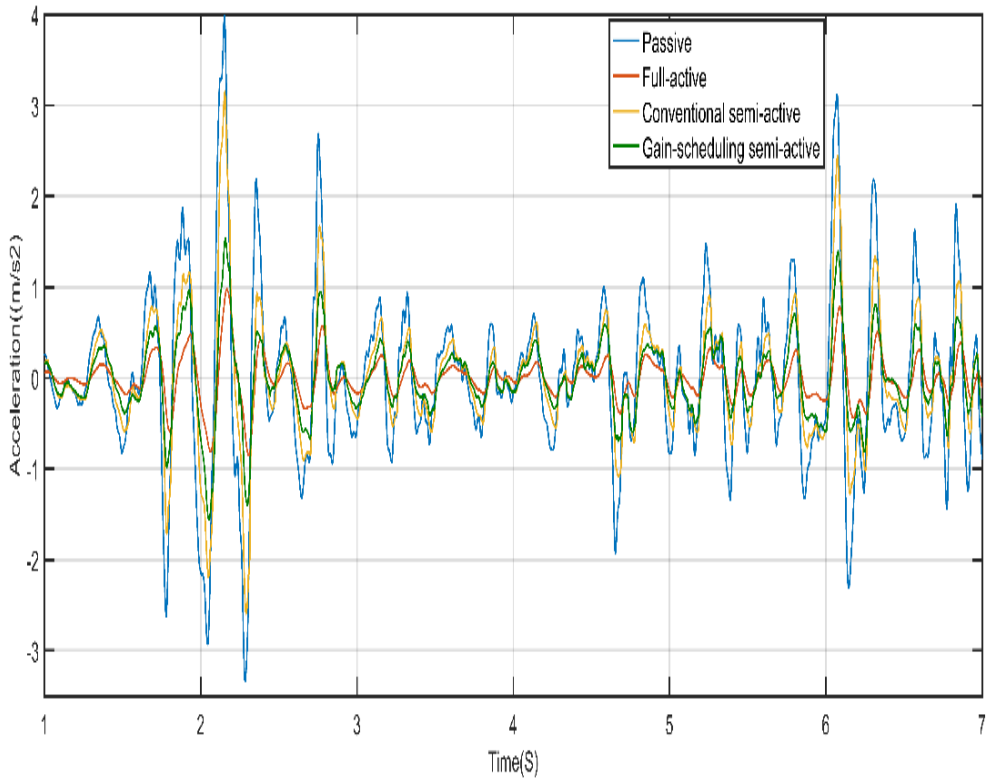

Figure 7.13: Vertical acceleration comparison at the rear of the vehicle body using measured track data input (track2)

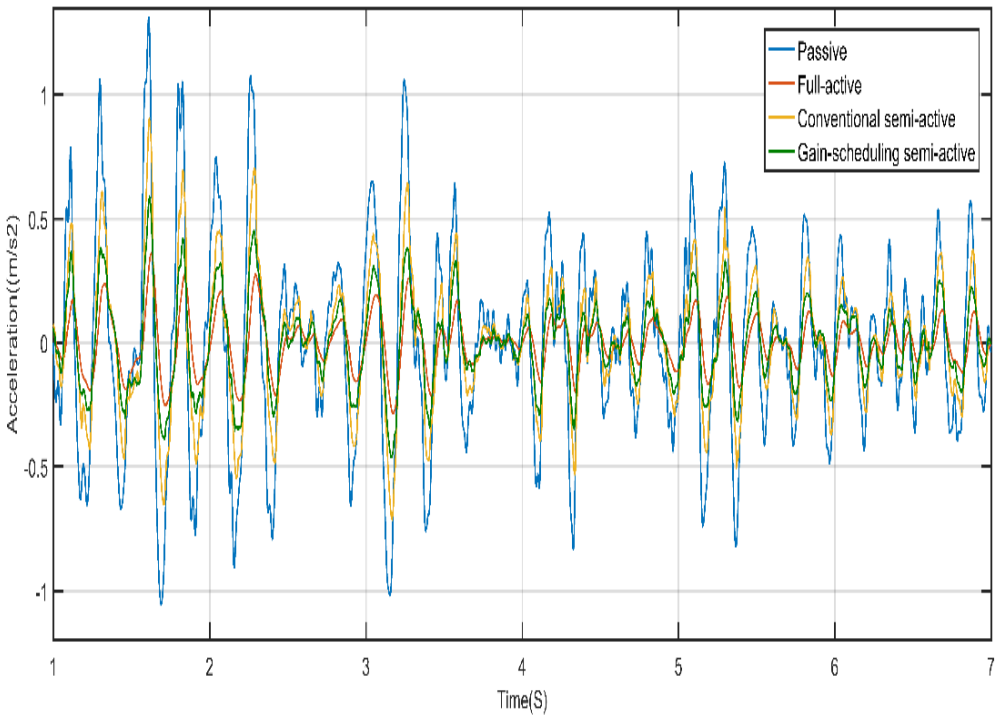

Figure 7.14: Vertical acceleration comparison at the centre of the vehicle body using measured track data input (track3)

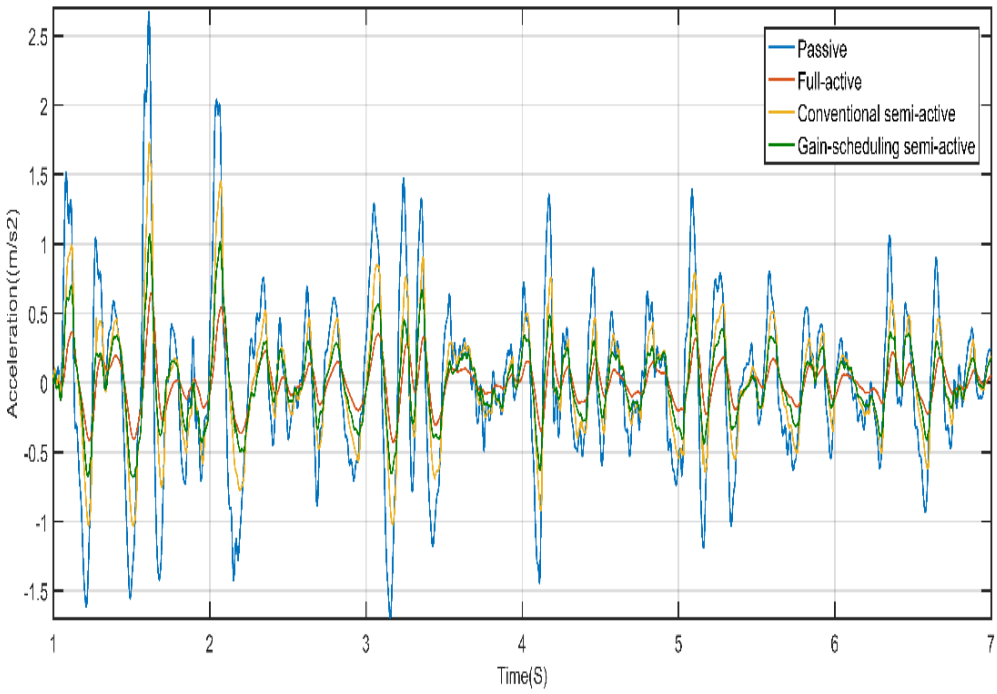

Figure 7.15: Vertical acceleration comparison at the front of the vehicle body using measured track data input (track3)

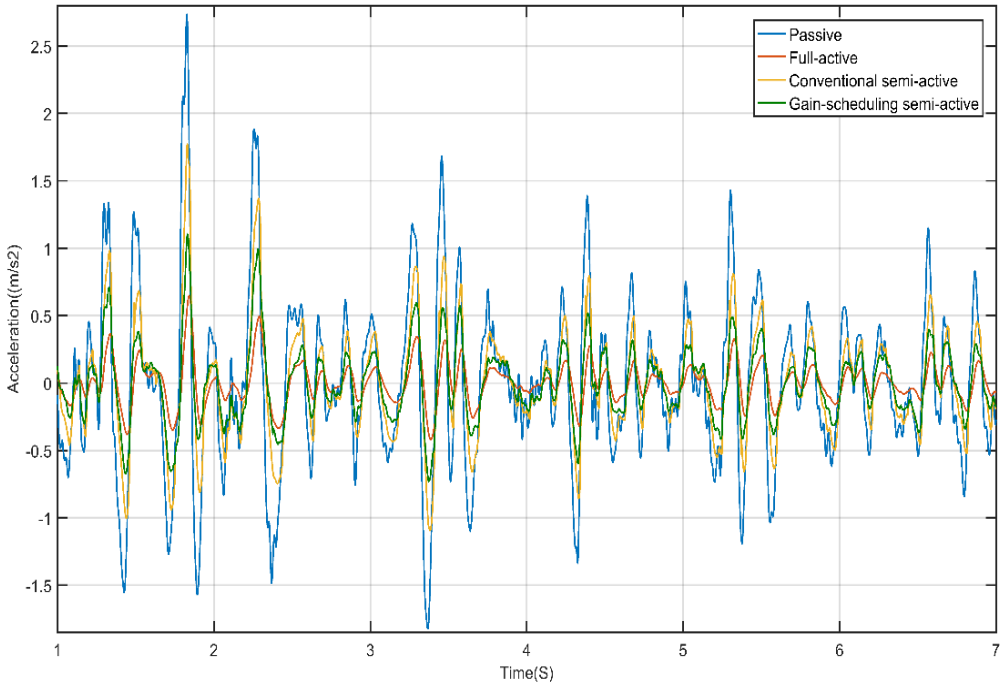

Figure 7.16: Vertical acceleration comparison at the rear of the vehicle body using measured track data input (track3)

The PSDs of the vehicle body accelerations of the railway vehicle with the passive, full-active, conventional semi-active, and gain-scheduling semi-active suspension systems were also studied, and the results using different track data to examine their effects regarding different frequencies. Figures 7.17~7.28 gives a clear view of the additional improvements achievable with the gain-scheduling controller solution, and it would be noted that the gain scheduling-based semi-active suspension improvement was much closer to that of the full-active control when compared with the conventional semi-active and passive suspensions.

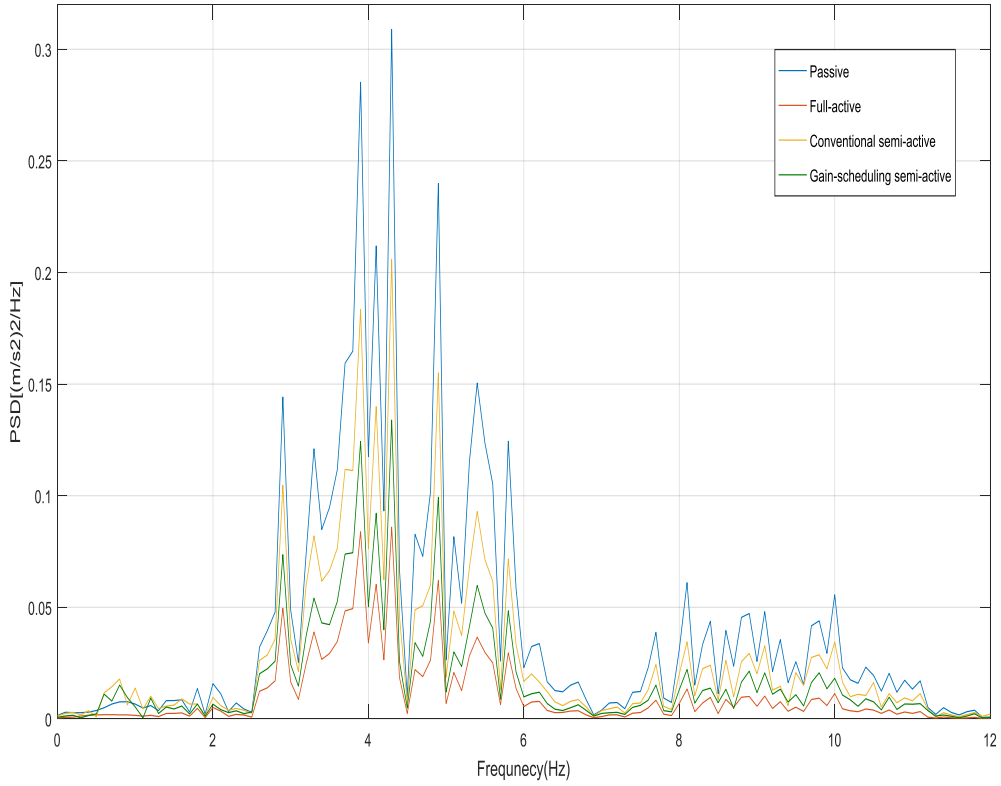

Figure 7.17: PSD of vertical accelerations at the centre of the vehicle body using measured track data input (track1)

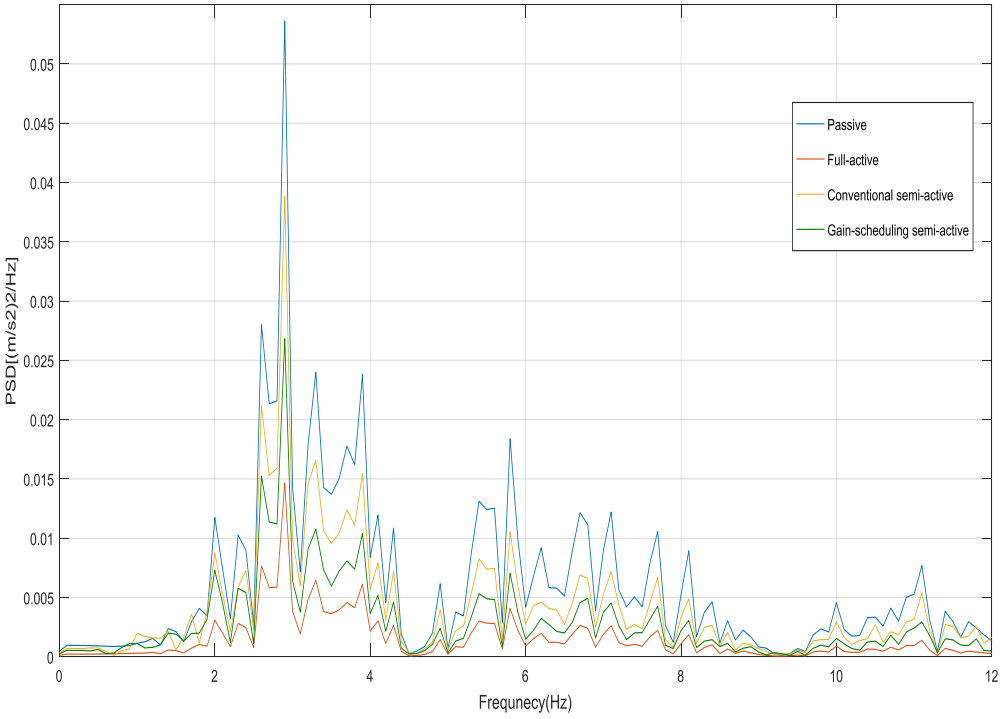

Figure 7.18: PSD of vertical accelerations at the pitch of the vehicle body using measured track data input (track1)

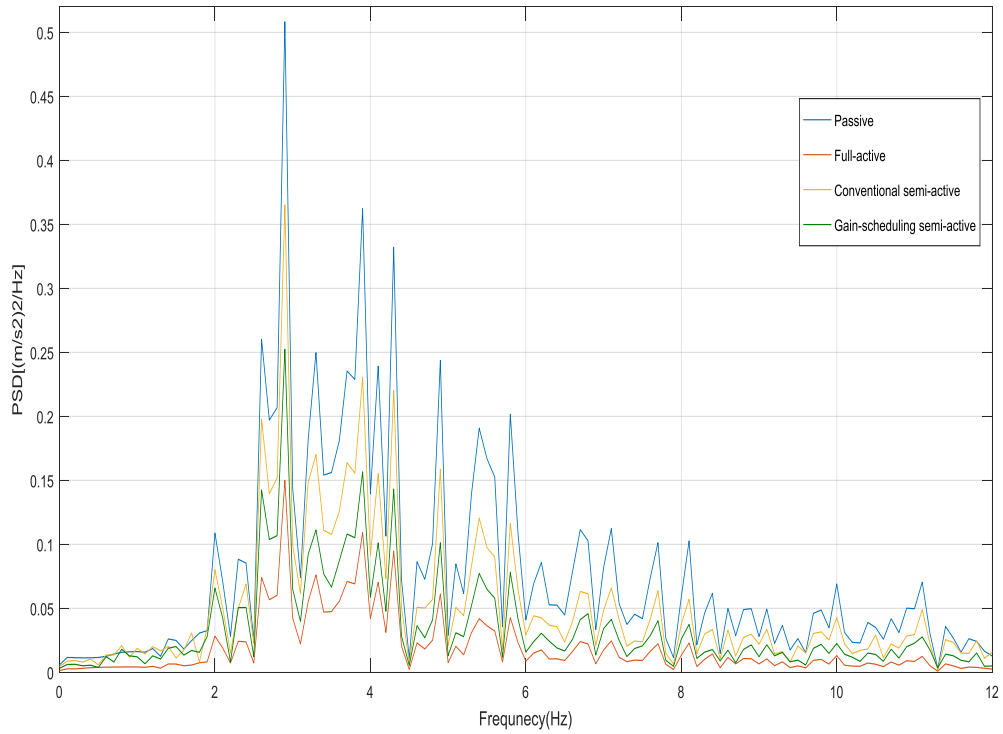

Figure 7.19: PSD of vertical comparison acceleration at the front of the vehicle body using measured track data input (track1)

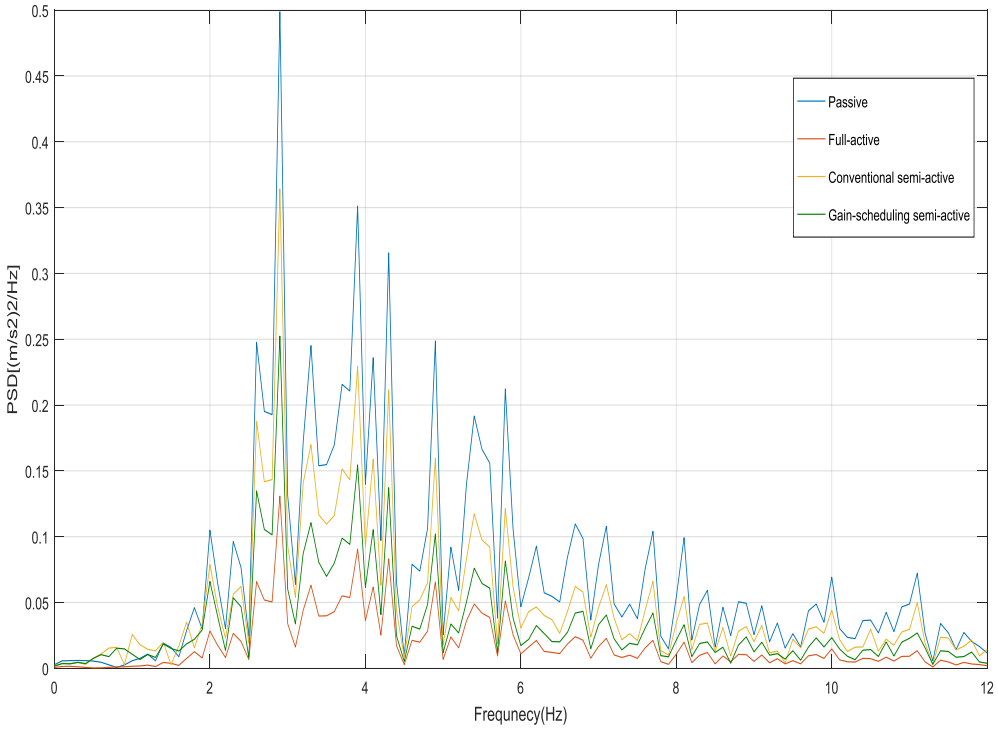

Figure 7.20: PSD of vertical comparison acceleration at the rear of the vehicle body using measured track data input (track1)

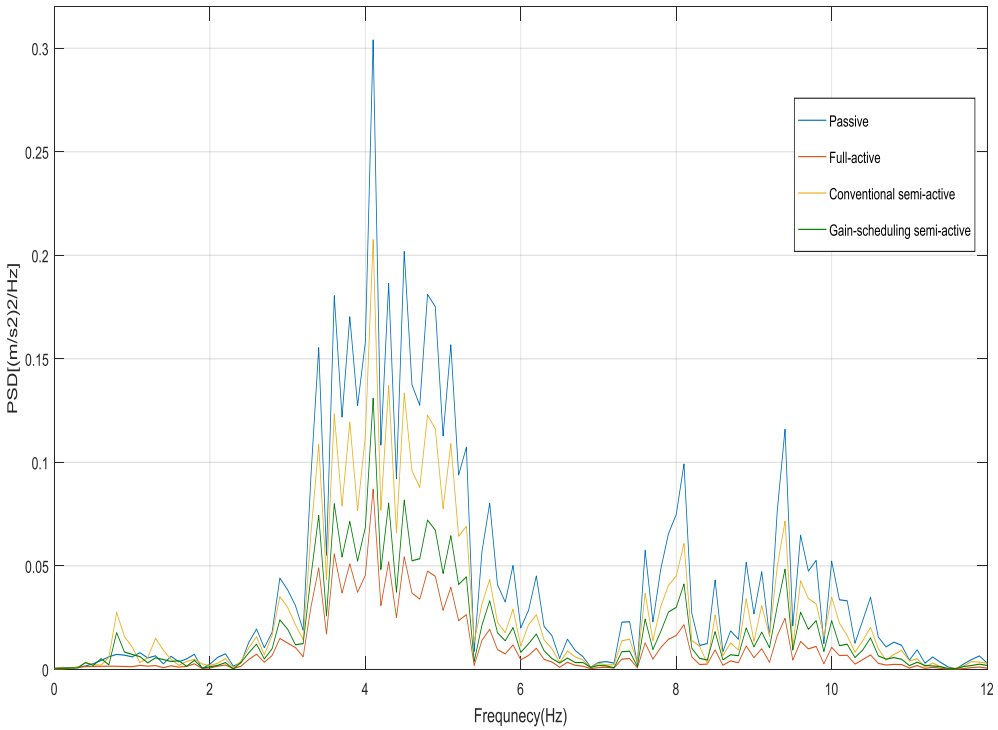

Figure 7.21: PSD of vertical comparison acceleration at the centre of the vehicle body using measured track data input (track2)

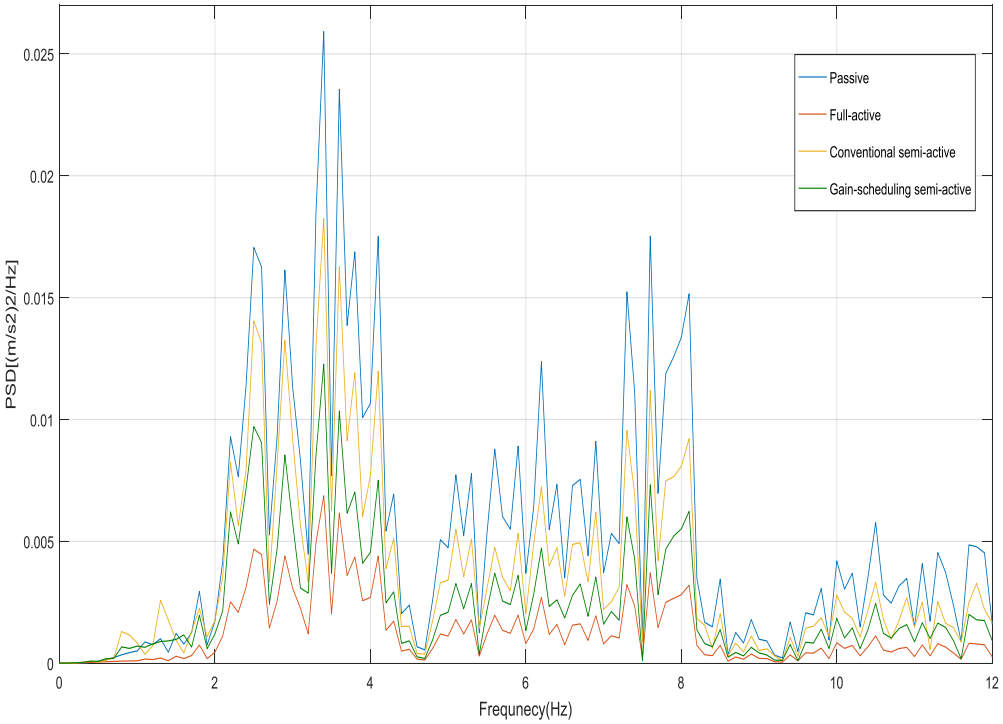

Figure 7.22: PSD of vertical comparison acceleration at the pitch of the vehicle body using measured track data input (track2)

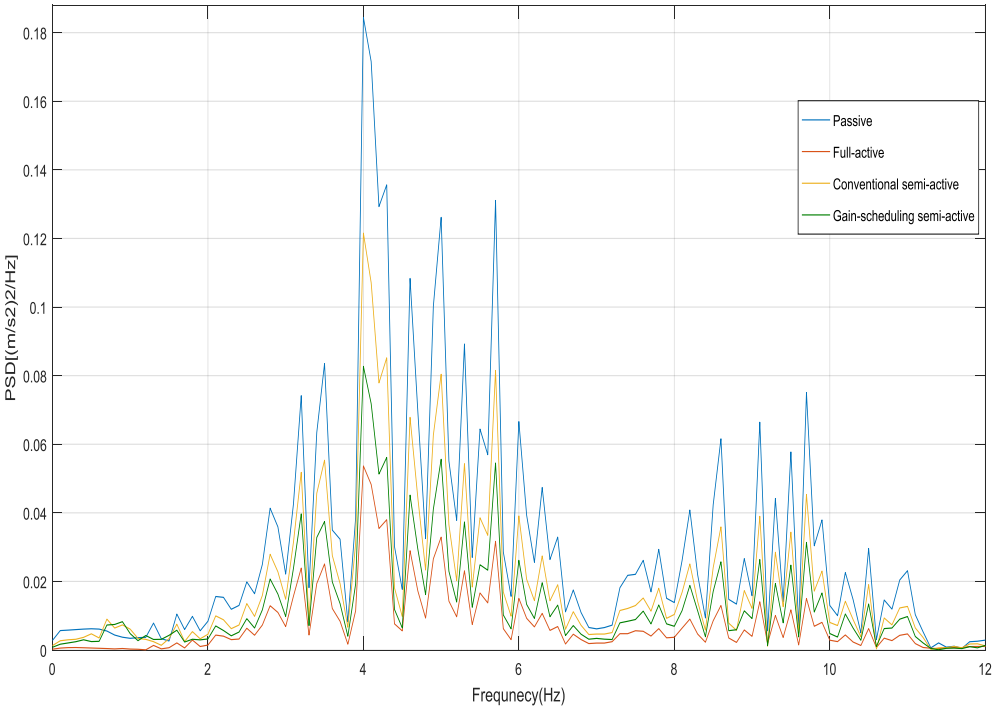

Figure 7.23: PSD of vertical comparison acceleration at the centre of the vehicle body using measured track data input (track3)

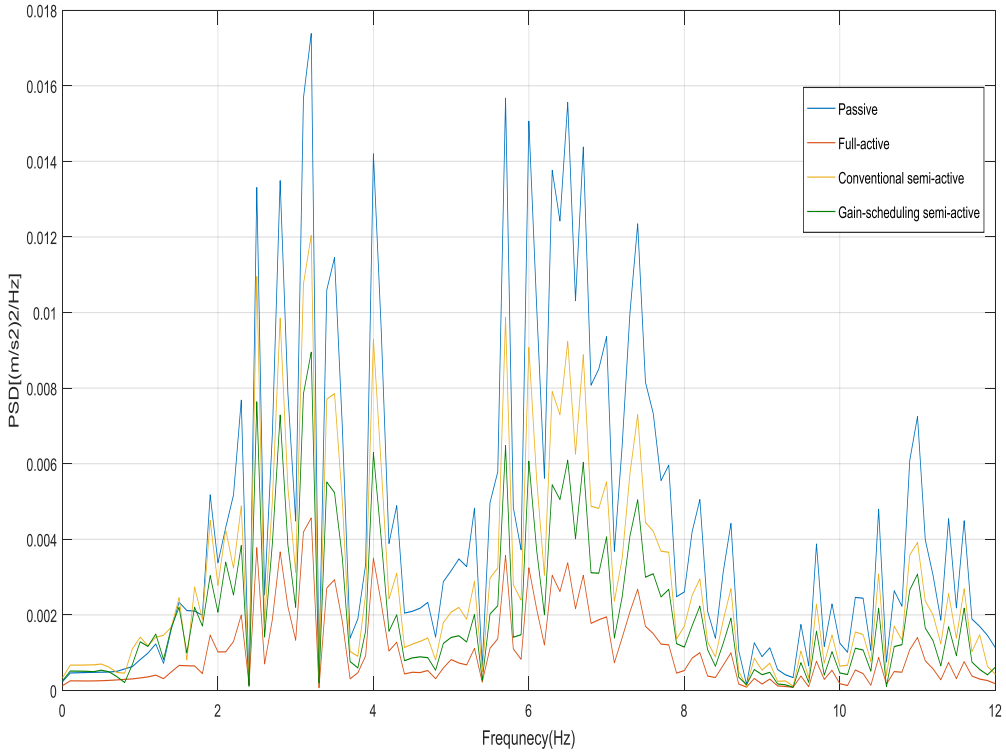

Figure 7.24: PSD of vertical comparison acceleration at the pitch of the vehicle body using measured track data input (track3)

7.2 Summary

Simulation works were performed in the Matlab Simulink environment to investigate the development of a nonlinear semi-active controller for improving the ride quality of railway vehicles and has evaluated the performance of the novel control approach against a passive suspension, a conventional semi-active and a full active control system.

In general, according to Tables 7.2, 7.3, and 7.4, the ride-quality improvements of the vertical and pitch acceleration of the railway vehicle with a full-active suspension system are similar to those of the railway vehicle with the full-active suspension system in Table7.1 and are around 75%. However, the ride quality improvements using conventional semi-active suspension system was approximately 25% in Table 7.1 (under random track irregularities) while quality improvements using conventional semi-active suspension was approximately 35% in Table 7.2, 7.3 and 7.4 (under measured track irregularities data for three different

sections). It is worth noting that the duration of the passive mode under random track irregularities (Table 7.1) was around 4 seconds, while the duration of the passive mode under measured track irregularities data for three different sections (Table 7.2, 7.3 and 7.4) was about 3 seconds.

Moreover, it can also be seen from Table 7.1 that the ride quality improvements using a gain-scheduling semi-active suspension system was about 35% and the duration of the passive mode was around 0.55 seconds. However, the improvements using gain-scheduling semi-active suspension under measured track irregularity data for three different sections (Table 7.2, 7.3, and 7.4) was around 55%, and the duration of the passive mode was less than 0.55 seconds. This indicates that the ride quality of semi-active suspension systems by extending the duration of the active mode is superior to those of the semi-active suspension systems whilst lowering the duration of the active mode.

Furthermore, it can be seen in Figures 7.4, 7.5, and 7.6 there are a very wide range of frequencies in the computer-generated track irregularities which reflects an improvement of around 10% for the gain scheduling-based semi-active control when compared with the conventional semi-active system listed in Table 7.1. Figures 7.11, 6.4, and 6.5 show a narrower range of frequencies from the measured track data, whilst Tables 7.2, 7.3, and 7.4 indicate an improvement of around 20% when compared with conventional semi-active suspension.

CHAPTER EIGHT

8 NUMERICAL SIMULATION OF LATERAL SECONDARY SUSPENSION

The proposed semi-active control using the gain-scheduling approach is also applied to the lateral secondary suspensions of a railway and evaluated as compared to the passive suspension, full-active suspension, and semi-active suspension with skyhook controller

8.1 Results of Lateral Secondary Suspension

Table 8.1 gives simulation results for the ride quality, and suspension deflection using computer-generated track data as input.

Table 8.1: Ride quality and suspension deflection results using computer-generated track data input

Control strategy	Front (m/s^2)	lateral (m/s^2)	Rear (m/s^2)	yaw (rad/s^2)	Time use min. damper at damper1	Time use min. damper at damper1	Def. damper1 (mm)	Def. Damper2 (mm)
Passive(RMS value)	0.67305	0.32661	0.7358	0.069435	-	-	41.6	47.362
Full-active with actuator	0.22348	0.10244	0.27499	0.025407	-	-	51.682	56.143
(%vs passive)	66.79%	68.63%	62.62%	63.40%				
Semi-active with MR damper	0.45258	0.22779	0.51614	0.047626	3.96 s	3.792 s	42.268	48.42
(% vs passive)	32.75%	30.25%	29.85%	31.41 %				
	0.39131	0.19966	0.45128	0.041354	0.311 s	0.373 s	41.84	48.63

Gain scheduling with MR damper (% vs passive)	41.86%	38.87 %	38.669	40.44%				

As shown in Table 8.1, the active suspension delivers the best ride quality improvement as expected. For the conventional semi-active, it should be noted that the time that the system is in the minimum damper setting of MR damper (i.e. the suspension is in the passive mode) is proximity 4 seconds for a simulation time of 10 seconds, and the ride quality improvements are around 30%. However, the time during which the MR damper is in the minimum setting (indicating the suspension is in the passive mode) in the semi-active suspension with a gain-scheduling controller is significantly decreased. As a result, the gain-scheduling semi-active suspension achieves a much better ride quality than the conventional semi-active suspension.

Moreover, Figures 8.1,8.2 and 8.3 show that the gain-scheduling semi-active suspension achieves a much smoother and lower acceleration (and closer to that of the full-active suspension) when compared with the conventional semi-active and passive suspensions.

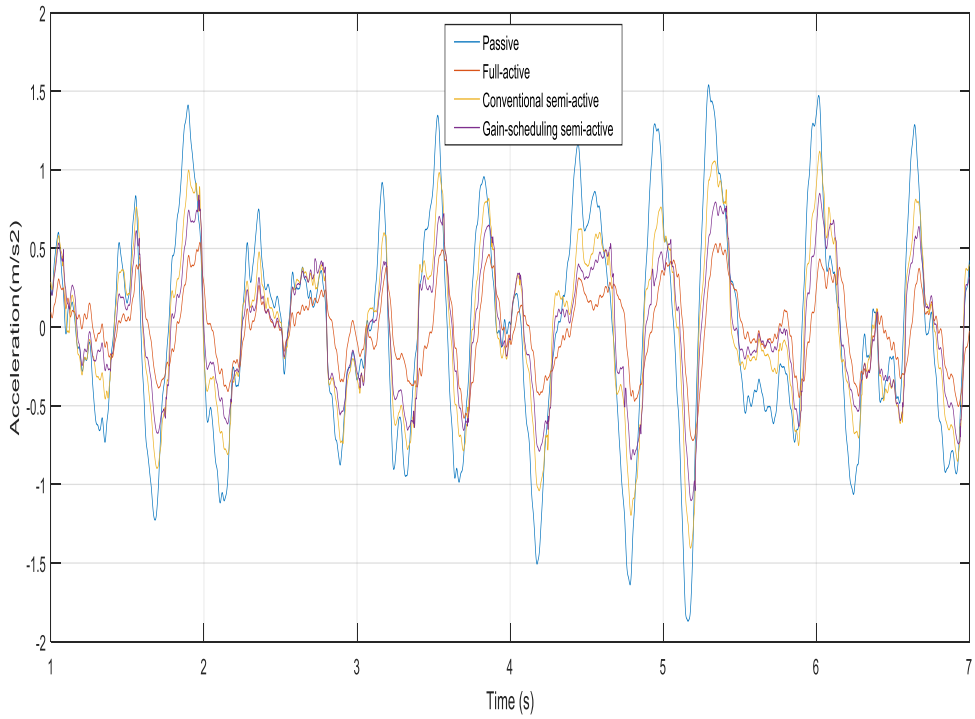

Figure 8.1: Acceleration comparison at the front of the vehicle body using computer-generated track data

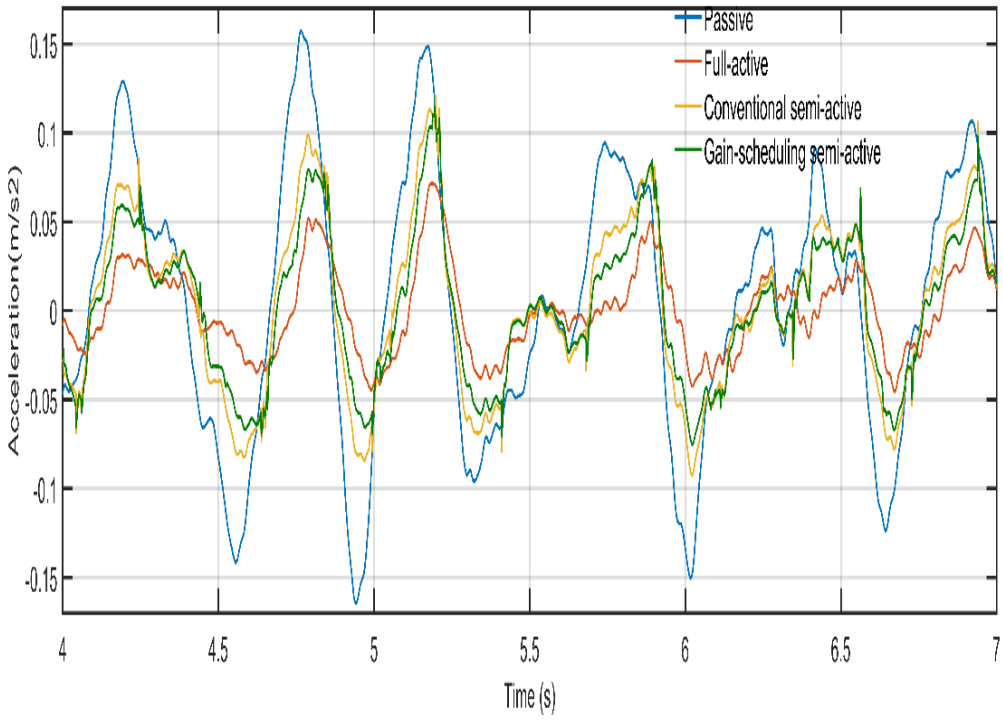

Figure 8.2: Acceleration comparison at the centre of the vehicle body using computer-generated track data

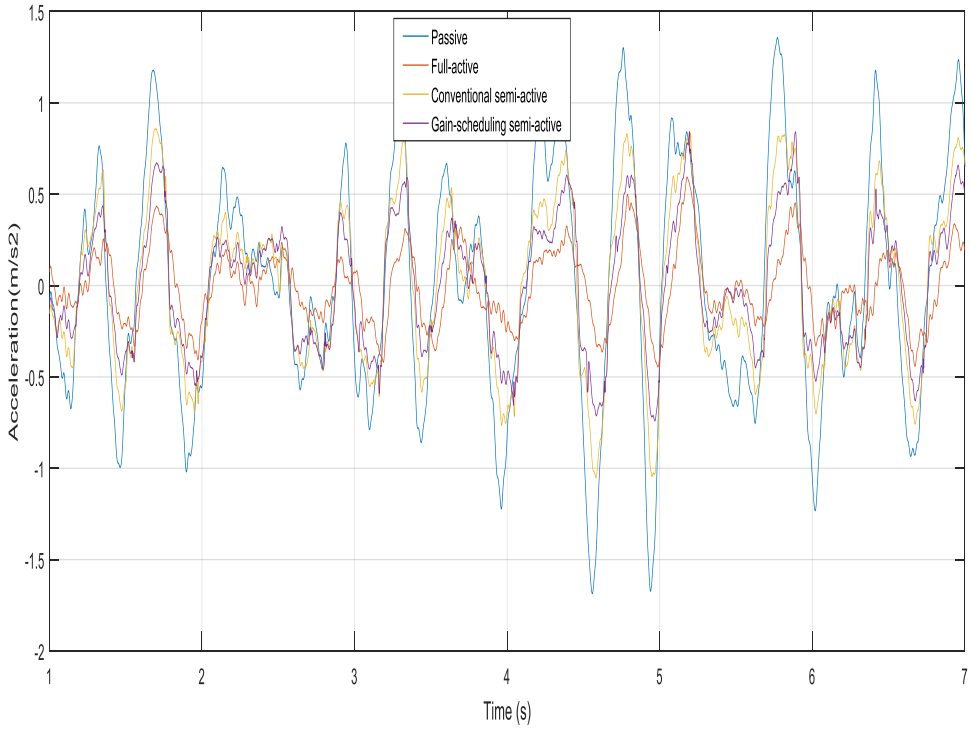

Figure 8.3: Acceleration comparison at the rear of the vehicle body using computer-generated track data

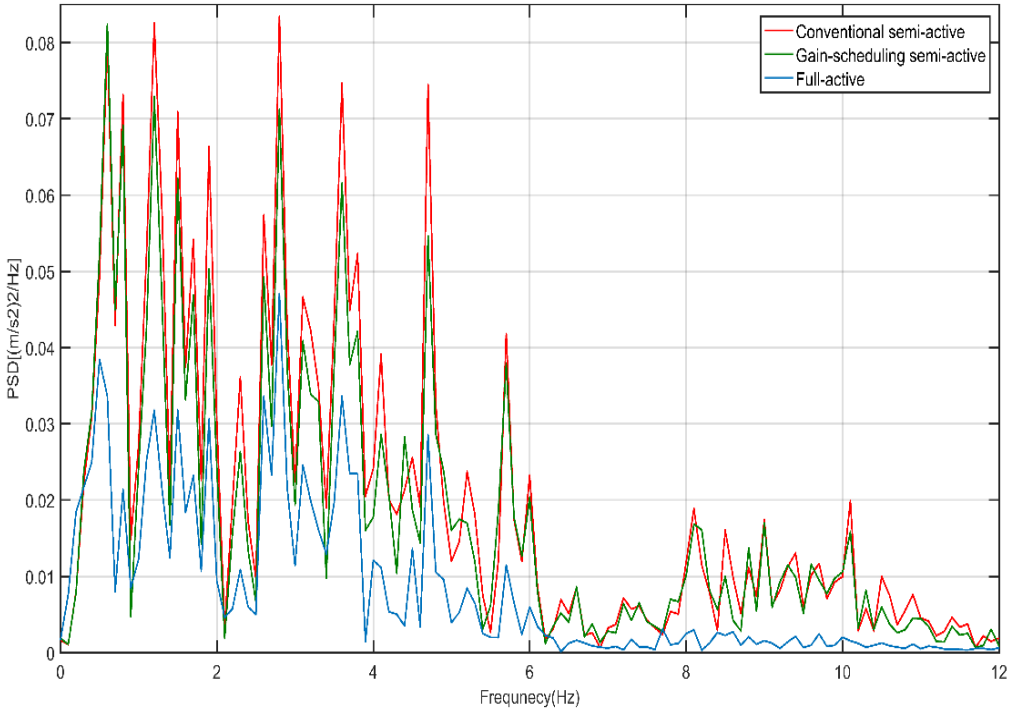

Figure 8.4: PSD of lateral acceleration at the centre of the vehicle body using computer-generated track data

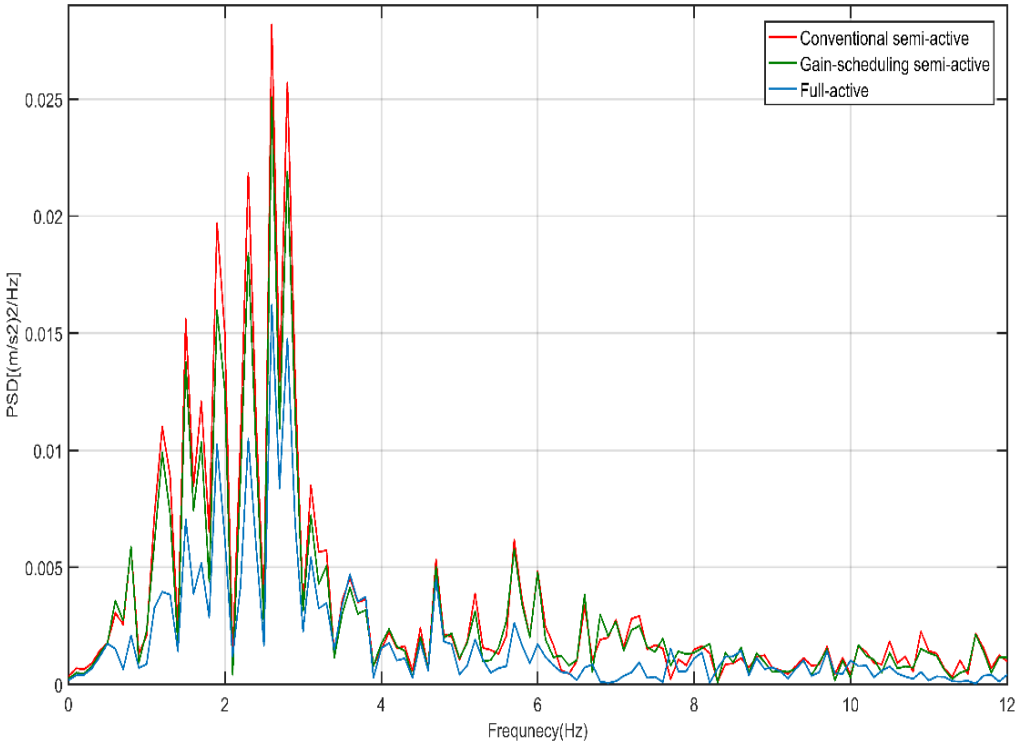

Figure 8.5: PSD of yaw comparison acceleration at the yaw of the vehicle body using computer-generated track data

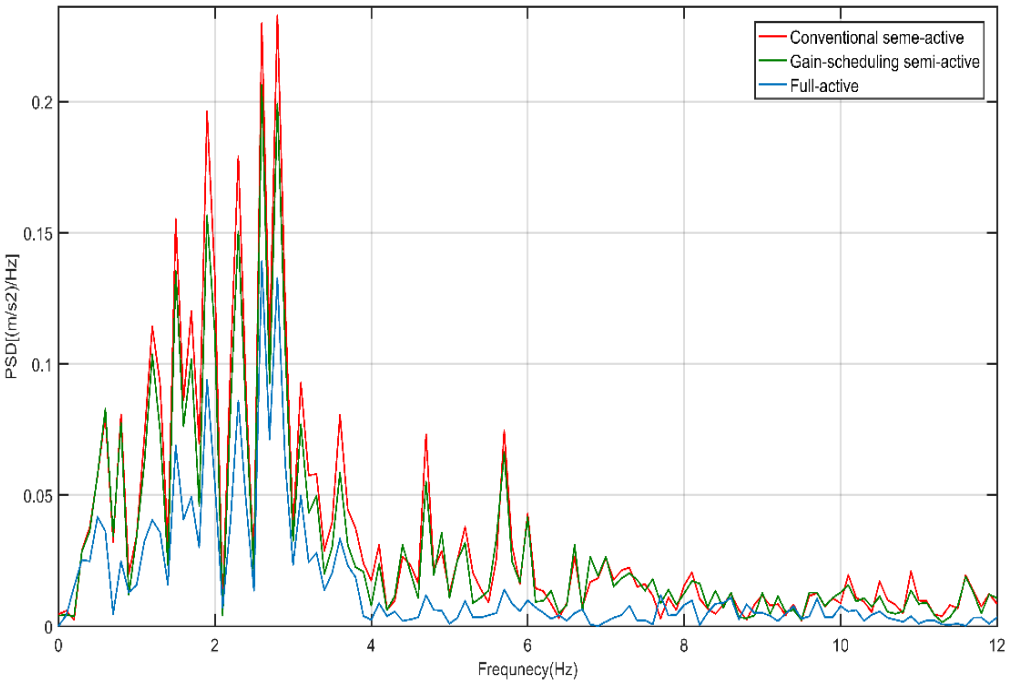

Figure 8.6: PSD of lateral comparison acceleration at the front of the vehicle body using computer-generated track data

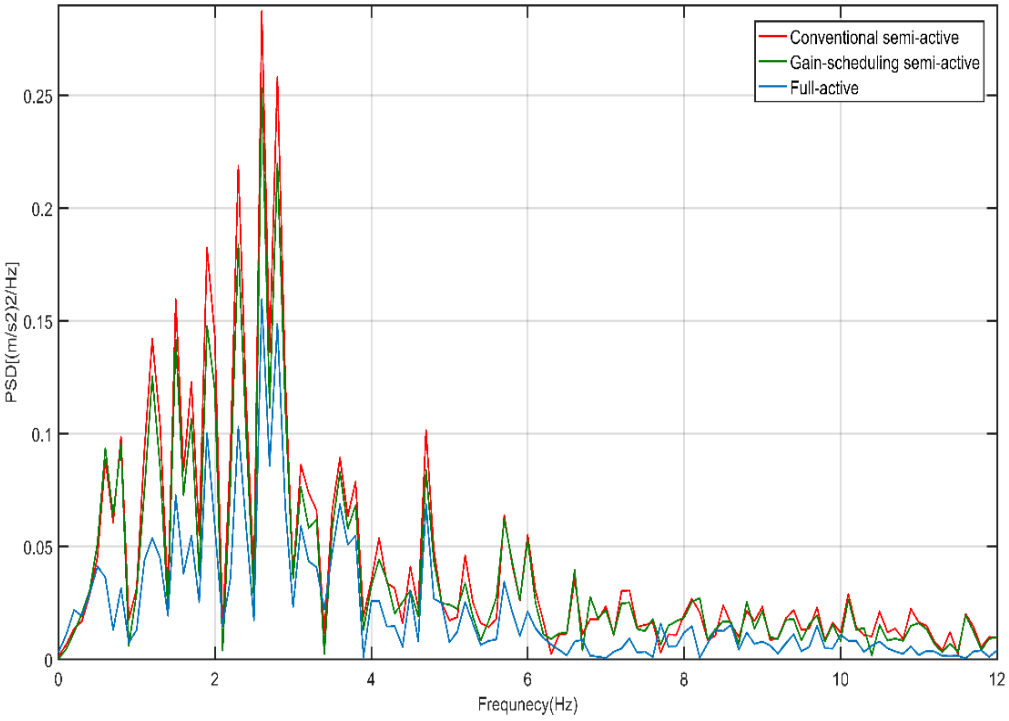

Figure 8.7: PSD of lateral comparison acceleration at the rear of the vehicle body using computer-generated track data

A comparison of ride quality improvements and maximum suspension deflection for three sections of the measured track data are shown in Tables 8.2, 8.3, and 8.4.

Table 8.2: Ride quality and suspension deflection results from time simulation using measured track data input (track1)

Control	Front (m/s^2)	lateral (m/s^2)	Rear (m/s^2)	yaw (rad/s^2)	Time use min. damper at damper1	Time use min. damper at damper1	Def. damper1 (mm)	Def. Damper2 (mm)
Passive(RMS value)	0.59489	0.21562	0.66584	0.06593			36.681	37.183
Full-active with actuator(%vs passive)	0.1967	0.05546	0.22791	0.02283	-	-	34.284	36.121
	66.93%	74.27%	65.77%	65.36%				
Semi-active with MR damper(% vs passive)	0.40042	0.14527	0.45471	0.04478	3.503	3.342	35.616	37.798
	32.69%	32.62%	31.70%	32.07%				
Gain scheduling with MR damper (% vs passive)	0.34103	0.12302	0.38693	0.03814	0.065	0.019	35.081	37.965
	42.673	42.948	41.889	42.143				

Table 8.3: Ride quality and suspension deflection results from time simulation using measured track data input (track2)

Control strategy	Front (m/s^2)	lateral (m/s^2)	Rear (m/s^2)	yaw (rad/s^2)	Time use min. damper at damper1	Time use min. damper at damper1	Def. damper 1(mm)	Def. Damper2 (mm)
Passive(RMS value)	0.52474	0.27955	0.644	0.05740	-	-	41.504	48.17
Full-active with actuator (%vs passive)	0.18497	0.07655	0.25371	0.02315	-	-	51.697	54.528
	64.75 %	72.61%	60.61%	59.66 %				
Semi-active with MR damper	0.37235	0.20096	0.46607	0.041209	3.931s	3.398 s	42.39	47.205
	29.04%	28.11%	27.62%	28.21 %				

(% vs passive)								
Gain scheduling with MR damper	0.2808	0.13239	0.36104	0.032787	0.458 s	0.043 s	47.967	51.931
(% vs passive)	46.487	52.642	43.937	42.882				

Table 8.4: Ride quality and suspension deflection results from time simulation using measured track data input (track3)

Control strategy	Front (m/s^2)	lateral (m/s^2)	Rear (m/s^2)	yaw (rad/s^2)	Time use min. damper at damper1	Time use min. damper at damper1	Def. damper1 (mm)	Def. Damper2 (mm)
Passive(RMS value)	0.3512	0.21573	0.41242	0.035167	-	-	18.031	19.68
Full-active with actuator	0.1101	0.05804	0.16755	0.014371	-	-	21.858	23.09
(%vs passive)	68.65 %	73.09%	59.37%	59.13%				
Semi-active with MR damper	0.2234	0.1391	0.28529	0.023909	3.612s	2.929 s	19.45	21.931
(% vs passive)	36.38%	35.52%	30.82%	32.01%				
Gain scheduling with MR damper	0.17505	0.10843	0.23875	0.019896	0.352 s	0.071 s	20.583	22.927
(% vs passive)	50.15%	49.73%	42.10%	43.42%				

Tables 8.2, 8.3, and 8.4 show the ride quality improvements of the gain-scheduling control based semi-active suspension in comparison to the conventional semi-active suspension on three real measured track inputs. In all cases, the time for the MR damper being set at the minimum damping (i.e., in the passive mode) is significantly reduced on every track section, and the ride quality is further improved by around 14% to 20% compared to the conventional semi-active control.

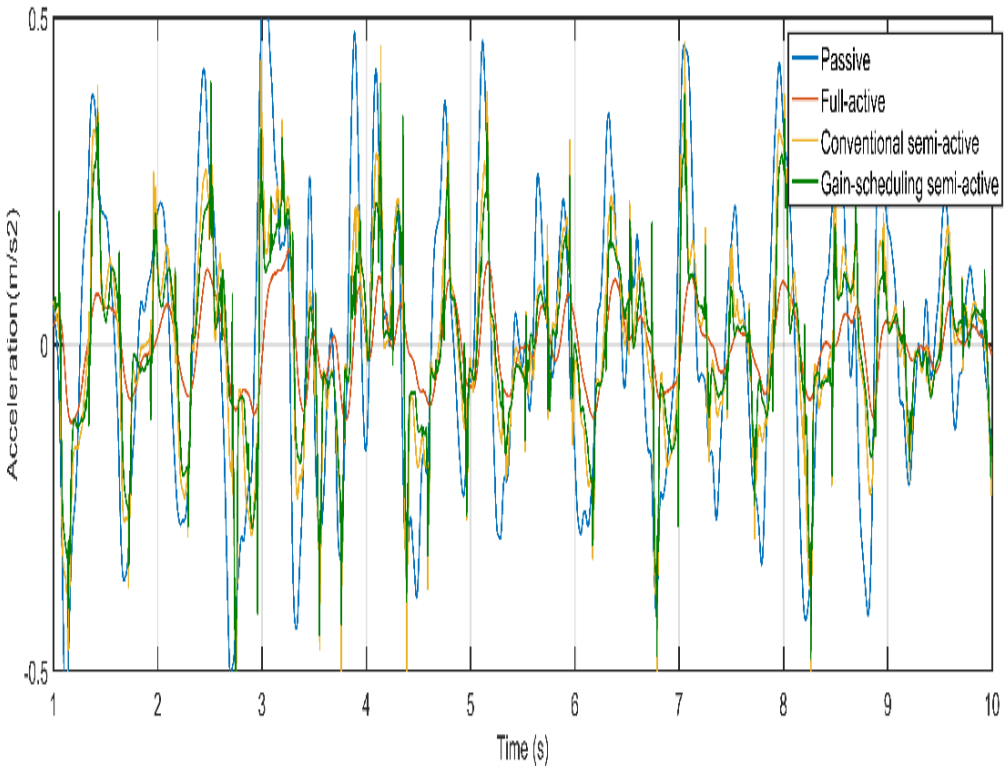

Figure 8.8: Acceleration comparison at the centre of the vehicle body using measured track data (track1)

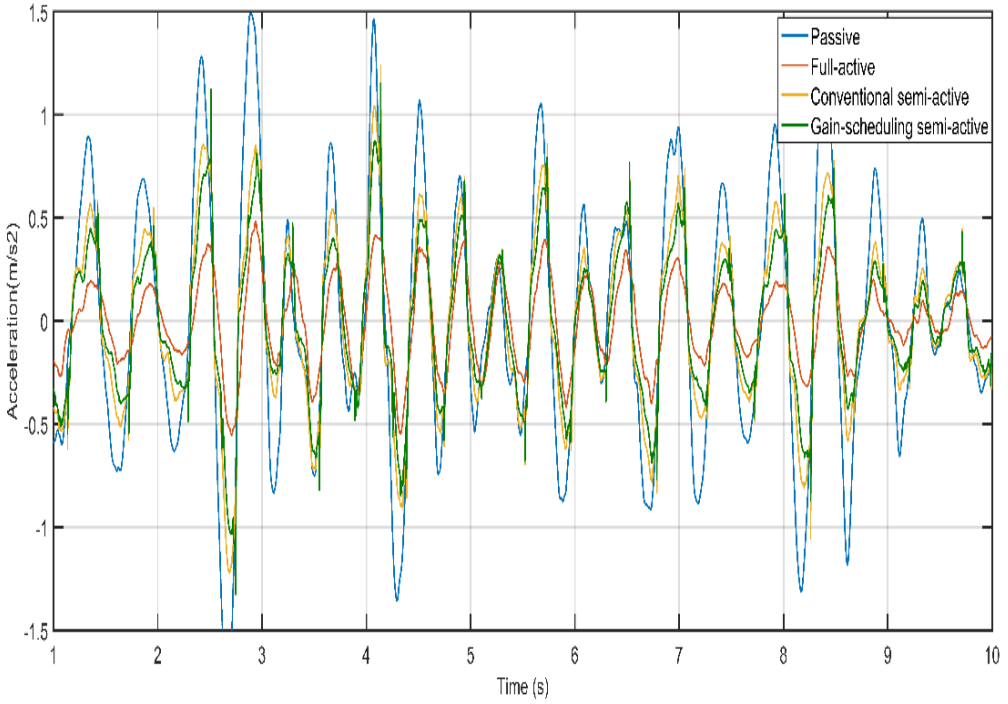

Figure 8.9: Acceleration comparison at the front of the vehicle body using measured track data (track1)

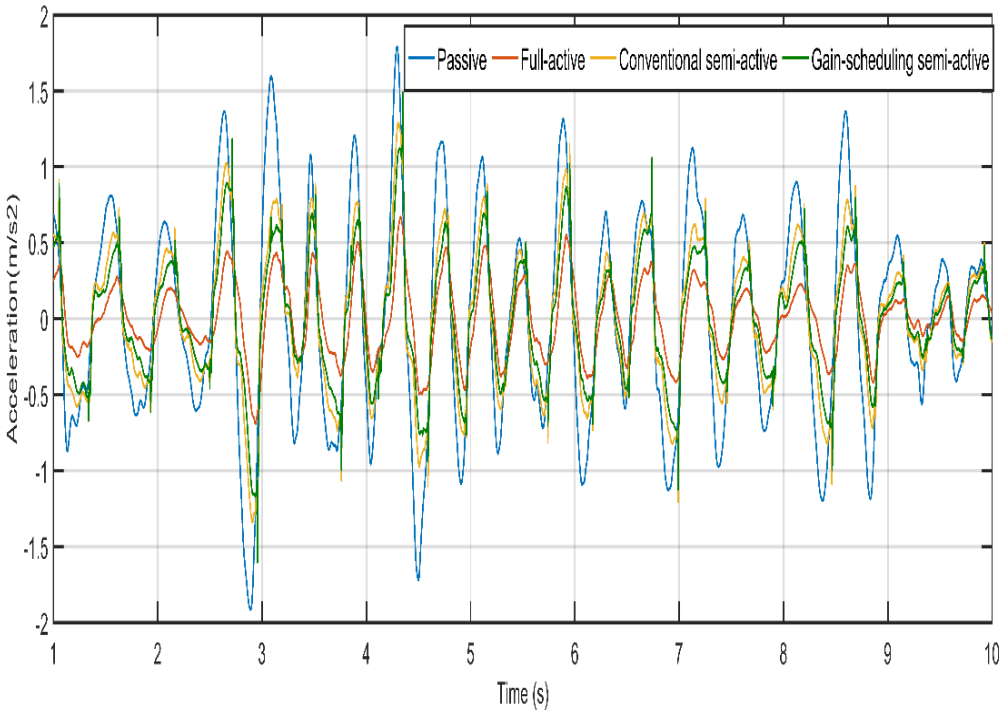

Figure 8.10: Acceleration comparison at the rear of the vehicle body using measured track data (track1)

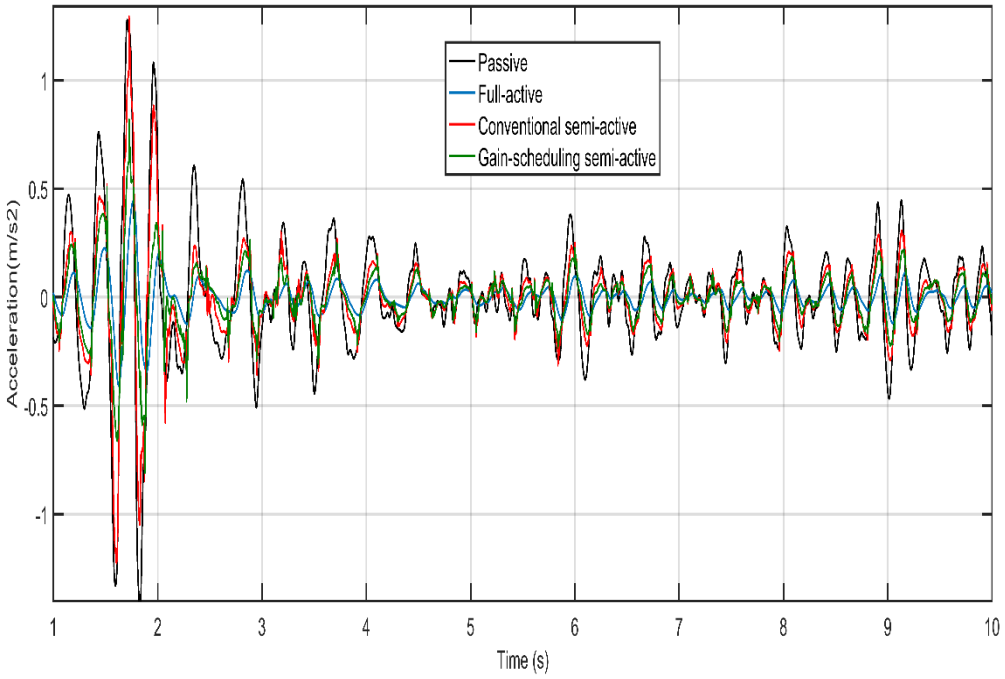

Figure 8.11: Lateral acceleration at the centre of the vehicle body using measured track data (track2)

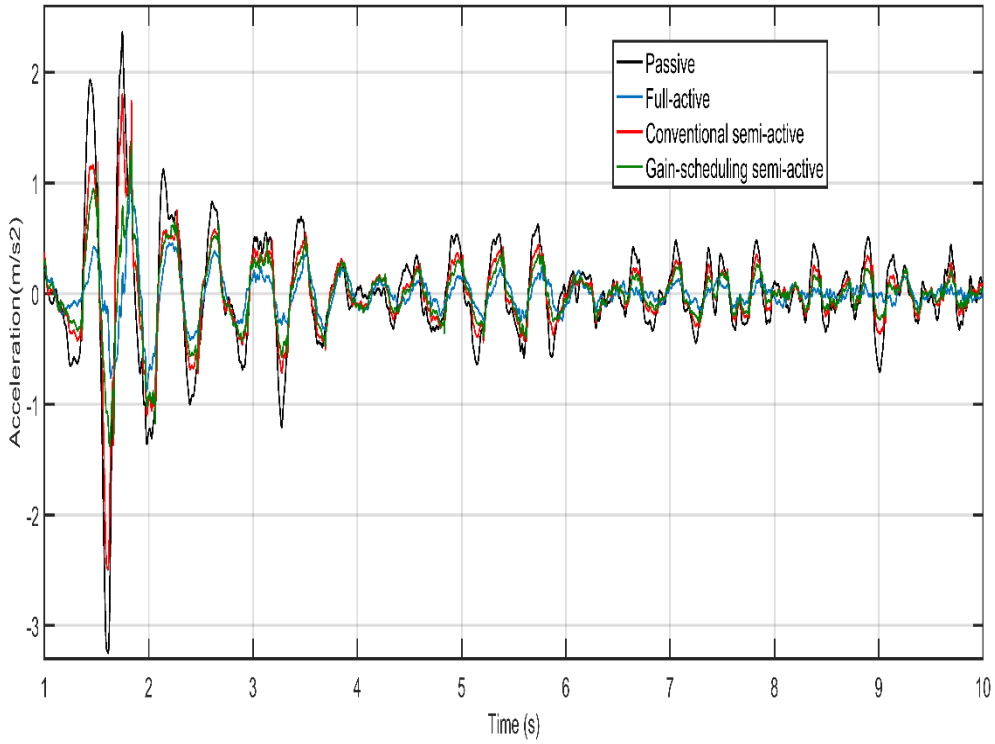

Figure 8.12: Lateral acceleration at the front of the vehicle body using measured track data (track2)

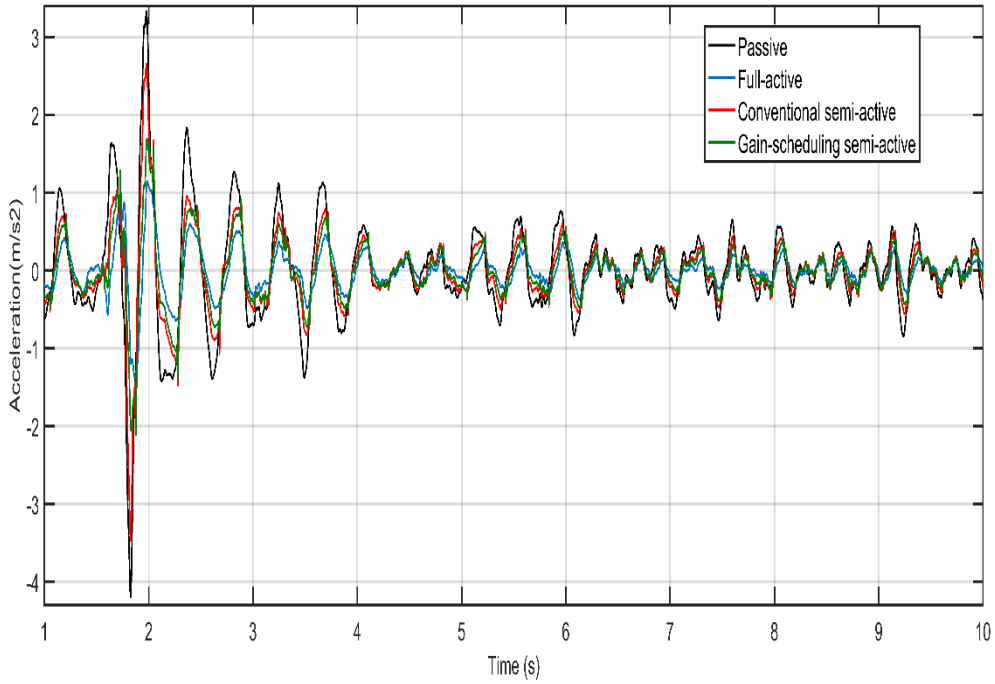

Figure 8.13: Lateral acceleration at the rear of the vehicle body using measured track data (track2)

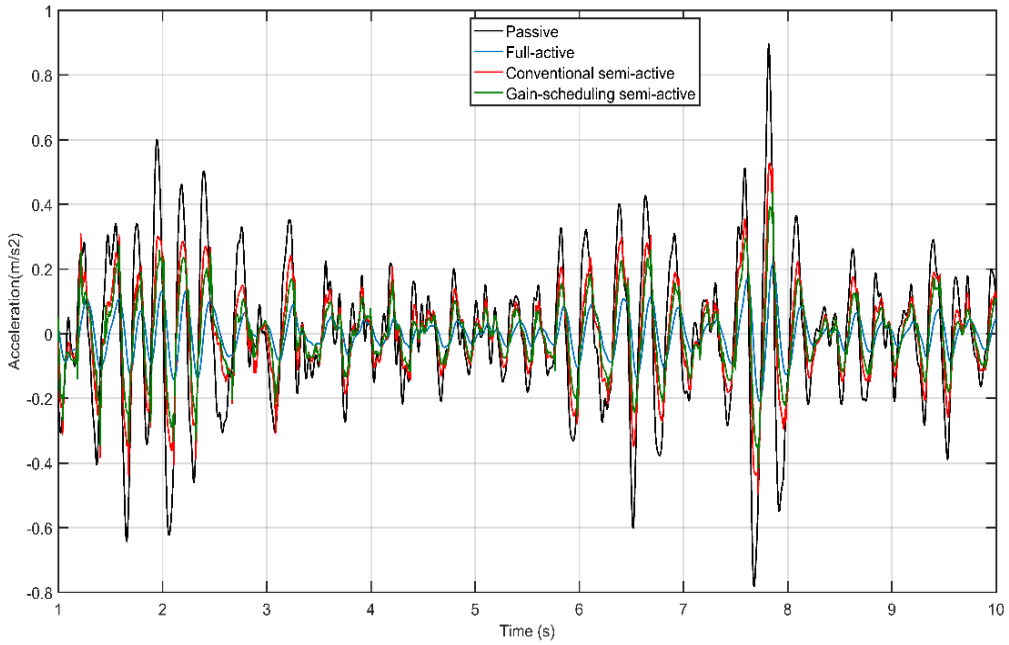

Figure 8.14: Acceleration comparison at the centre of the vehicle body using measured track data (track3)

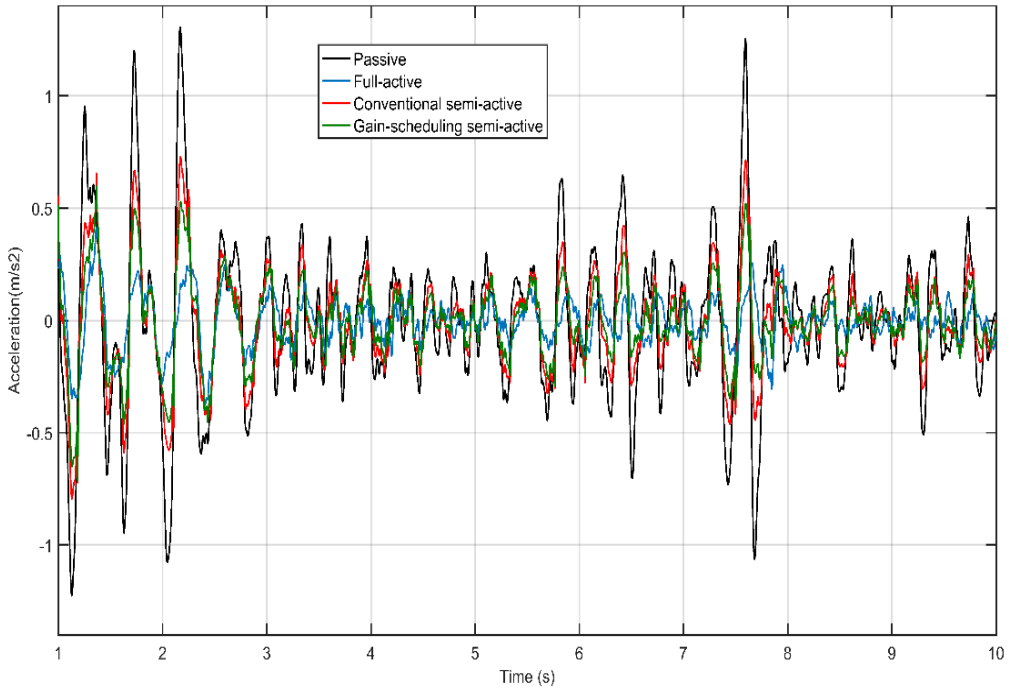

Figure 8.15: Acceleration comparison at the front of the vehicle body using measured track data (track3)

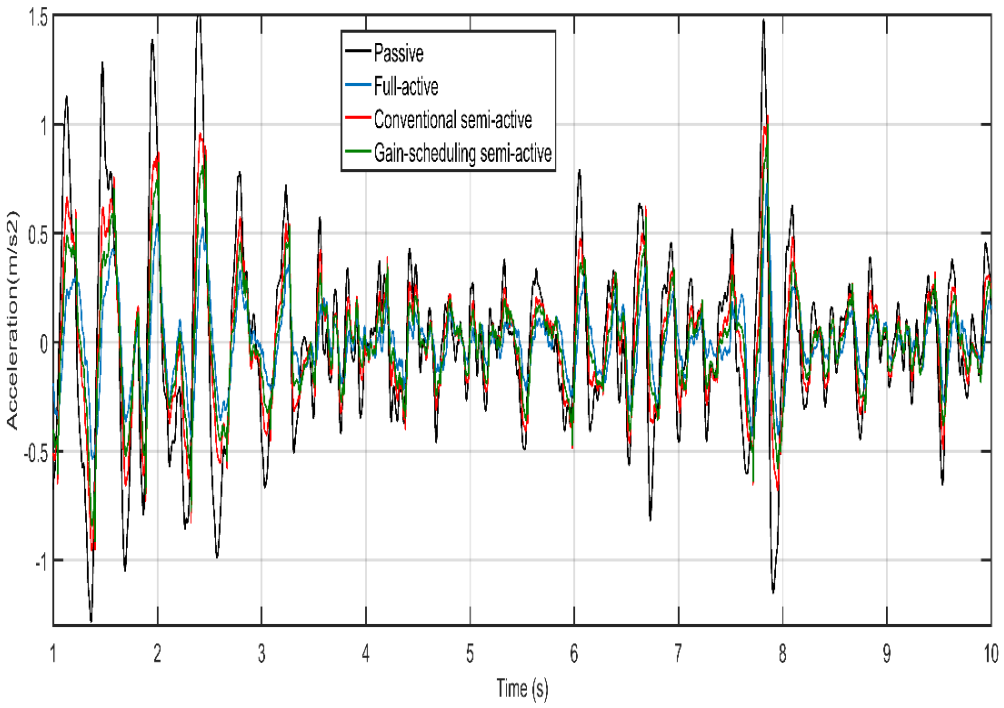

Figure 8.16: Acceleration comparison at the rear of the vehicle body using measured track data (track3)

The PSD of the vehicle body acceleration with the proposed control, conventional semi-active and full-active strategies is also studied and the results using different track data to evaluate their effects in terms of different frequencies.

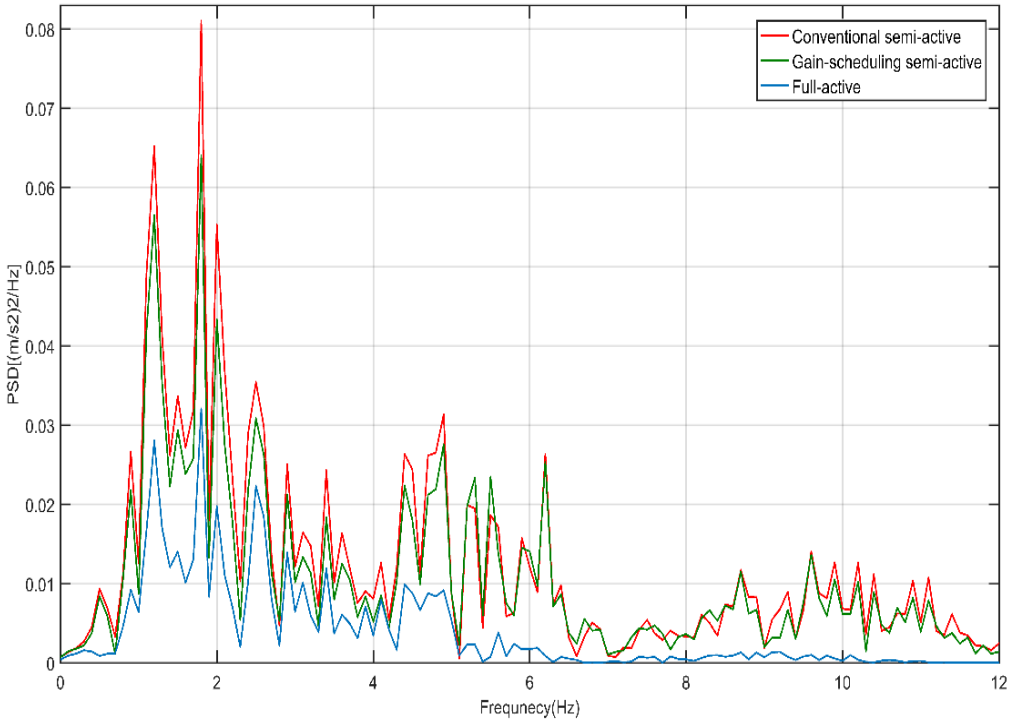

Figure 8.17: PSD of lateral acceleration at the centre of the vehicle body using measured track data (track1)

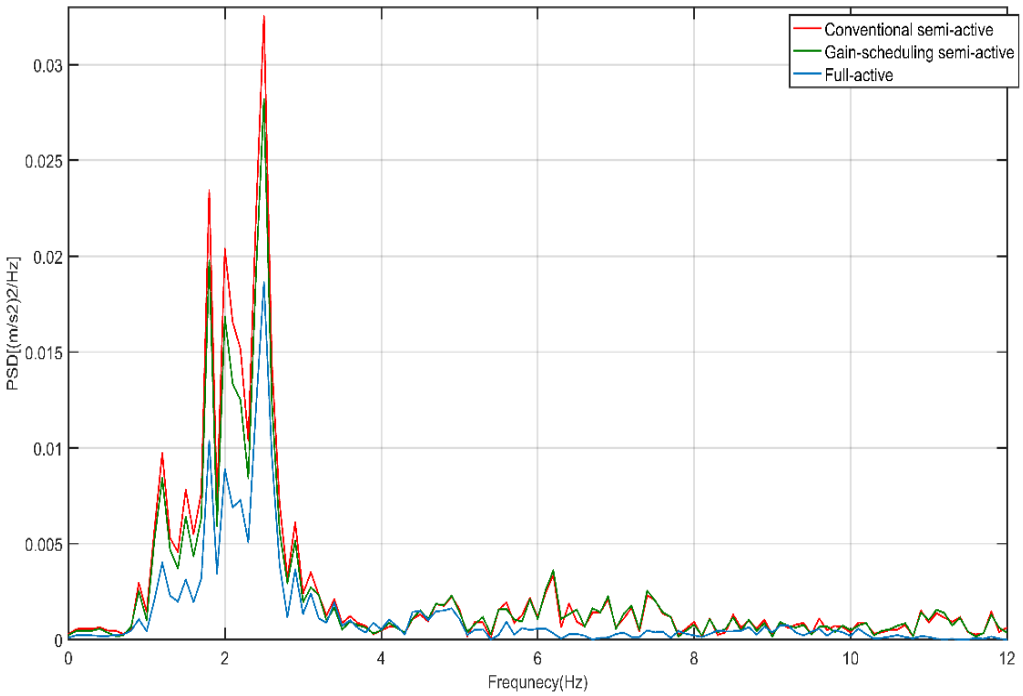

Figure 8.18: PSD of lateral acceleration at the yaw of the vehicle body using measured track data (track1)

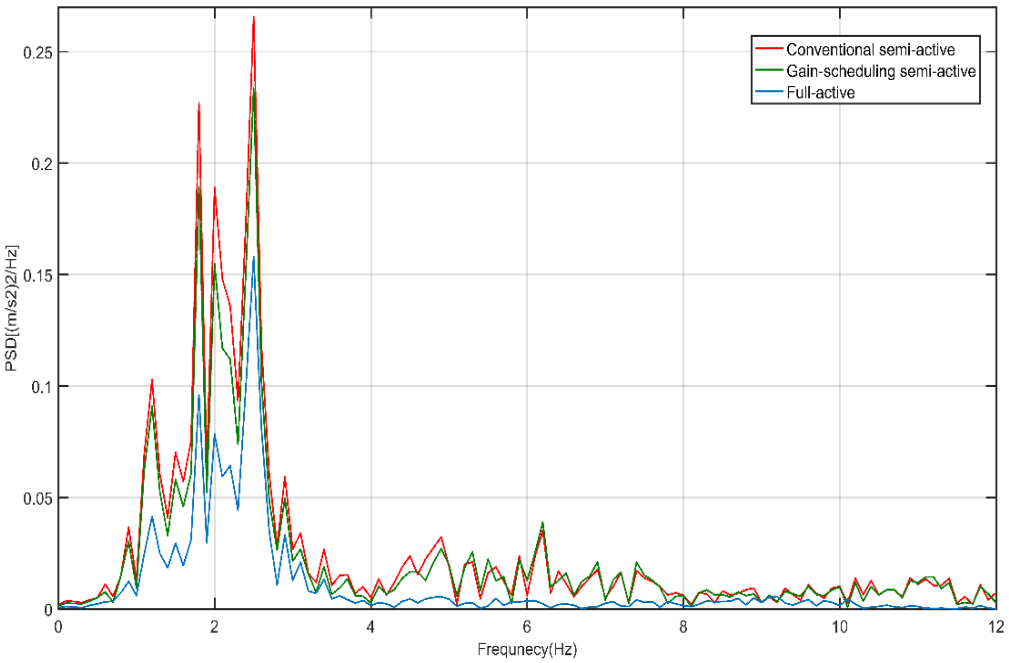

Figure 8.19: PSD of lateral acceleration at the front of the vehicle body using measured track data (track1)

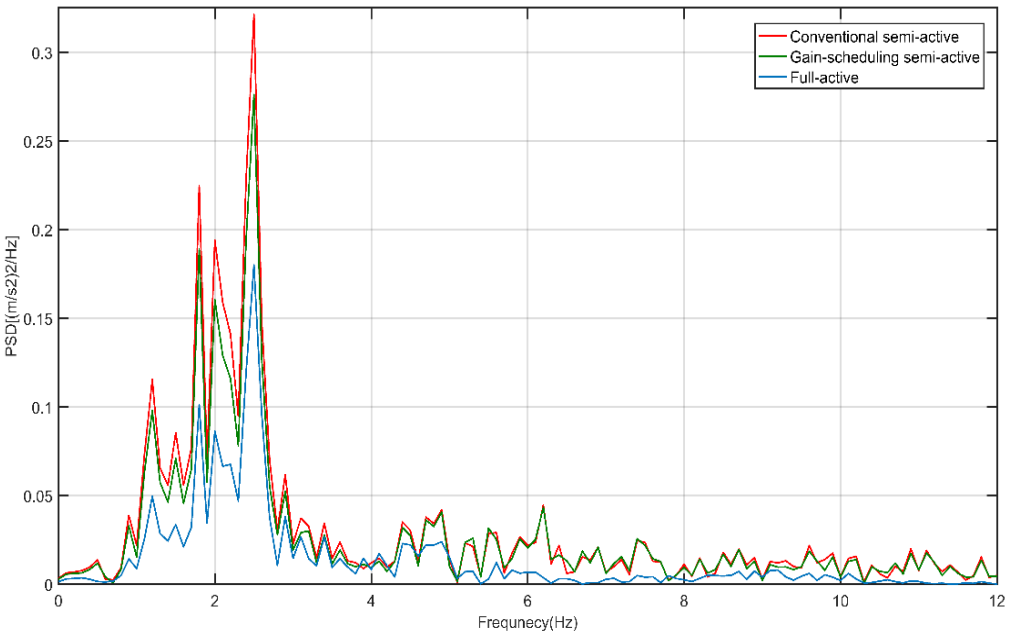

Figure 8.20: PSD of lateral acceleration at the rear of the vehicle body using measured track data (track1)

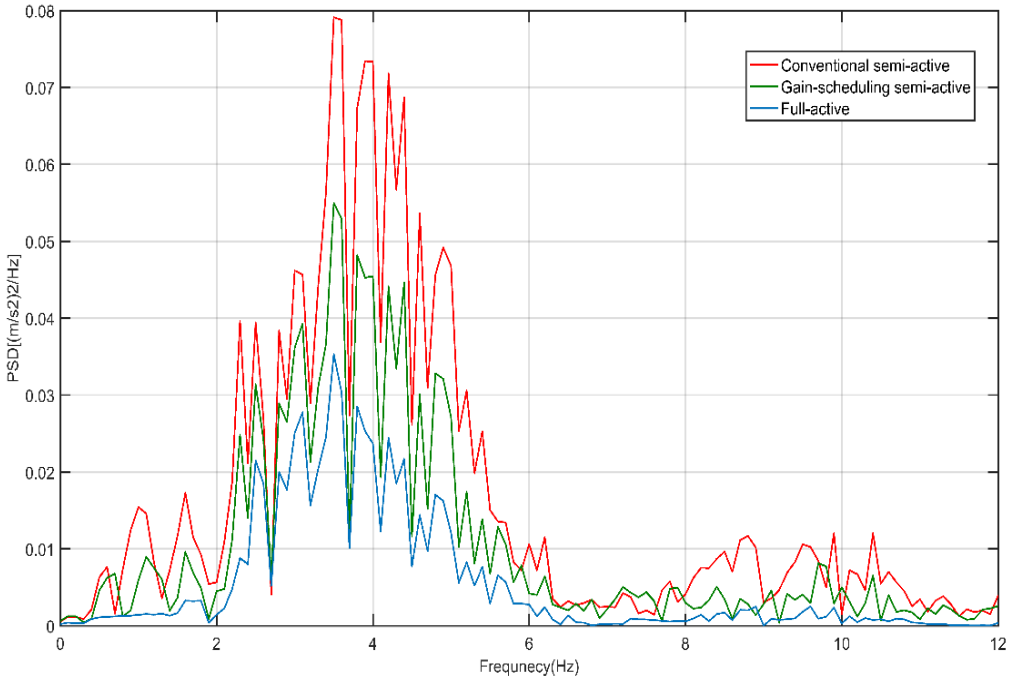

Figure 8.21: PSD of lateral acceleration at the centre of the vehicle body using measured track data (track2)

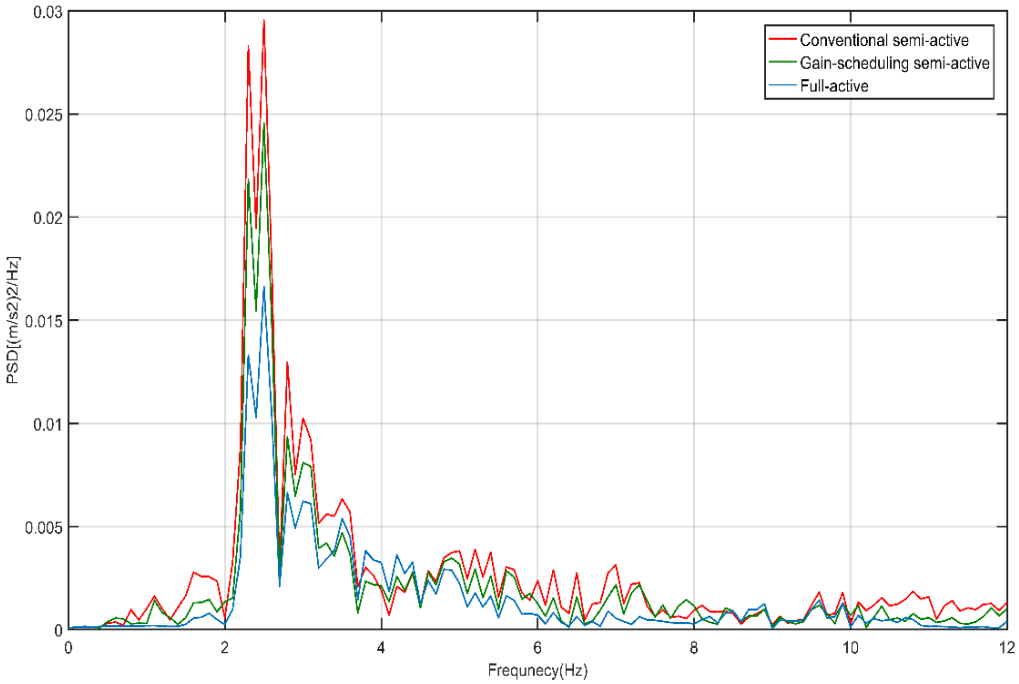

Figure 8.22: PSD of lateral acceleration at the yaw of the vehicle body using measured track data (track2)

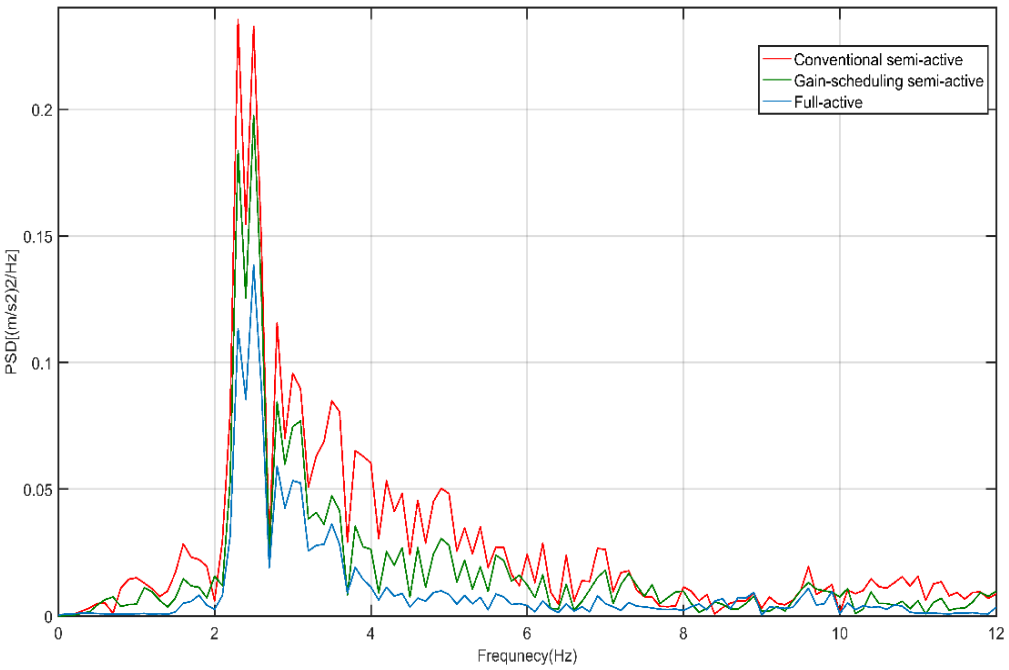

Figure 8.23: PSD of lateral acceleration at the front of the vehicle body using measured track data (track2)

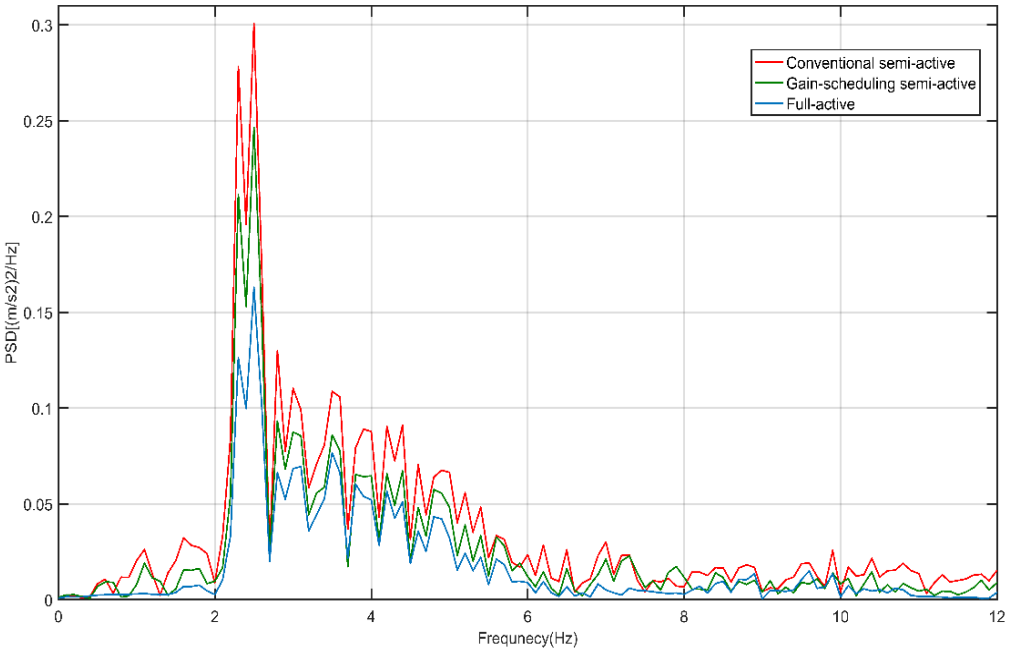

Figure 8.24: PSD of lateral acceleration at the rear of the vehicle body using measured track data (track2)

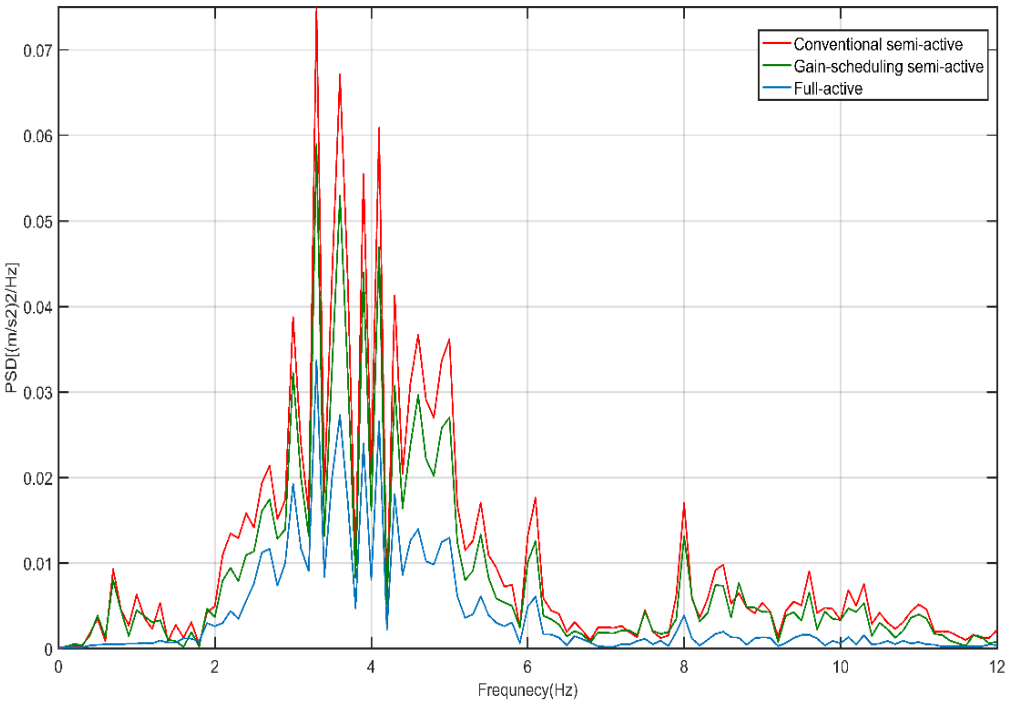

Figure 8.25: PSD of lateral acceleration at the centre of the vehicle body using measured track data (track3)

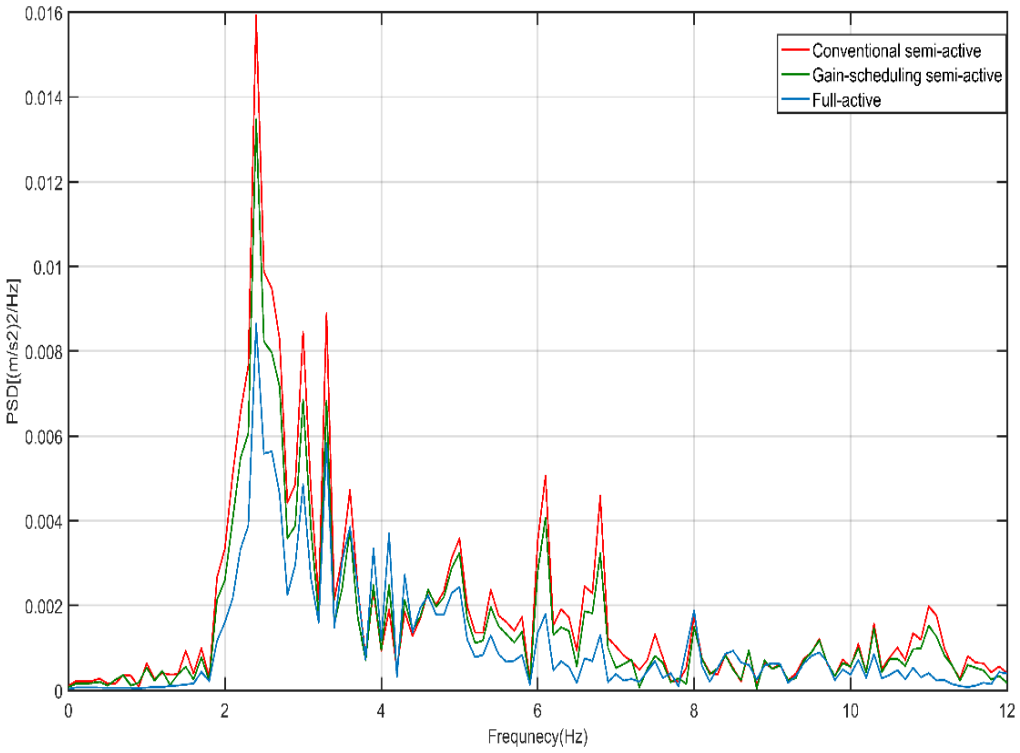

Figure 8.26: PSD of lateral acceleration at the yaw of the vehicle body using measured track data (track3)

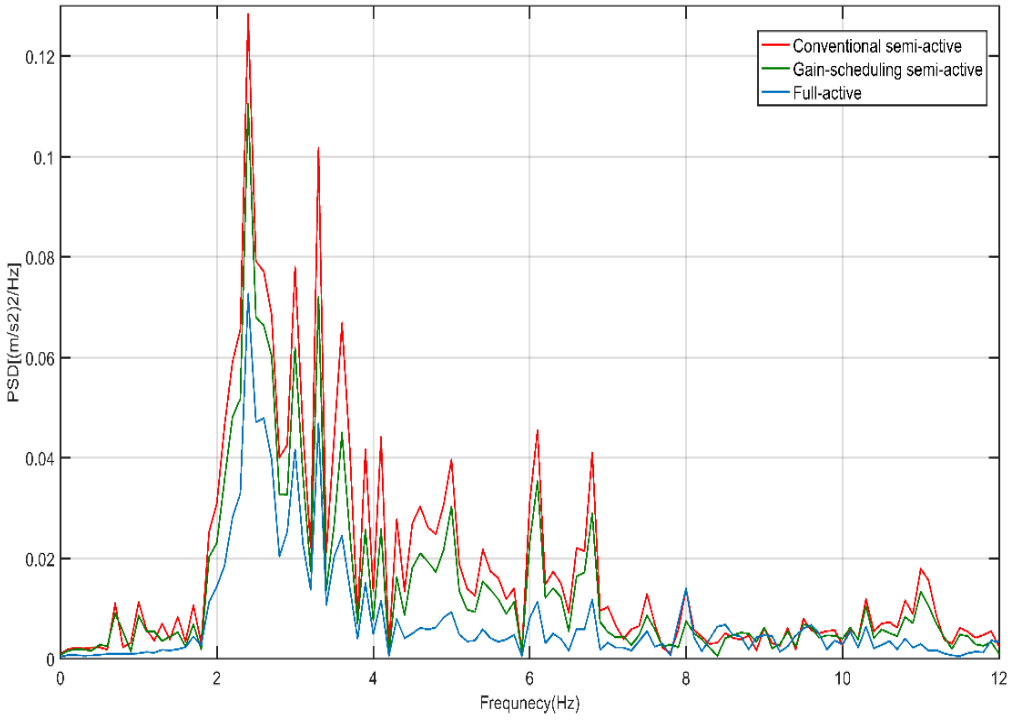

Figure 8.27: PSD of lateral acceleration at the front of the vehicle body using measured track data (track3)

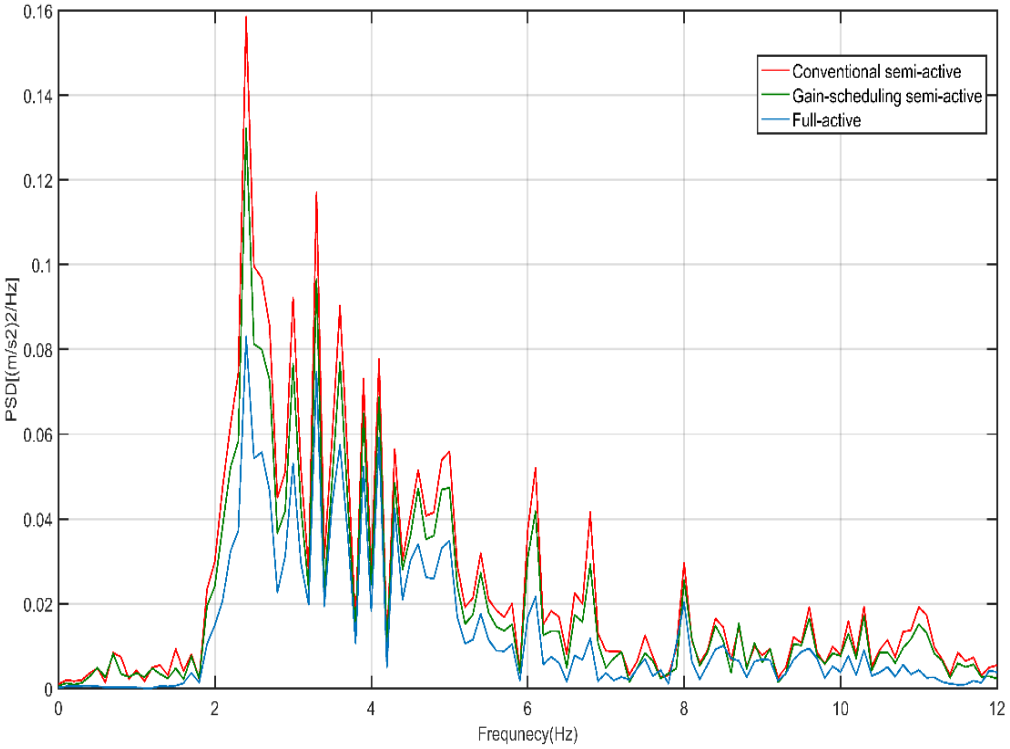

Figure 8.28: PSD of lateral acceleration at the rear of the vehicle body using measured track data (track3)

8.2 Summary

In this chapter, the study has investigated the development of a nonlinear semi-active controller for lateral secondary suspension for improving the ride quality of railway vehicles and has evaluated the performance of the novel control approach against a passive suspension, a conventional semi-active and a full active control system.

In general, according to Tables 8.2, 8.3, and 8.4, the ride-quality improvements of the lateral and yaw acceleration of the railway vehicle with a full-active suspension system on real measured track input are consistent with that using the generic track data as given in Table8.1 and are around 65%. However, the ride quality improvements using conventional semi-active suspension system was approximately 30% in Table 8.1 (under generic track irregularities) while quality improvements using conventional semi-active suspension was approximately 35% in Table 8.2, 8.3 and 8.4 (under measured track irregularities data for three different

sections). It is worth noting that the duration of the passive mode under random track irregularities (Table 8.1) was around 4 seconds, while the duration of the passive mode under measured track irregularities data for three different sections (Table 8.2, 8.3 and 8.4) was about 3 seconds.

Moreover, it can also be seen from Table 8.1 that the ride quality improvements using a gain-scheduling semi-active suspension system was about 38% and the duration of the passive mode was around 0.55 seconds. However, the improvements using the gain-scheduling semi-active suspension under measured track irregularity data for three different sections (Table 8.2, 8.3, and 8.4) was around 50% and the duration of the passive mode was lower than 0.55 seconds which indicates that the ride quality of semi-active suspension systems by extending the duration of the active mode is superior to those of the semi-active suspension systems whilst lowering the duration of the active mode.

Moreover, broad frequencies are noticed for the computer-generated track irregularities in Figures 8.4, which reflects an improvement of around 10% for the gain scheduling-based semi-active control when compared with the conventional semi-active system listed in Table 8.1. Figures 8.17, 8.21, and 8.25 shows a narrower range of frequencies from the measured track data, whilst Tables 8.2, 8.3, and 8.4 indicate an improvement of around 20% when compared with conventional semi-active suspension.

CHAPTER NINE

9 CONCLUSIONS AND FUTURE WORK

9.1 Conclusions

This chapter contains the general conclusions of this thesis. Detailed findings are included in each chapter. Throughout the thesis, the study has covered aspects involving the development of a nonlinear control strategy for semi-active suspensions based on Magnetorheological (MR) dampers for a railway vehicle using gain-scheduling structure control. The aim of the research was to overcome the constraints of the conventional linear control strategies and improve the semi-active suspensions to gain a performance close to that of full-active systems.

For the purposes of performance comparison, a semi-active controller based on skyhook damping control integrated with MR dampers and a vehicle with passive suspension were used as the benchmark, and are used as a reference case for assessment of the proposed design.

Computer simulation using the model of a conventional bogie vehicle was performed in the Matlab Simulink environment to investigate the performance of different control strategies for the secondary suspension system of the railway vehicle. The performance of the proposed controller is investigated in term of car body acceleration and the relative displacement of the suspension units. For the purposes of control design and assessment, a generalised computer data was used to represent track irregularities. Then, for research assessment, real measured data for track irregularities were also used. Numerical simulation for semi-active secondary suspension cases was used to study the effectiveness and efficiency of the proposed control strategy. Potentially, this kind of adaptive capability with variable control approaches may be used to deliver the level of the performance that is currently only possible with a full-active suspension without incurring the associated high costs and power consumption.

The results are presented by PSDs and RMS values for vehicle accelerations. According to the simulation and analyses, it can be established that:

- The simulation results show that the full-active-based skyhook control always provides the best performance over a wide range of frequencies than passive, conventional semi-active, and gain-scheduling semi-active suspensions.
- For the full-active suspension system-based skyhook control, it should be noted that vertical full-active suspension delivers better ride quality than lateral full-active suspension. This is mainly because the full-active suspension is affected by two conflicting factors that have an influence on its performance, namely the suspension deflection and the ride quality. The lateral full-active suspension is more restricted to trade-offs between the performance and the suspension deflection because the lateral suspension system is affected by low-frequency track irregularities.
- The simulation result indicates that the lookup table inverse model of the MR damper can satisfy the needs of the application where the inverse model was employed to track the desired damping force.
- For conventional semi-active suspension, the results showed that percentage of time when the semi-active damper is in active-mode is dependent on the frequency of track irregularity input, which indicates that the switching of the semi-active control may depend on the amplitude and frequency of the irregularities.
- It should be noted that the split in time between the active and passive modes for the conventional semi-active control strategies has an impact on ride-quality improvements. Results indicate that the ride quality of semi-active suspension systems with longer active-

mode durations deliver better ride quality than those of the semi-active suspension systems with shorter active-mode durations.

- The results illustrate that the gain-scheduling controller delivers smooth switching behaviour as it enables the maximum use of possible damping forces hence minimises the time when the semi-active control is switched to passive mode.
- This study has shown that a significant improvement in vehicle ride quality is achieved using gain scheduling control integrated with the MR damper of the secondary suspension. It has shown that, in comparison to the conventional semi-active controller, the ride quality of the vehicle would be improved by around 15% to 20% when the gain-scheduling controller is applied. In addition, the results obtained with the use of gain-scheduling controller show a potential to reduce the use of the minimum damper setting. It has been illustrated that the gain-scheduling controller delivers smooth switching behaviour as it enables the maximum use of possible damping forces hence minimises the time when the semi-active control is switched to passive mode.

9.2 Recommendations for Future Work

This thesis presents the development of a non-linear control strategy for semi-active suspension that can be used to deliver the level of the performance that is currently only possible with full-active suspension without incurring the associated high costs and power consumption. This thesis presents a scientific contribution to a new approach to the above ends. Further research directions that need to be pursued to bring such a system to industrial adoption are as follows:

- A semi-active device with higher damping on active state and lower damping on passive state would work best.

- Research into the design control strategy using alternative semi-active devices could be of value.
- The research is carried out assuming the vehicle is moving on a straight track, which can further be extended for both deterministic (low-frequency signals) and the random track inputs (high-frequency signals) as well.
- This study is carried out using the dynamic model of two-stage suspension systems, with the potential of this research being assessed using a single-stage suspension model. The research idea can be further extended to achieve a better compromise between stability and guidance.
- Finally, experimental implementation and validation of the semi-active suspension-based gain-scheduling control will be required before it can be used in practical applications.

10 APPENDIX: LIST OF PUBLICATIONS

1. Husam Hammood and Mie TX, “Variable structure control for railway vehicle semi-active suspension”. Proceedings of the Salford Postgraduate Annual Research Conference 2017, 27-29 June 2017, University of Salford UK, p.30-31
2. H. Hammood and Mie TX, “Gain-scheduling control for railway vehicle semi-active suspension”, Proceedings of the 25th Symposium of the International Association of Vehicle System Dynamics (IAVSD 2017), Rockhampton, Queensland, Australia, 14–18 August 2017
3. Husam Hammood and Mie TX, “Improvement of semi-active suspensions based on gain-scheduling control”. Proceedings of the Salford Postgraduate Annual Research Conference 2018,4-5 July 2018,University of Salford UK,p.123-124
4. Husam Hammood and Mie TX, “Gain-scheduling Control for Semi-active Suspensions”, (under review)

11 REFERENCES

[1] J. Fagerlund, "Towards Active Car Body Suspension in Railway Vehicles," LEng thesis, Chalmers University of Technology, Goteborg, Sweden, 2009.

[2] K. Tanifuji, S. Koizumi, and R. Shimamune, "Mechatronics in Japanese rail vehicles: active and semi-active suspensions," *Control Engineering Practice*, vol. 10, pp. 999-1004, Sep 2002.

[3] L. Tianye, W. Zhongdong, T. M. Xiang, and Z. Wanling, "Study on Semi-active Secondary Suspension of Railway Vehicle," *International Conference on Transportation, Mechanical, and Electrical Engineering (TMEE)*, pp. 237–253, 2011.

[4] Y. Zhiqiang, Z. Baoan, Z. Jimin, and W. Chenhui, "Research on Semi-active Control of High-speed Railway Vehicle Based on Neural Network-PID Control," presented at the Seventh International Conference on Natural Computation, 2011.

[5] D. S. Pour and S. Behbahani, "Semi-active fuzzy control of machine tool chatter vibration using smart MR dampers," *International Journal of Advanced Manufacturing Technology*, vol. 83, pp. 421-428, Mar 2016.

[6] X. Wei, M. Zhu, and L. Jia, "A semi-active control suspension system for railway vehicles with magnetorheological fluid dampers," *Vehicle System Dynamics*, vol. 54, pp. 982-1003, Jul 2016.

[7] D. Karnopp, M. J. Crosby, and R. Harwood, "Vibration control using semi-active force generators," *Journal of Engineering for Industry*, vol. 96, pp. 619-626, 1974.

[8] M. H. A. Talib and I. Z. M. Darus, "Self-Tuning PID Controller with MR damper and Hydraulic Actuator for Suspension System," pp. 119-124, 2013.

[9] C. Lin, W. Liu, and H. B. Ren, "Neutral network-PID control algorithm for semi-active suspensions with magneto-rheological damper," *Journal of Vibroengineering*, vol. 17, pp. 4432-4444, Dec 2015.

[10] M. L. Aggarwal, "Comparative Analysis of Passenger Ride Comfort using Various Semi-Active Suspension Alternatives," *International Journal of Recent advances in Mechanical Engineering*, vol. 3, pp. 79-89, 2014.

[11] L. C. Félix-Herrán, J. d. J. Rodríguez-Ortiz, R. Soto, and R. Ramírez-Mendoza, "Modeling and Control for a Semi-active Suspension with a Magnetorheological Damper Including the Actuator Dynamics," pp. 338-343, 2008.

[12] A. K-Karamodin and H. H-Kazemi, "Semi-active control of structures using neuro-predictive algorithm for MR dampers," *Structural Control and Health Monitoring*, pp. 237–253, 2008.

[13] S.-Y. Ok, D.-S. Kim, K.-S. Park, and H.-M. Koh, "Semi-active fuzzy control of cable-stayed bridges using magneto-rheological dampers," *Engineering Structures*, vol. 29, pp. 776-788, 2007.

[14] J. C. Tudon-Martinez and R. Morales-Menendez, "Adaptive Vibration Control System for MR Damper Faults," *Shock and Vibration*, 2015 2015.

[15] S. Iwnicki, *Handbook of railway vehicle dynamics*. Boca Raton, FL: CRC press, 2006.

[16] A. Orvnäs, *Active secondary suspension in trains: A literature survey of concepts and previous work*: KTH, 2008.

[17] B. Ebrahimi, "Development of Hybrid Electromagnetic Dampers for Vehicle Suspension Systems," PhD thesis, University of Waterloo, Waterloo, Ontario, 2009.

[18] R. M. Goodall, S. Bruni, and T. X. Mei, "Concepts and prospects for actively controlled railway running gear," *Vehicle System Dynamics,* vol. 44, pp. 60-70, 2006.

[19] S. Bruni, R. Goodall, T. Mei, and H. Tsunashima, "Control and monitoring for railway vehicle dynamics," *Vehicle System Dynamics,* vol. 45, pp. 743-779, 2007.

[20] R. Goodall, "Active Railway Suspensions: Implementation Status and Technological Trends," *Vehicle System Dynamics,* vol. 28, pp. 87-117, 1997.

[21] S. Sun, H. Deng, W. Li, H. Du, Y. Q. Ni, J. Zhang, *et al.*, "Improving the critical speeds of high-speed trains using magnetorheological technology," *Smart Materials and Structures,* vol. 22, p. 115012, 2013.

[22] Y. Liu, "Semi-active damping control for vibration isolation of base disturbances," PhD thesis, University of Southampton, Southampton, 2004.

[23] R. M. Goodall and W. Kort, "Mechatronic developments for railway vehicles of the future," *Control Engineering Practice,* vol. 10, pp. 887–898, 2002.

[24] H. Li and R. Goodall, "Distinguishing between Random and Deterministic Track Inputs for Active Railway Suspensions," *Vehicle System Dynamics,* vol. 29, pp. 772-777, 1998.

[25] H. Li and R. M. Goodall, "Linear and non-linear skyhook damping control laws for active railway suspensions," *Control Engineering Practice*, vol. 7, pp. 843-850, Jul 1999.

[26] T. X. Mei, H. Li, and R. M. Goodall, "Kalman filters applied to actively controlled railway vehicle suspensions," *Transactions of the Institute of Measurement and Control,* vol. 23, pp. 163-181, 2001 2001.

[27] J. Pombo and J. Ambrosio, "An alternative method to include track irregularities in railway vehicle dynamic analyses," *Nonlinear Dynamics,* vol. 68, pp. 161-176, Apr 2012.

[28] L.-H. Zong, X.-L. Gong, S.-H. Xuan, and C.-Y. Guo, "Semi-active H∞ control of high-speed railway vehicle suspension with magnetorheological dampers," *Vehicle System Dynamics,* vol. 51, pp. 600-626, 2013.

[29] R. Goodall, G. Freudenthaler, and R. Dixon, "Hydraulic actuation technology for full- and semi-active railway suspensions," *Vehicle System Dynamics,* vol. 52, pp. 1642-1657, 2014.

[30] J. Zhou, G. Shen, H. Zhang, and L. Ren, "Application of modal parameters on ride quality improvement of railway vehicles," *Vehicle System Dynamics,* vol. 46, pp. 629-641, 2008.

[31] H. B. Zheng, Q. S. Yan, J. L. Hu, and Z. Chen, "Numerical Simulation of Railway Track Irregularities Based on Stochastic Expansion Method of Standard Orthogonal Bases," in *Sustainable Environment and Transportation, Pts 1-4*. vol. 178-181, M. J. Chu, H. H. Xu, Z. Jia, Y. Fan, and J. P. Xu, Eds., ed Durnten-Zurich: Trans Tech Publications Ltd, 2012, pp. 1373-1378.

[32] H. Claus and W. Schiehlen, "Modeling and simulation of railway bogie structural vibrations," *Vehicle System Dynamics,* vol. 29, pp. 538-552, 1998.

[33] E. Foo and R. M. Goodall, "Active suspension control of flexible-bodied railway vehicles using electro-hydraulic and electro-magnetic actuators," *Control Engineering Practice,* vol. 8, pp. 507-518, May 2000.

[34] H. M. Yusof, R. Goodall, and R. Dixon, "Active railway suspension controllers using electro-mechanical actuation technology," presented at the Control 2010, UKACC International Conference on Control, Coventry, UK 2010.

[35] R. Zhou, A. Zolotas, and R. Goodall, "H∞-based control system and its digital implementation for the integrated tilt with active lateral secondary suspensions in high," presented at the 32nd Chinse Control Conference, Xian, China, 2013.

[36] A. C. Zolotas and R. M. Goodall, "Modelling and control of railway vehicle suspensions," in *Lecture Notes in Control and Information Sciences, Mathematical Methods for Robust and Nonlinear Control*, M. C. Turner and D. G. Bates, Eds., ed New York: Springer, 2007, pp. 373-412.

[37] A. C. Zolotas, R. M. Goodall, and G. D. Halikias, "Recent results in tilt control design and assessment of high-speed railway vehicles," *Proceedings of the Institution of Mechanical Engineers Part F-Journal of Rail and Rapid Transit*, vol. 221, pp. 291-312, Jun 2007.

[38] C. C. Smith, D. Y. McGehee, and A. J. Healey, "Prediction of passenger riding comfort from acceleration data," *Journal of Dynamic Systems Measurement and Control-Transactions of the Asme*, vol. 100, pp. 34-41, 1978.

[39] S. D. Nie, Y. Zhuang, W. P. Liu, and F. Chen, "A semi-active suspension control algorithm for vehicle comprehensive vertical dynamics performance," *Vehicle System Dynamics*, vol. 55, pp. 1099-1122, Aug 2017.

[40] H. E. Tseng and D. Hrovat, "State of the art survey: active and semi-active suspension control," *Vehicle System Dynamics*, vol. 53, pp. 1034-1062, Jul 3 2015.

[41] C. C. Smith, "Using ISO standard to evaluate ride quality of broad-band vibration-spectra in transportation vehicles," *Journal of Dynamic Systems Measurement and Control-Transactions of the Asme,* vol. 98, pp. 440-443, 1976.

[42] J. J. Allan and E. Arias, "Computers in Railways XI: Computer System Design and Operation in the Railway and Other Transit Systems." vol. 11, ed: WIT Press, 2008.

[43] D. G. Stephens and American Society of Mechanical Engineers, "Comparative vibration environments of transportation vehicles," presented at the ASME AMD, Passenger Vib in Transp Veh, Chicago, 1977.

[44] W. S. Yoo, C. H. Lee, W. B. Jeong, and S. H. Kim, "Development and application of new evaluation system for ride comfort and vibration on railway vehicles," *Journal of Mechanical Science and Technology,* vol. 19, pp. 1469-1477, Jul 2005.

[45] K. Abood and R. Khan, "Hunting phenomenon study of railway conventional truck on tangent tracks due to change in rail wheel geometry," *Journal of Engineering Science and Technology,* vol. 6, pp. 146-160, 2011.

[46] T. X. Mei and R. M. Goodall, "Recent Development in Active Steering of Railway Vehicles," *Vehicle System Dynamics,* vol. 39, pp. 415-436, 2003.

[47] G. Diana, S. Bruni, F. Cheli, and F. Resta, "Active control of the running behaviour of a railway vehicle: Stability and curving performances," *Vehicle System Dynamics,* vol. 37, pp. 157-170, 2002.

[48] F. Braghin, S. Bruni, and F. Resta, "Active yaw damper for the improvement of railway vehicle stability and curving performances: simulations and experimental results," *Vehicle System Dynamics,* vol. 44, pp. 857-869, Nov 2006.

[49] G. Shen and R. Goodall, "Active yaw relaxation for improved bogie performance," *Vehicle System Dynamics,* vol. 28, pp. 273-289, Oct 1997.

[50] A. H. Wickens, "Dynamic stability of articulated and steered railway vehicles guided by lateral displacement feedback," *Vehicle System Dynamics,* vol. 23, pp. 541-553, 1994.

[51] A. Orvn, "On Active Secondary Suspension in Rail Vehicles to Improve Ride Comfort," PhD thesis, KTH Engineering Sciences, Stockholm, 2011.

[52] N. Al-Holou, A. Bajwa, and D. S. Joo, "Computer controlled individual semi-active suspension system," presented at the Circuits and Systems, 1993., Proceedings of the 36th Midwest Symposium on, 1993.

[53] Goodall and Roger, "Tilting trains and beyond-the future for active railway suspensions. Part 1: Improving passenger comfort," *Computing & Control Engineering Journal,* vol. 10, pp. 153-160, 1999.

[54] R. Persson, "Tilting trains: enhanced benefits and strategies for less motion sickness," PhD Thesis, KTH Royal Institute of Technology, Stockholm, 2011.

[55] A. C. Mellado, C. Casanueva, J. Vinolas, and J. G. Giménez, "A lateral active suspension for conventional railway bogies " *Vehicle System Dynamics,* vol. 47, pp. 1-14, 2009.

[56] A. OrvnÄS, S. Stichel, and R. Persson, "Ride Comfort Improvements in a High-Speed Train with Active Secondary Suspension," *Journal of Mechanical Systems for Transportation and Logistics,* vol. 3, pp. 206-215, 2010.

[57] S. Alfi, S. Bruni, G. Diana, A. Facchinetti, and L. Mazzola, "Active control of airspring secondary suspension to improve ride quality and safety against crosswinds,"

Proceedings of the Institution of Mechanical Engineers, Part F: Journal of Rail and Rapid Transit, vol. 225, pp. 84-98, 2011.

[58] A. Pacchioni, R. M. Goodall, and S. Bruni, "Active suspension for a two-axle railway vehicle," *Vehicle System Dynamics,* vol. 48, pp. 105-120, 2010.

[59] E. Foo and R. Goodall, "Active suspension control strategies for flexible-bodied railway vehicles," in *Control'98. UKACC International Conference on (Conf. Publ. No. 455)*, 1998, pp. 1300-1305.

[60] G. Schandl, P. Lugner, C. Benatzky, M. Kozek, and A. Stribersky, "Comfort enhancement by an active vibration reduction system for a flexible railway car body," *Vehicle System Dynamics,* vol. 45, pp. 835-847, 2007.

[61] H. Zhang, L. Ren, R. Goodall, and J. Zhou, "Influences of car body vertical flexibility on ride quality of passenger railway vehicles," *Proceedings of the Institution of Mechanical Engineers, Part F: Journal of Rail and Rapid Transit,* vol. 223, pp. 461-471, 2009.

[62] Y. Suda, S. Nakadai, and K. Nakano, "Hybrid Suspension System with Skyhook Control and Energy Regeneration (Development of Self-Powered Active Suspension)," *Vehicle System Dynamics,* vol. 29, pp. 619-634, 1998.

[63] Y. Suda, "Study on the self-powered active vibration control," *JSME International Journal Series C Mechanical Systems, Machine Elements and Manufacturing Vol. 43(2000) No. 3,* pp. 726-731, 2000.

[64] K. Singal and R. Rajamani, "Simulation study of a novel self-powered active suspension system for automobiles," in *Proceedings of the 2011 American Control Conference,* 2011, pp. 3332-3337.

[65] P. Wang, T. Mei, J. Zhang, and H. Li, "Self-Powered Active Lateral Secondary Suspension for Railway Vehicles," *IEEE Transactions on Vehicular Technology*, vol. 65, pp. 1121-1129, 2016.

[66] P. Wang, T. Mei, and J. Zhang, "Towards self-powered lateral active suspension for railway vehicles," in *Control (CONTROL), 2014 UKACC International Conference on*, 2014, pp. 567-572.

[67] H. Selamat and S. D. A. Bilong, "Optimal Controller Design for a Railway Vehicle Suspension System Using Particle Swarm Optimization," *2013 9th Asian Control Conference (Ascc)*, 2013.

[68] T. X. Mei and R. M. Goodall, "Modal Controllers for Active Steering of Railway Vehicles with Solid Axle Wheelsets," *Vehicle System Dynamics*, vol. 34, pp. 25-41, 2000.

[69] R. Zhou, A. Zolotas, and R. Goodall, "Integrated tilt with active lateral secondary suspension control for high speed railway vehicles," *Mechatronics*, vol. 21, pp. 1108-1122, 2011.

[70] R. Zhou, A. Zolotas, and R. Goodall, "H-infinity based control system and its digital implementation for the integrated tilt with active lateral secondary suspensions in high speed trains," in *Control Conference (CCC), 2013 32nd Chinese*, China, 2013.

[71] R. Zhou, A. Zolotas, and R. Goodall, "Robust system state estimation for active suspension control in high-speed tilting trains," *Vehicle System Dynamics*, vol. 52, pp. 355-369, 2014.

[72] H. Yabuno, T. Okamoto, and N. Aoshima, "Stabilization control for the hunting motion of a railway wheelset," *Vehicle System Dynamics*, vol. 35, pp. 41-55, 2001.

[73] A. K. Mohamadi and N. Al-e-Ali, "Active Control of Lateral Vibration for Bogie Using Variable Structure Model Reference Adaptive Control," presented at the 2008 International Conference on Computational Intelligence for Modelling Control & Automation (CIMCA 2008)(CIMCA), Vienna, Austria, 2008.

[74] J. Pearson, R. Goodall, T. Mei, and G. Himmelstein, "Active stability control strategies for a high speed bogie," *Control Engineering Practice,* vol. 12, pp. 1381-1391, 2004.

[75] P. E. Orukpe, X. Zheng, I. M. Jaimoukha, A. C. Zolotas, and R. M. Goodall, "Model predictive control based on mixed $\mathcal{H}2/\mathcal{H}\infty$control approach for active vibration control of railway vehicles," *Vehicle System Dynamics,* vol. 46, pp. 151-160, 2008.

[76] W. Liao and D. Wang, "Semiactive vibration control of train suspension systems via magnetorheological dampers," *Journal of Intelligent Material Systems and Structures,* vol. 14, pp. 161-172, 2003.

[77] S. B. Choi, W. H. Li, M. Yu, H. P. Du, J. Fu, and P. X. Do, "State of the art of control schemes for smart systems featuring magneto-rheological materials," *Smart Materials and Structures,* vol. 25, p. 24, Apr 2016.

[78] D. H. Wang and W. H. Liao, *Application of MR dampers for semiactive suspension of railway vehicles* vol. 10, 2000.

[79] A. Stribersky, A. Kienberger, G. Wagner, and H. Muller, "Design and evaluation of a semi-active damping system for rail vehicles," *Vehicle System Dynamics,* vol. 29, pp. 669-681, 1998.

[80] G. S. Gao and S. P. Yang, "Semi-active Control Performance of Railway Vehicle Suspension Featuring Magnetorheological Dampers," presented at the 2006 1ST IEEE Conference on Industrial Electronics and Applications, Singapore, 2006.

[81] C. Spelta, S. M. Savaresi, F. Codecà, M. Montiglio, and M. Ieluzzi, "Smart-Bogie: Semi-Active Lateral Control of Railway Vehicles," *Asian Journal of Control,* vol. 14, pp. 875-890, 2012.

[82] K. Hudha, M. H. Harun, M. H. Harun, and H. Jamaluddin, "Lateral Suspension Control of Railway Vehicle Using Semi-Active Magnetorheological Damper," presented at the 2011 IEEE Intelligent Vehicles Symposium (IV), Germany, 2011.

[83] W. H. Liao and D. H. Wang, "Semiactive vibration control of train suspension systems via magnetorheological dampers," *Journal of Intelligent Material Systems and Structures,* vol. 14, pp. 161-172, Mar 2003.

[84] Y. Lau and W. Liao, "Design and analysis of magnetorheological dampers for train suspension," *Proceedings of the Institution of Mechanical Engineers, Part F: Journal of Rail and Rapid Transit,* vol. 219, pp. 261-276, 2005.

[85] D. H. Wang and W. H. Liao, "Semi-active suspension systems for railway vehicles using magnetorheological dampers. Part I: system integration and modelling," *Vehicle System Dynamics,* vol. 47, pp. 1305-1325, 2009.

[86] B. Allotta, L. Pugi, F. Bartolini, F. Cangioli, and V. Colla, "Comparison of different control approaches aiming at enhancing the comfort of a railway vehicle," in *2010 IEEE/ASME International Conference on Advanced Intelligent Mechatronics*, 2010, pp. 676-681.

[87] S. H. Ha, S. B. Choi, G. S. Lee, and W. H. Yoo, "Control performance evaluation of railway vehicle MR suspension using fuzzy sky-ground hook control algorithm," *13th International Conference on Electrorheological Fluids and Magnetorheological Suspensions (Ermr2012),* vol. 412, 2013 2013.

[88] K. H. A. Abood and R. A. Khan, "Hunting Phenomenon Study of Railway Conventional Truck on Tangent Tracks Due to Changein Rail Wheel Geometry," *Journal of Engineering Science and Technology* vol. 6, pp. 146-160, 2011.

[89] D. H. Wang and W. H. Liao, "Semi-active suspension systems for railway vehicles using magnetorheological dampers. Part II: simulation and analysis," *Vehicle System Dynamics*, vol. 47, pp. 1439-1471, 2009.

[90] K. Hudha, M. H. Harun, M. H. Harun, H. Jamaluddin, and Ieee, "Lateral Suspension Control of Railway Vehicle Using Semi-Active Magnetorheological Damper," *IEEE Intelligent Vehicles Symposium (IV)*, pp. 728-733, 2011.

[91] H. Scheffel, R. D. Frohling, and P. S. Heyns, "Curving and stability analysis of self-steering bogies having a variable yaw constraint," *Vehicle System Dynamics*, vol. 23, pp. 425-436, 1994.

[92] S. H. Ha, S. B. Choi, G. S. Lee, and W. H. Yoo, "Control performance evaluation of railway vehicle MR suspension using fuzzy sky-ground hook control algorithm," in *13th International Conference on Electrorheological Fluids and Magnetorheological Suspensions*. vol. 412, H. I. Unal, Ed., ed, 2013.

[93] Karnopp and Dean, "Active and semi-active vibration isolation," in *Current Advances in Mechanical Design and Production VI*, ed: Elsevier, 1995, pp. 409-423.

[94] S. B. A. Kashem, S. Roy, and R. Mukharjee, "A modified skyhook control system (SKDT) to improve suspension control strategy of vehicles," in *Informatics, Electronics & Vision (ICIEV), 2014 International Conference on*, 2014, pp. 1-8.

[95] A. Z. Solehin and C. Hasan, "Modelling and simulation of modified skyhook control for semi-active suspension," Universiti Malaysia Pahang, 2011.

[96] K. J. Åström and B. Wittenmark, *Adaptive control*: Courier Corporation, 2013.

[97] M. Rahman, Z. C. Ong, S. Julai, M. M. Ferdaus, and R. Ahamed, "A review of advances in magnetorheological dampers: their design optimization and applications," *Journal of Zhejiang University-Science A,* vol. 18, pp. 991-1010, Dec 2017.

[98] J. D. Carlson, "A growing attraction to magnetic fluids," *Machine Design,* vol. 66, pp. 61-64, Aug 1994.

[99] O. Ashour, C. A. Rogers, and W. Kordonsky, "Magnetorheological fluids: Materials, characterization, and devices," *Journal of Intelligent Material Systems and Structures,* vol. 7, pp. 123-130, Mar 1996.

[100] N. I. N. Ismail and S. Kamaruddin, "Development of Magnetorheological Elastomers based on Deproteinised Natural Rubber as Smart Damping Materials," in *Advanced Materials for Sustainability and Growth*. vol. 1901, S. M. Ibrahim and K. Noorsal, Eds., ed Melville: Amer Inst Physics, 2017.

[101] K. D. Weiss, J. D. Carlson, and D. A. Nixon, "Viscoelastic properties of magnetorheological and electrorheological fluids," *Journal of Intelligent Material Systems and Structures,* vol. 5, pp. 772-775, Nov 1994.

[102] J. H. Koo, F. D. Goncalves, and M. Ahmadian, "A comprehensive analysis of the response time of MR dampers," *Smart Materials & Structures,* vol. 15, pp. 351-358, Apr 2006.

[103] M. Ahmadian, "Magneto-rheological suspensions for improving ground vehicle's ride comfort, stability, and handling," *Vehicle System Dynamics,* vol. 55, pp. 1618-1642, 2017.

[104] H. A. Metered, "Modelling and control of magnetorheological dampers for vehicle suspension systems," University of Manchester, 2010.

[105] D. Wang and W. H. Liao, "Magnetorheological fluid dampers: a review of parametric modelling," *Smart materials and structures,* vol. 20, p. 023001, 2011.

[106] B. Spencer, S. Dyke, M. Sain, and J. Carlson, "Phenomenological model for magnetorheological dampers," *Journal of engineering mechanics,* vol. 123, pp. 230-238, 1997.

[107] M. Bideleh, S. Milad, and V. Berbyuk, "Application of Semi-Active Control Strategies in Bogie Primary Suspension System," in *Proceedings of the Second International Conference on Railway Technology: Research, Development and Maintenance, J. Pombo,(Editor), Civil-Comp Press, Stirlingshire, United Kingdom, paper 318*, 2014.

[108] L.-H. Zong, X.-L. Gong, C.-Y. Guo, and S.-H. Xuan, "Inverse neuro-fuzzy MR damper model and its application in vibration control of vehicle suspension system," *Vehicle System Dynamics,* vol. 50, pp. 1025-1041, 2012 2012.

[109] P.-Q. Xia, "An inverse model of MR damper using optimal neural network and system identification," *Journal of Sound and Vibration,* vol. 266, pp. 1009-1023, 2003.

[110] H. Wang and H. Hu, "The Neuro-fuzzy Identification of MR Damper," pp. 464-468, 2009.

[111] D. J. Leith and W. E. Leithead, "Survey of gain-scheduling analysis and design," *International Journal of Control,* vol. 73, pp. 1001-1025, Jul 2000.

[112] T. Chaiyatham and I. Ngamroo, "Improvement of Power System Transient Stability by PV Farm With Fuzzy Gain Scheduling of PID Controller," *IEEE Systems Journal,* vol. 11, pp. 1684-1691, Sep 2017.

[113] J. A. Brizuela-Mendoza, C. M. Astorga-Zaragoza, A. Zavala-Rio, F. Canales-Abarca, and M. Martinez-Garcia, "Gain-scheduled linear quadratic regulator applied to the stabilization of a riderless bicycle," *Proceedings of the Institution of Mechanical Engineers Part I-Journal of Systems and Control Engineering,* vol. 231, pp. 669-682, Sep 2017.